CHAPTER 6

STATIC SCANNING

6.1 Introduction

Static scanning is a means of converting both amplitude and phase information, contained in the profile of a periodic light intensity distribution, into equivalent electrical signals. It was developed for the purpose of measuring position and contrast of periodic shadows when determining Fourier coefficients, avoiding mechanical movement for high speed work.

Static scanning is based on sampling a periodic light intensity distribution at a number of points within a period. A pure sinewave must be sampled in at least two places according to the sampling theorem stated by Weaver[83]. A sinewave shadow, however, is always accompanied by a d.c. light background. The minimum number of samples that may be taken in this case is three since the d.c. term has to be eliminated. It may assist signal processing if more frequent samples are taken. This is exemplified by the quadrant sampling mask method described later. The three parameters associated with a sinusoidal light intensity profile, a, $\emptyset$ and H are illustrated in Fig. 6.1.

6.1.1 Method of Sampling

Single point or slit sampling is impracticable with little light transmitted for detection. This is marginally improved with a grid of slits having the same period as the shadow. Such a grid situated in the shadow plane constitutes a single sampling point.

A more efficient sampling mask producing the same net result as a set of slits is a grid with a sinusoidal transmission profile. When placed in the shadow plane with its stripes parallel to the shadow stripes, its total light transmission summed over a period d, is expressed by:-

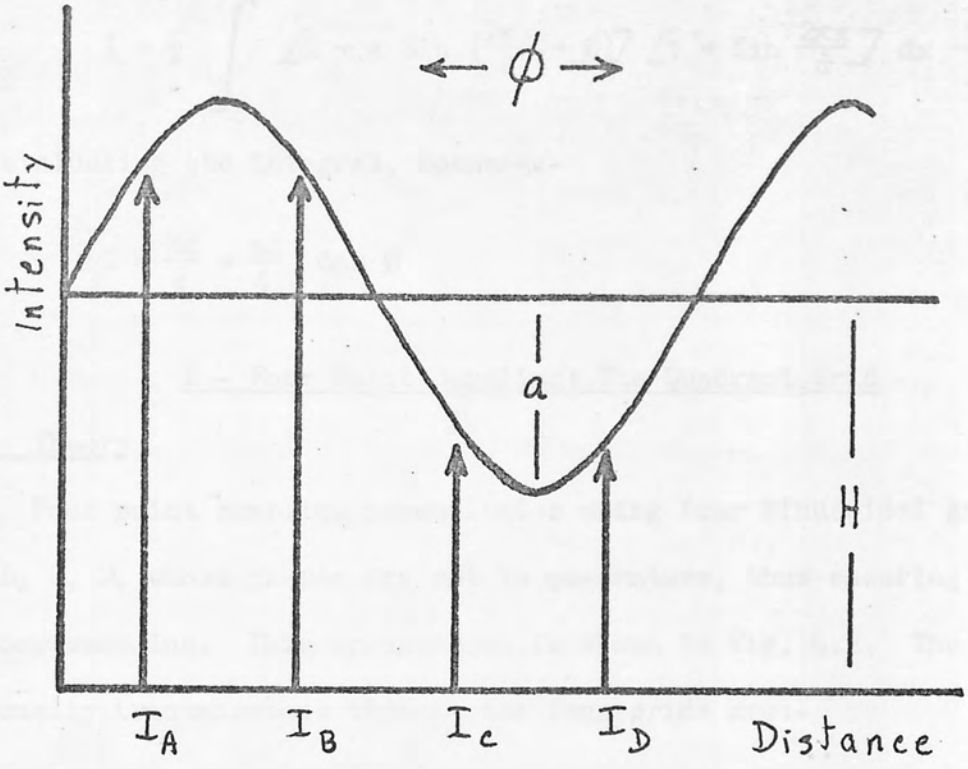

Fig. 6.1

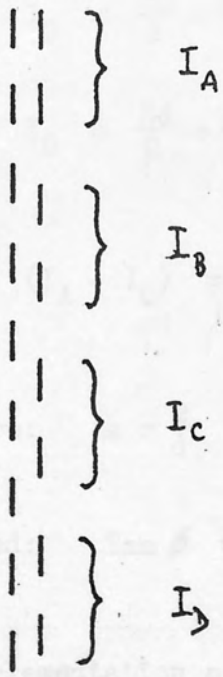

Fig. 6.2 Quadrature Sampling Masks.

$$I = \tfrac{1}{2} \int_0^d \left[H + a \text{ Sin } \left(\frac{2\pi x}{d} + \phi\right)\right] \left[1 + \text{Sin } \frac{2\pi x}{d}\right] dx$$

On evaluating the integral, becomes:-

$$I = \frac{Hd}{2} + \frac{ad}{4} \text{ Cos } \phi$$

I - Four Point Sampling: The Quadrant Grid

6.2 Theory

Four point sampling necessitates using four sinusoidal grids, A, B, C, D, whose phases are set in quadrature, thus ensuring equispaced shadow sampling. This arrangement is shown in Fig. 6.2. The light intensity transmissions through the four grids are:-

$$I_A = \frac{Hd}{2} + \frac{ad}{4} \text{ Cos } \phi \quad \ldots\ldots\ldots\ldots\ldots 1$$

$$I_B = \frac{Hd}{2} - \frac{ad}{4} \text{ Sin } \phi \quad \ldots\ldots\ldots\ldots\ldots 2$$

$$I_C = \frac{Hd}{2} - \frac{ad}{4} \text{ Cos } \phi \quad \ldots\ldots\ldots\ldots\ldots 3$$

$$I_D = \frac{Hd}{2} + \frac{ad}{4} \text{ Sin } \phi \quad \ldots\ldots\ldots\ldots\ldots 4$$

$$(I_A - I_C) = \frac{ad}{2} \text{ Cos } \phi \text{ and } (I_D - I_B) = \frac{ad}{2} \text{ Sin } \phi$$

Therefore: $$a = \frac{2}{d} \left((I_A - I_C)^2 + (I_D - I_B)^2 \right)^{\frac{1}{2}}$$

And: $$\text{Tan } \phi = \frac{I_D - I_B}{I_A - I_C}$$

6.3 Implementation of the Theory

On the face of it, the obvious thing to do is to collect light transmitted by each mask onto suitable photo-detectors and then perform the mathematical operations electronically. High stability low drift

detectors would be necessary to collect the d.c. light intensities. Subtraction can be performed using low offset differential operational amplifiers. Precise determination of "a" and "tan ϕ" would entail using non-linear elements for which some sophistication of circuit design is necessary.

The mathematical operations can be very elegantly performed if the analogue d.c. signals are modulated. Modulation techniques have a two fold advantage over the d.c. approach:-

1. Increased stability.
2. Signal processing is facilitated.

6.4 Signal Modulation

6.4.1 Signal Processing Philosophy

The signals, that is the values of light intensities transmitted by each mask, are modulated at an early stage (preferably optically) and assigned phases equivalent to the spatial phases of the masking grids. There are a number of ways of accomplishing this in practice but the final result is the same for each. Mathematically, the modulation may be expressed by the equations:-

$$\left.\begin{aligned} I'_A &= \frac{d}{4}\left[H + \frac{a}{2}\,\mathrm{Cos}\,\phi\right]\left[1 + \mathrm{Cos}\,wt\right] \\ I'_B &= \frac{d}{4}\left[H - \frac{a}{2}\,\mathrm{Sin}\,\phi\right]\left[1 - \mathrm{Sin}\,wt\right] \\ I'_C &= \frac{d}{4}\left[H - \frac{a}{2}\,\mathrm{Cos}\,\phi\right]\left[1 - \mathrm{Cos}\,wt\right] \\ I'_D &= \frac{d}{4}\left[H + \frac{a}{2}\,\mathrm{Sin}\,\phi\right]\left[1 + \mathrm{Sin}\,wt\right] \end{aligned}\right\} \quad \ldots\ldots\ldots 5$$

Which, when added, produce:-

$$d\left[1 + \frac{a}{4}\,\mathrm{Cos}\,(\phi + wt)\right]$$

The temporal modulation term contains both phase and amplitude information of the original spatial shadow.

6.5 Light Modulation Techniques

Light illuminating the object may be modulated by any suitable method provided it does not disturb the passage of light rays producing the shadows. Modulation depth should be large; unmodulated light constitutes noise. Methods of light intensity modulation include: mechanical choppers; electro-optic and electro-magnetic modulators; light source modulation.

Source modulation was used for much of the development. This was simply a source running off 50 cycles mains supply. Tungsten filament lamps produced an excellent 100 Hz sinewave modulation but their depth of molulation was found to be poor, the a.c. : d.c. ratio being approximately 1 : 7. A mercury lamp had good modulation depth but with a triangular shaped waveform. This, however, is not a serious drawback and the mercury lamp was adopted for experimentation with the quadrant grids.

6.6 Experimental Details

An optical arrangement shown in Fig. 6.3 was set up on an optical bench.

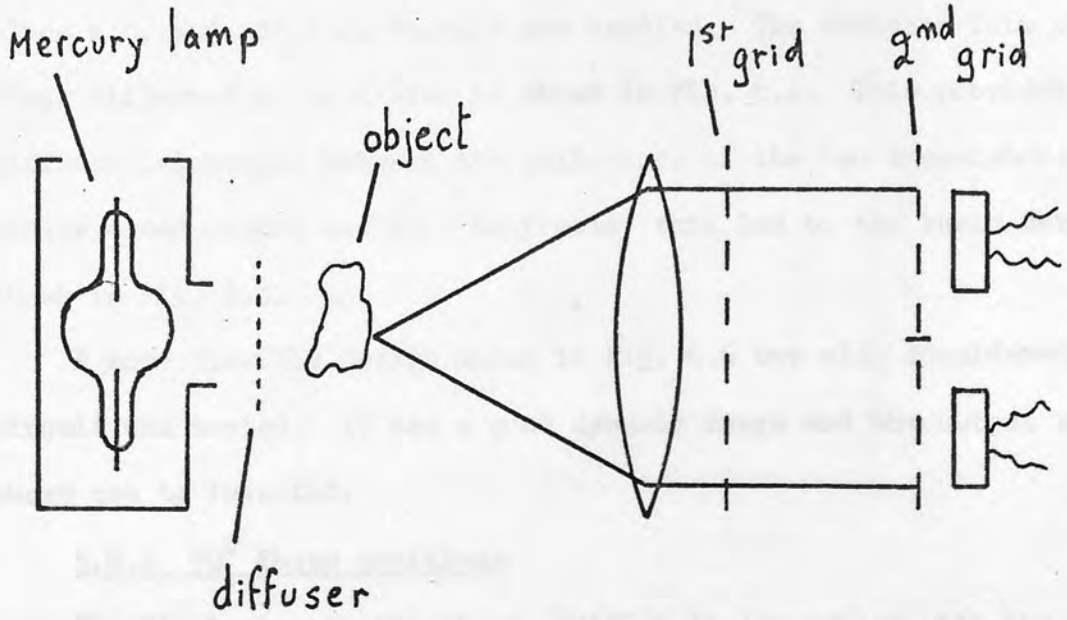

Fig. 6.3

A specimen character was shadowed through a single grid. ORP12 cadmium sulphide photo-conductive cells were used to detect light. These have a relatively slow response time but are adequate at 100 Hz. Their sensitive areas are grid structured, so, as a safeguard against interaction with the shadows, a diffusing screen was inserted between the quadrant grid and the detectors. Four detectors, one behind each quadrant, collect all light transmitted by each quadrant. The modulated light source gives rise to a corresponding modulation in the conductivity of each photo-cell. This is translated into an electrical signal using the same potentiometer circuit shown in Fig. 3.3. These signals must be assigned their correct phase relationships in accordance with the theory.

One virtue of the quadrant grid (4 samples) now becomes apparent. Two pairs of quadrants require their signals to be in antiphase on inspection of the modulation equations. The appropriate pairs of signals are merely fed into two differential amplifiers which effectively add pairs of input signals in antiphase.

6.6.1 Differential Amplifier Design

Special differential amplifier design technique was not essential since a.c. and not d.c. signals are handled. The standard form of single stage differential amplifier is shown in Fig. 6.4. This provides a differential output between the collectors of the two transistors. A single ended output was more desirable, this led to the basic design shown in Fig. 6.5.

A more flexible design shown in Fig. 6.6 was also considered. This circuit was tested. It has a good dynamic range and the output waveform phase can be inverted.

6.6.2 90° Phase Additions

The final step in the phase addition in accordance with the equations involves a 90° phase shift.

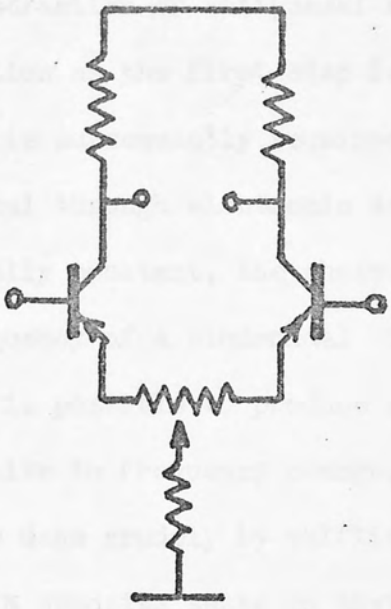

Fig. 6.4

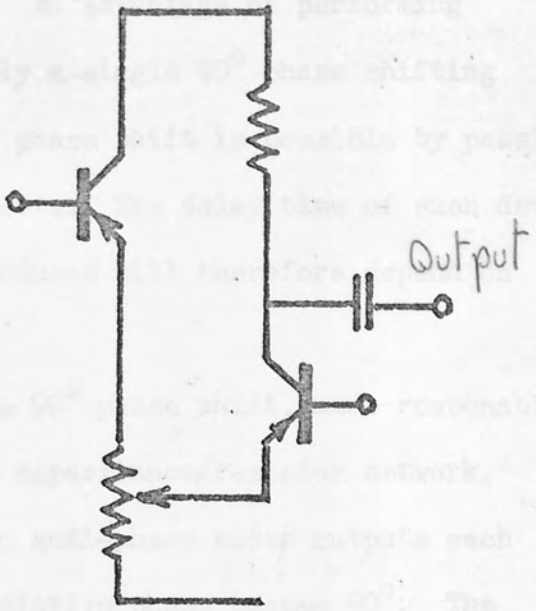

Fig. 6.5

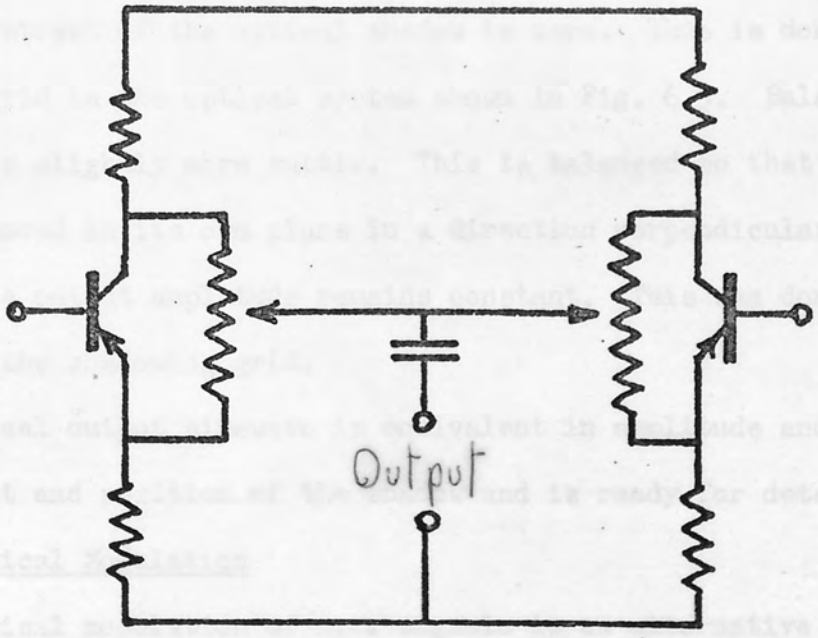

Fig. 6.6

90° phase shifting is slightly more cumbersome to perform electronically than subtraction or antiphasal addition. An advantage of performing subtraction as the first step is that only a single 90° phase shifting circuit is subsequently required. A 90° phase shift is possible by passing the signal through electronic delay elements. The delay time of such devices is normally constant, the phase shift produced will therefore depend on the frequency of a sinusoidal signal.

It is possible to produce a relative 90° phase shift, made reasonably insensitive to frequency change, using a capacitance/resistor network. This was done crudely by shifting the two anti-phase adder outputs each by 45° in opposite sense so that their relative phase became 90°. The circuit built to do this is shown in Fig. 6.7. A balancing potenticmeter is connected between the collectors of the output transistors.

6.6.3 Note on Balancing

All final balancing is done electronically. The differential amplifiers are balanced so that there is zero modulation at their outputs when the contrast of the optical shadow is zero. This is done by removing the first grid in the optical system shown in Fig. 6.3. Balancing the 90° adder is slightly more subtle. This is balanced so that when the shadow is moved in its own plane in a direction perpendicular to the stripes, the output amplitude remains constant. This was done by traversing the shadowing grid.

The final output sinewave is equivalent in amplitude and phase to the contrast and position of the shadow and is ready for detection.

6.7 Electrical Modulation

Electrical modulation of d.c. signals is an alternative to optical modulation and offers more scope for phase addition. The phase addition principle is the same.

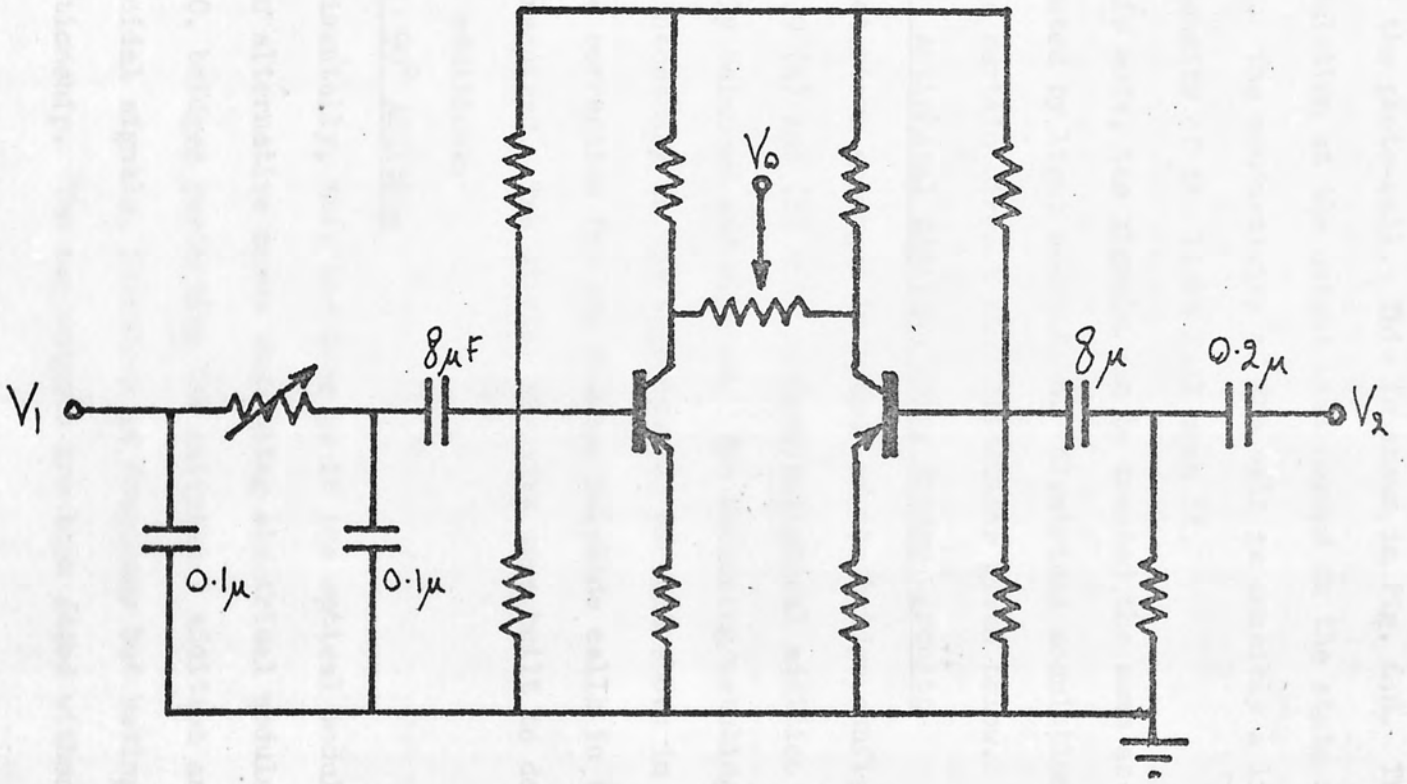

Fig. 6.4 90° Phase Shift Circuit

6.7.1 Experimental Detail

Detectors used in these experimental circuits were cadmium sulphide photo-conductive cells. These were chosen for convenience and compatability with fixed resistors. Signals are modulated by applying an a.c. voltage (in the order of a few volts) to a potentiometer containing the photo-cell. This is shown in Fig. 6.8. The amplitude of the modulation at the output will depend on the state of conduction of the photo-cell. The conductivity of the cell is sensibly a linear function of the intensity of the light fall upon it.

In this mode, the signals can be treated the same as if they had been generated by light modulation. Electrical modulation does, however, provide for certain circuit simplifications given below.

6.7.2 Antiphasal Addition Using Bridge Circuits

Two detectors arranged in either of the bridge configurations shown in Figs. 6.9 (a) and (b) will perform antiphasal addition provided they are properly balanced and matched. Two balancing/matching potentiometers were found necessary in the experimental circuit shown in Fig. 6.10. Capacitance correction for the cadmium sulphide cells in the order of 100pF was required. Two similar circuits were built to do both pairs of antiphasal additions.

6.7.3 90° Addition

Experimentally, this was done as in the optical modulation case. There is an alternative means when using electrical modulation. The pair of A.C. bridges performing the antiphasal addition are supplied with sinusoidal signals, identical in frequency but having a 90° relative phase relationship. The two outputs are then added without further phase shifting.

6.8 Discussion on Optical and Electrical Modulation Techniques

Electrical modulation is convenient and flexible but was found to be less stable than optical modulation, i.e. balance settings were prone to drift. Modulation can be regarded as chopper stabilisation and

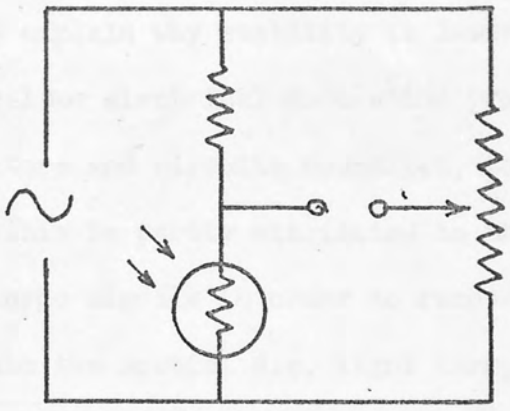

Fig. 6.8

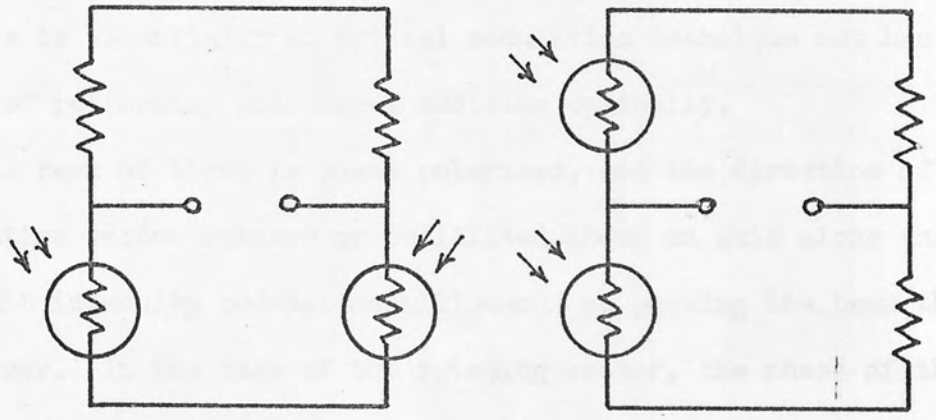

Fig. 6.9

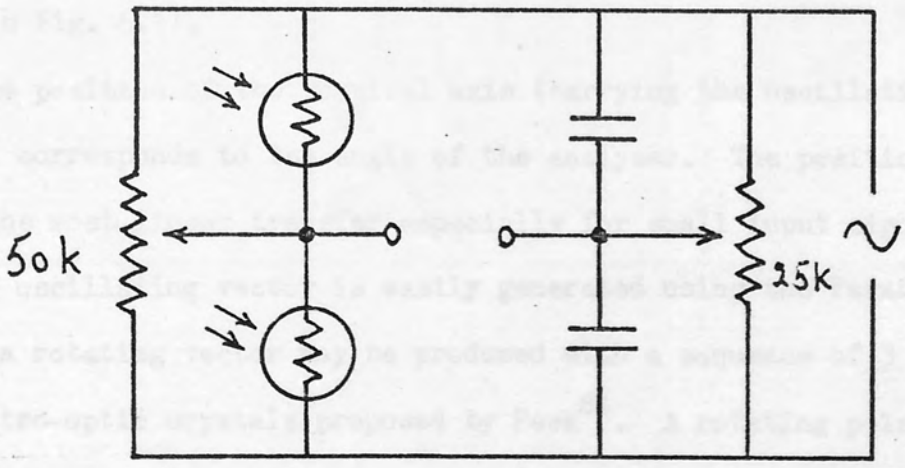

Fig. 6.10

would explain why stability is lower using electrical modulation. Neither opticalnor electrical modulation produced enough stability, using the detectors and circuits described, to ensure reliable amplitude measurements.

This is partly attributed to the inherent difficulty in subtracting two large signals in order to recover a small one. The large signals contain the spatial d.c. light term, which is generally high compared with the shadow contrast. This led to a concept of optical antiphasal addition using an oscillating or rotating polarisation vector.

6.9 Light Modulation using Rotating Polarisation Vector

This is essentially an optical modulation technique but has the novel feature of performing antiphasal addition optically.

If a beam of light is plane polarised, and the direction of the polarisation vector rotated or oscillated about an axis along the beam, then light intensity modulation will result on passing the beam through an analyser. In the case of the rotating vector, the phase of the modulation will depend on the orientation of the analyser. If the vector is rotating with angular velocity wt, then the modulation is given by $\mathrm{Sin}^2(wt + \phi)$ where ϕ is the angle of the polaroid relative to an arbitrary reference. If the vector is oscillating, the transmission amplitude can be derived using the angular intensity transfer diagram of polariser shown in Fig. 6.11.

The position of the vertical axis (carrying the oscillating input vector) corresponds to the angle of the analyser. The position shown gives the most linear transfer especially for small input signals.

An oscillating vector is easily generated using the Faraday effect; whilst a rotating vector may be produced with a sequence of 3 (possibly 2) electro-optic crystals proposed by Peek[84]. A rotating polarisation vector may conveniently be generated by mechanically rotating a polarising sheet. Frequency doubling of the modulation is possible by rotating a half wave plate. These systems are described by Rogers[85] and Jaumann[86(a)].

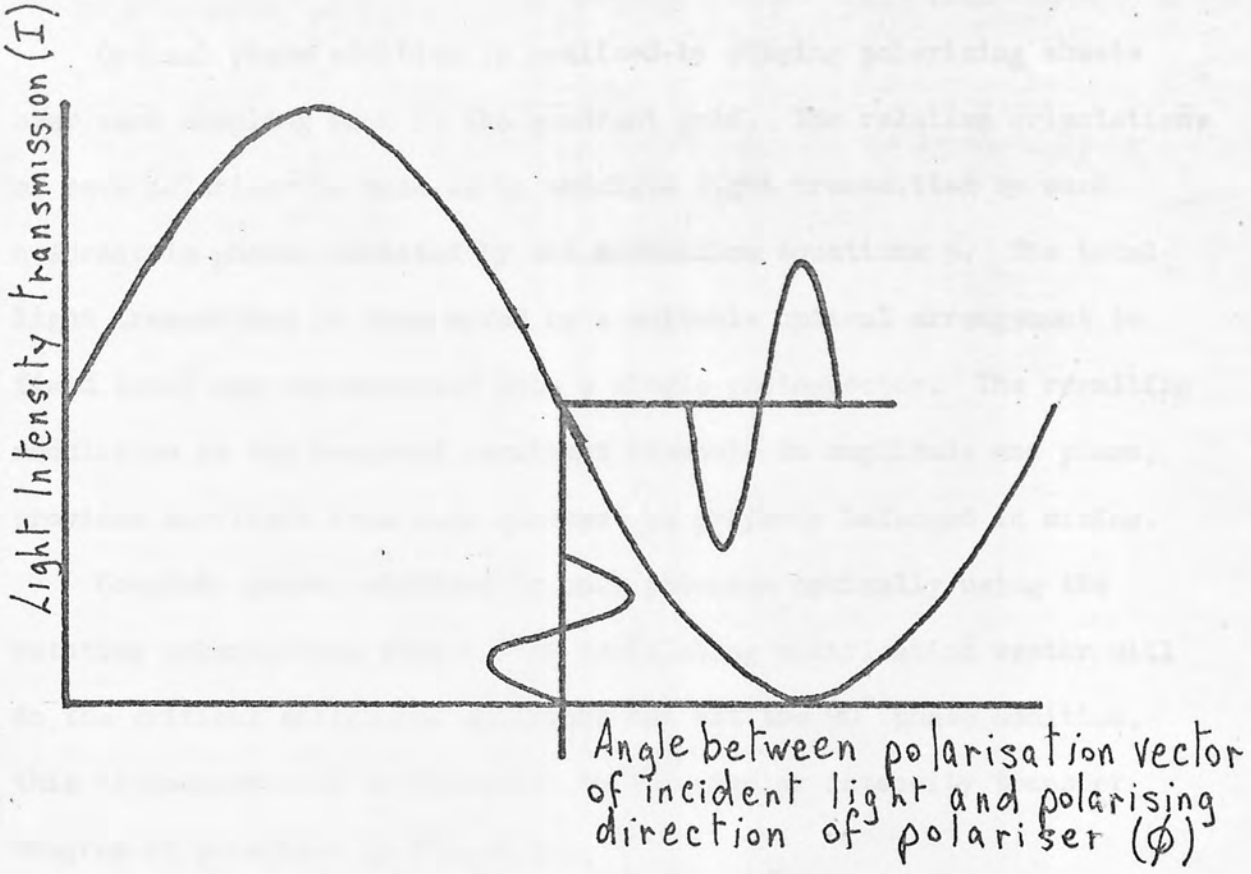

Fig. 6·11 Angular Intensity Function of Polaroid

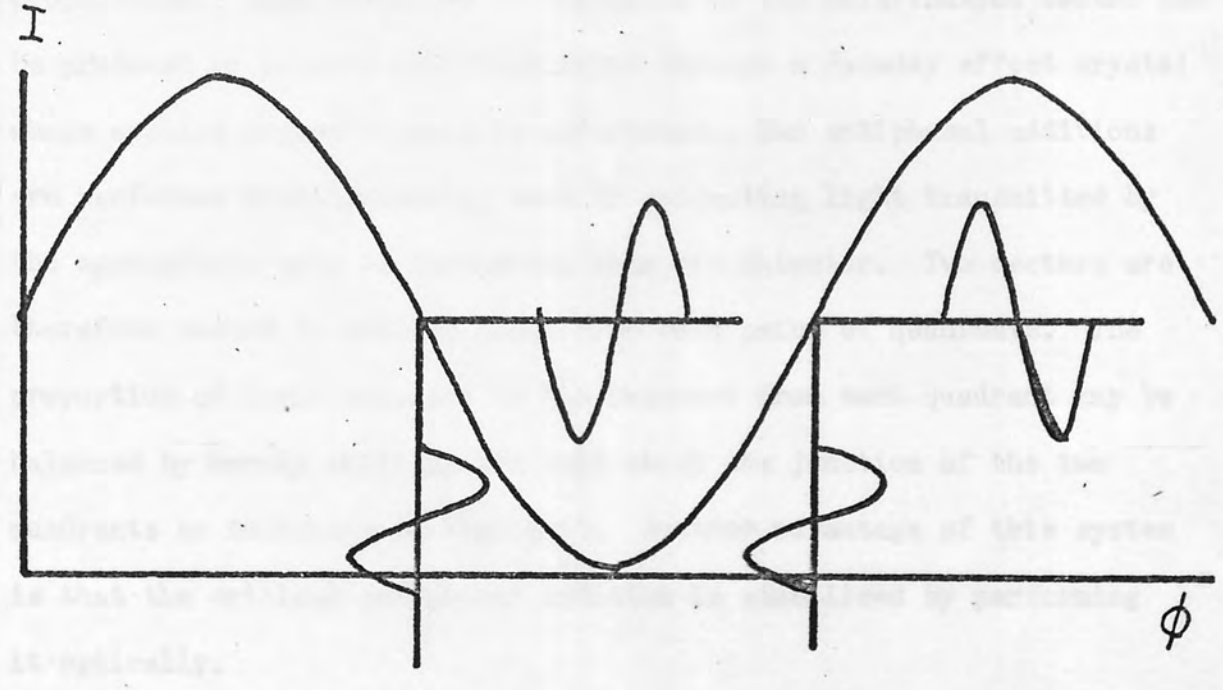

Fig. 6·12 Antiphasal Intensity Transfer of two Oscillating Polarisation Vectors

Optical phase addition is realised by placing polarising sheets over each sampling mask in the quadrant grid. The relative orientations of each polariser is such as to modulate light transmitted by each quadrant in phases dictated by the modulation equations 5. The total light transmitted is then mixed by a suitable optical arrangement (a field lens) and concentrated onto a single photo-dector. The resulting modulation is the required resultant sinusoid in amplitude and phase, provided the light from each quadrant is properly balanced in mixing.

Complete phasal addition is only possible optically using the rotating polarisation vector. An oscillating polarisation vector will do the critical antiphasal additions but not the 90^{o} phase addition, this is demonstrated by reference to the angular intensity transfer diagram of polariser in Fig. 6.12.

There are certain practical considerations which make the use of the oscillating polarisation vector for antiphasal addition an attractive proposition. High frequency oscillations of the polarisation vector can be produced by passing polarised light through a Faraday effect crystal whose applied magnetic field is alternated.. Two antiphasal additions are performed simultaneously, each by collecting light transmitted by the appropriate pair of quadrants, onto one detector. Two dectors are therefore needed to collect light from both pairs of quadrants. The proportion of light received by the detector from each quadrant may be balanced by merely shifting the cell about the junction of the two quadrants as indicated in Fig. 6.13. Another advantage of this system is that the critical antiphasal addition is stabilised by performing it optically.

6.10 Experimentation with a YIG Faraday Effect Crystal

An oscillating vector system was developed with antiphasal addition using two photo-detectors. An Yttrium Iron Garnet crystal placed inside

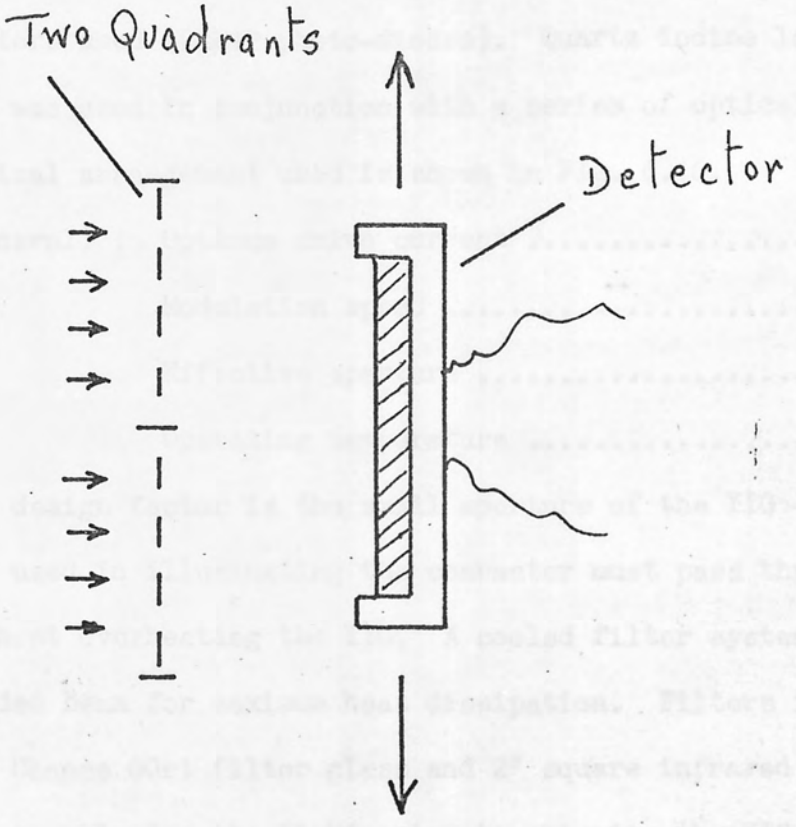

Fig. 6.13

a coil carrying an a.c. current serves to oscillate the plane of the polarisation vector. The crystal is arranged so that the light travels through it parallel to the lines of magnetic flux shown in Fig. 6.14. The YIG crystal transmits in the near infrared. It is most efficient in the spectral range between 1 and 2 μ.

The opto-electronic system was designed round the YIG in order to benefit fully from it. The graph in Fig. 6.15 gives spectral information about the YIG together with a suitable polariser and the spectral response of the detectors used (OAP12 photo-diodes). Quartz iodine lamp illumination was used in conjunction with a series of optical filters.

The optical arrangement used is shown in Fig. 6.16.

YIG Data (General) : Optimum drive current ..... 25 m.a.
Modulation speed ..... 0 - 100KHz
Effective aperture ..... 4 mm.
Operating temperature ..... 80°C.

A major design factor is the small aperture of the YIG - 4 mm. All of the light used in illuminating the character must pass through this aperture without overheating the YIG. A cooled filter system was inserted in the expanded beam for maximum heat dissipation. Filters included: $2\frac{1}{2}$" diameter Chance OGr1 filter glass and 2" square infrared polaroid serving also to polarise the light prior to entering the YIG crystal.

To assist in aligning the optical components, the polarising filter is removed and the YIG replaced by an equivalent aperture. Visible green transmitted by the OGr1 filter can then be used for visual alignment.

The YIG was driven by a low impedence sinewave generator at frequencies ranging between 1K - 10K Hz. during trials.

6.10.1 Detectors and Circuitry

The germanium OAP12 photo-diodes have a peak spectral sensitivity in the region in which the YIG is most efficient. The disadvantage in this application is their small sensitive area which involves the use of

FARADAY EFFECT

Plane of Polarisation of incident I.R. beam rotated through angle of θ where

$\theta = f(H, t, \lambda)$

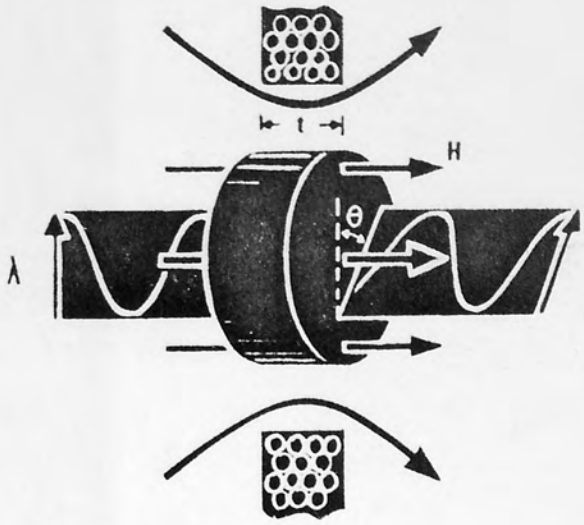

Fig 6·14 **The 'YIG' Modulator**

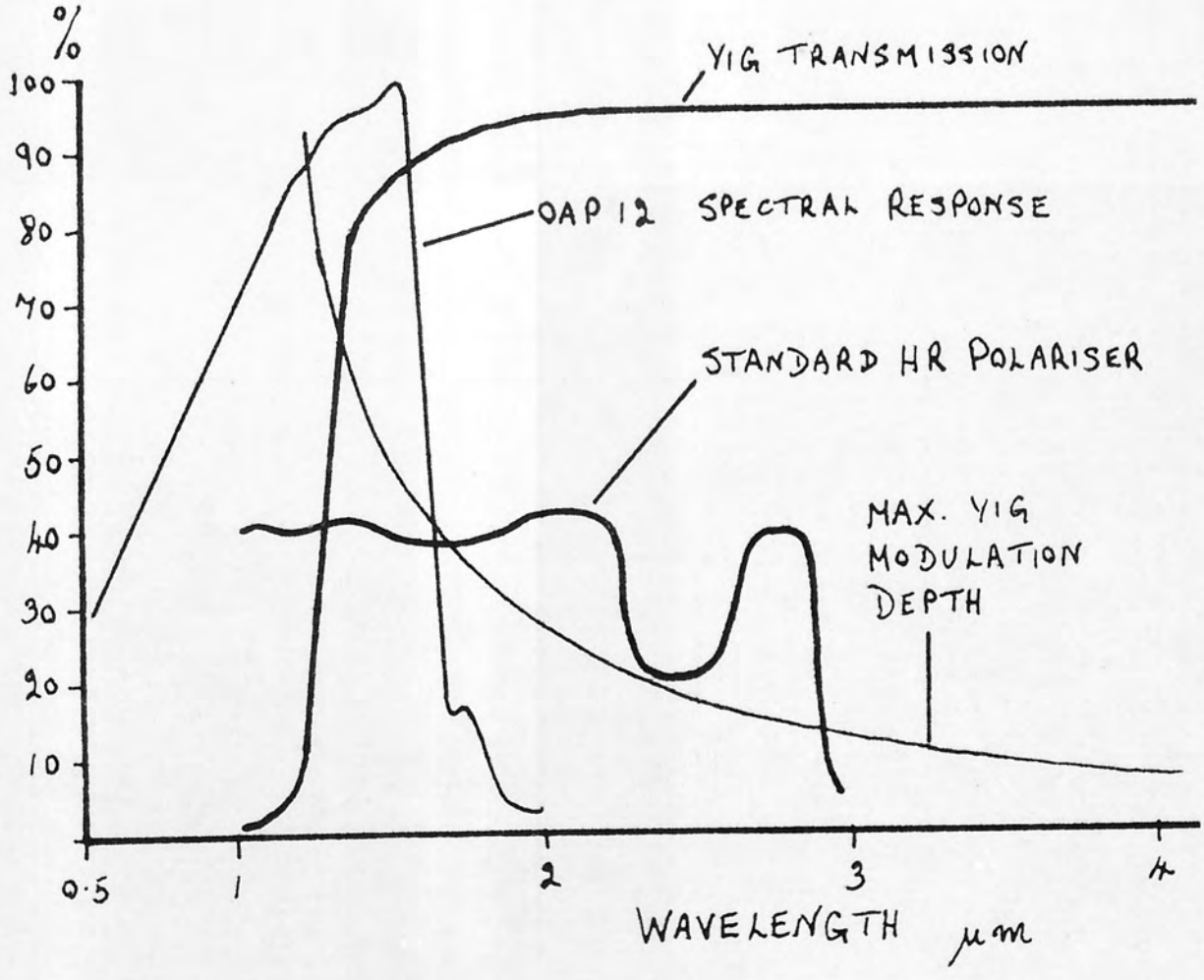

Fig. 6·15

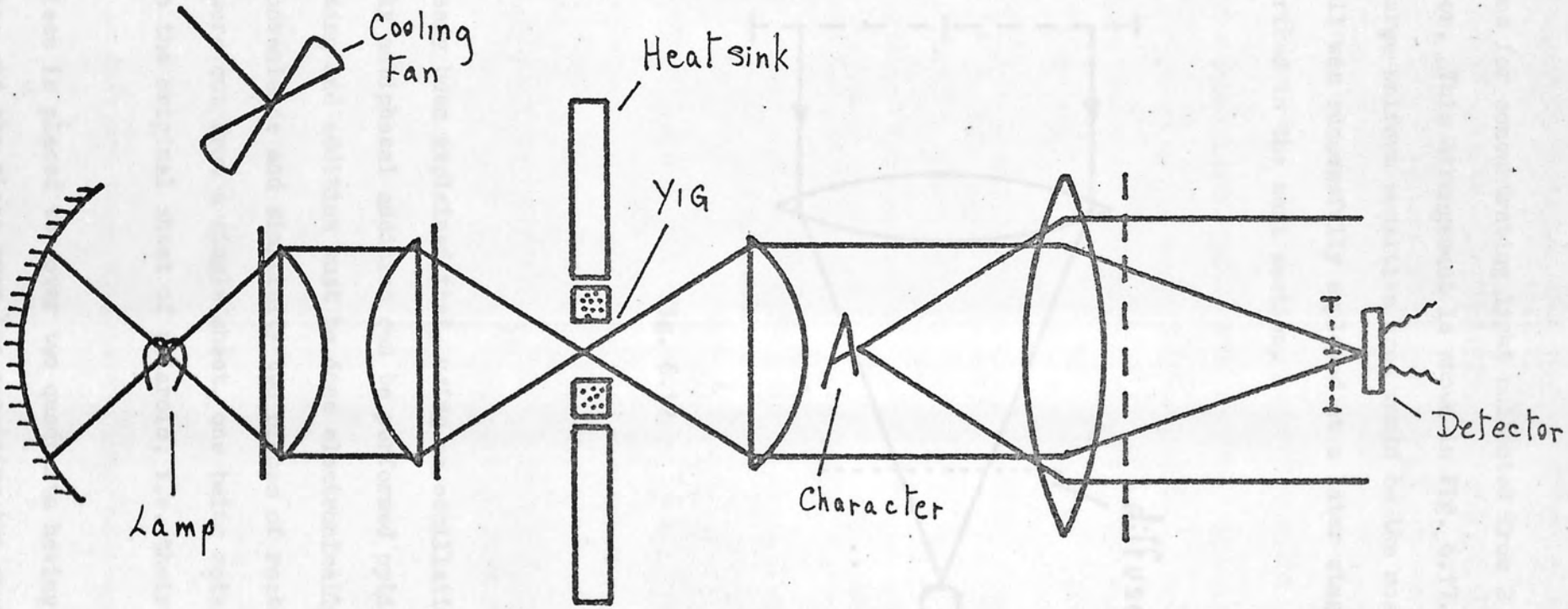

Fig. 6·16 Optics Used With Y.I.G. Modulator

a field lens for concentrating light collected from 2 quadrants, onto the detector. This arrangement is shown in Fig. 6.17. A detector having a large uniform sensitive area would be the most suitable. This type of cell was successfully employed at a later stage with the triple grid, described in the next section.

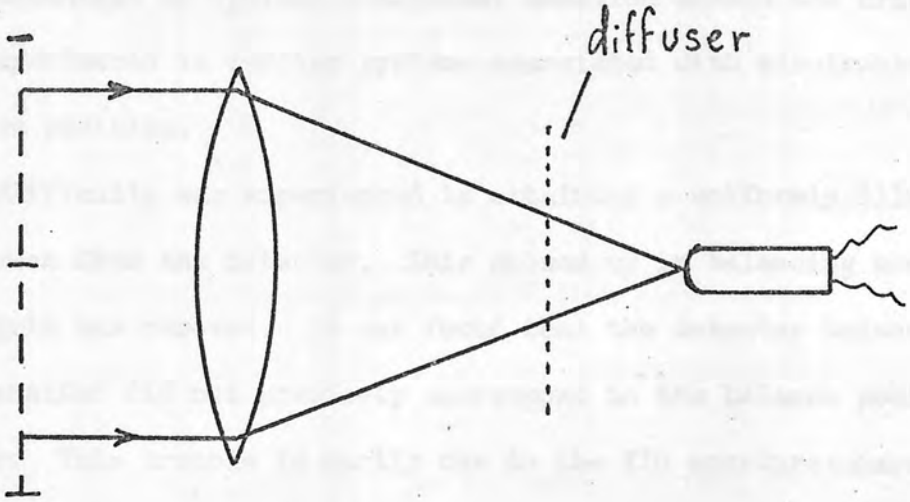

Fig. 6.17

It has already been explained that, using an oscillating polarisation vector, only antiphasal addition can be performed optically. The 90° phase shifting and addition must be done electronically.

For convenience and simplicity two pieces of rectangular shaped polaroids were cut from a single sheet, one being rotated through 90° relative to the original sheet of polaroid, i.e. their polarisation axes crossed.

One piece is placed to cover two quadrants having a 90° relative spatial phase and the piece over the remaining two quadrants also having 90° relative spatial phase. Light, however, is collected and mixed from pairs of quadrants having a 180° spatial phase relation, i.e. those pairs

having "crossed" polaroids. This arrangement is illustrated in Fig. 6.18 (a) and (b). Care must be taken to ensure that there is no leakage of light across the central vertical boundary. Part of the circuit showing one of the detectors designed for 90° phase addition of signals collected by the germanium photo-diodes is shown in Fig. 6.19.

6.10.2 Remarks and Conclusions

This technique of optical antiphasal addition solved the drift problems experienced in earlier systems associated with electronic means of antiphase addition.

Some difficulty was experienced in obtaining a uniformly illuminated character seen from the detector. This showed up in balancing when the shadowing grid was removed. It was found that the detector balance position for one character did not precisely correspond to the balance position for another. This trouble is partly due to the YIG aperture:character size ratio being low.

The problem was substantially overcome by adjusting the spacing between optical components and inserting a diffusing screen in a suitable plane behind the character.

II - Three Point Sampling: The Triple Grid

6.11 Theory

This concept is based on the minimum number of samples for collecting both phase and amplitude information of a sine wave which is accompanied by a d.c. background. It is described by Rogers[55(b)] in relation to optical sampling techniques.

Three samples are taken at $\frac{1}{3}$ period intervals shown in Fig. 6.20.

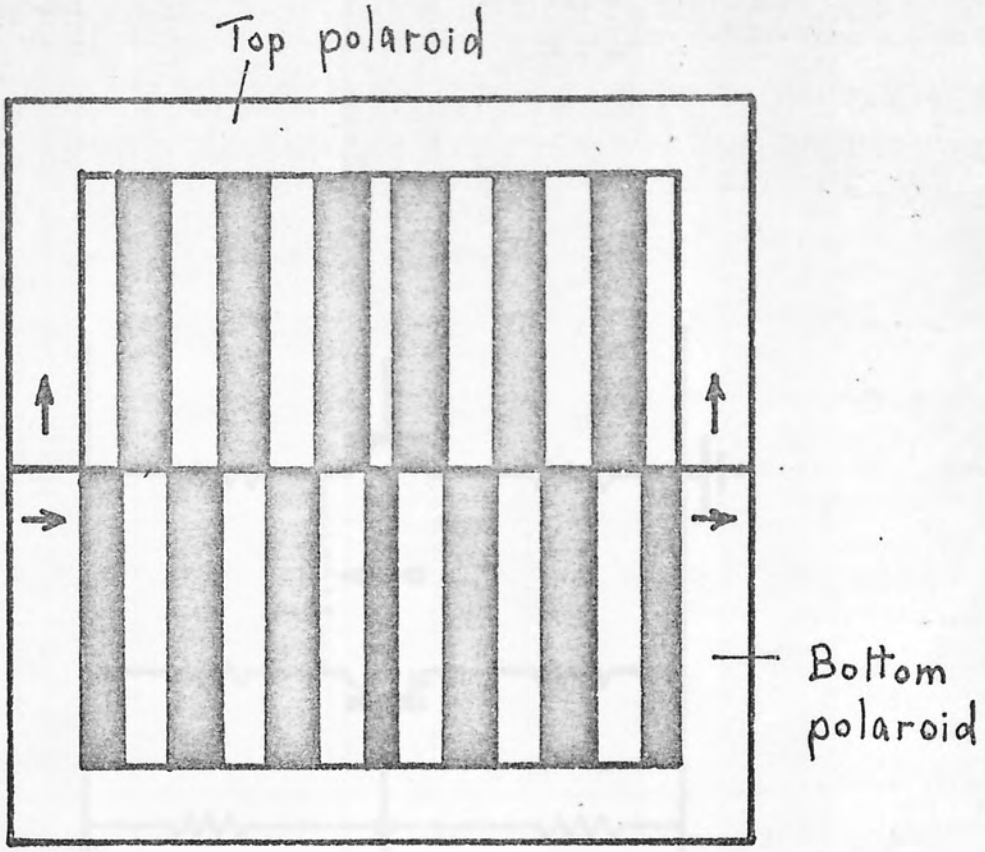

Fig. 6.18 (a)

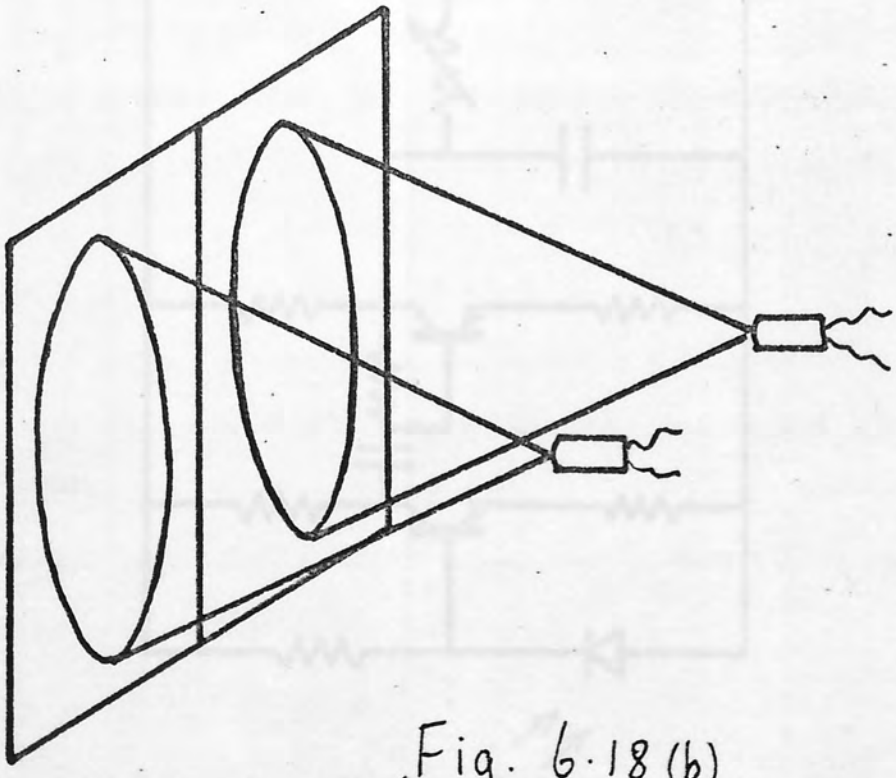

Fig. 6.18 (b)

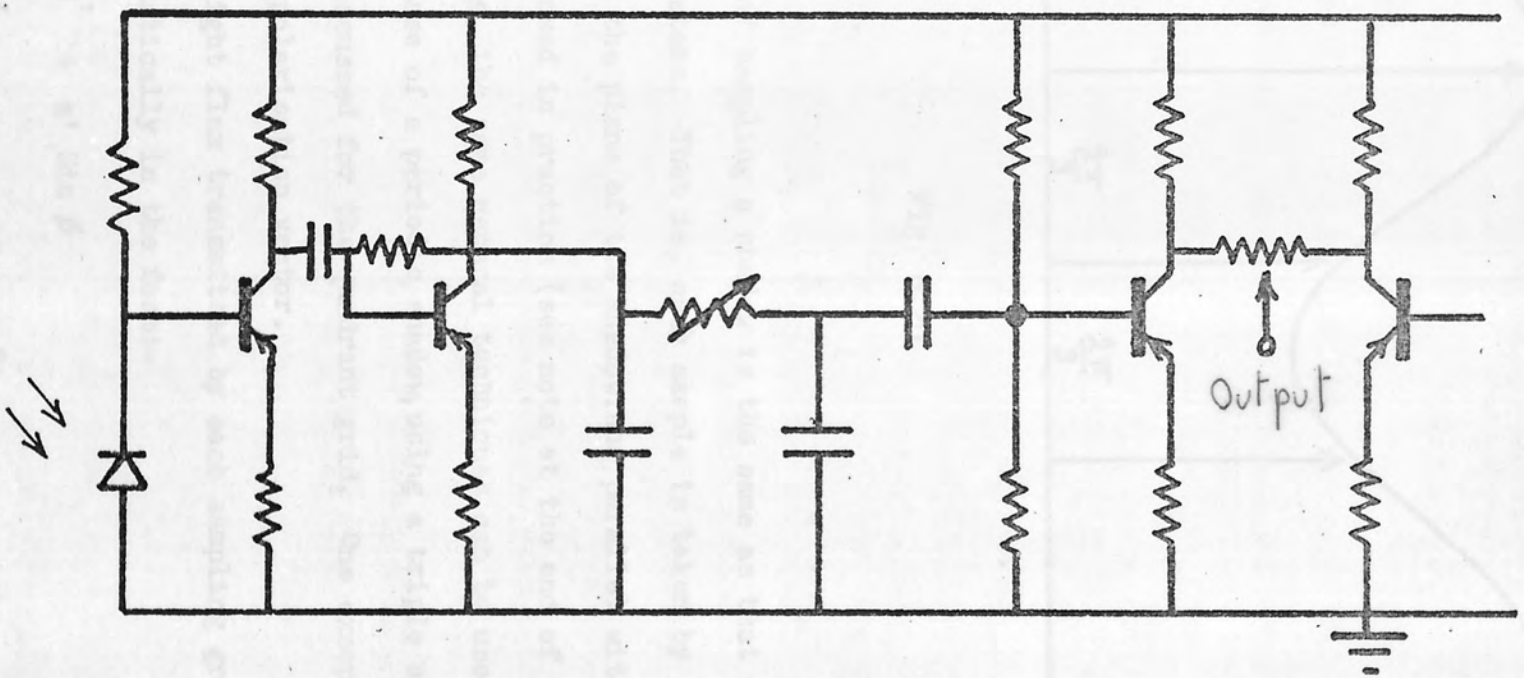

Fig. 6.19

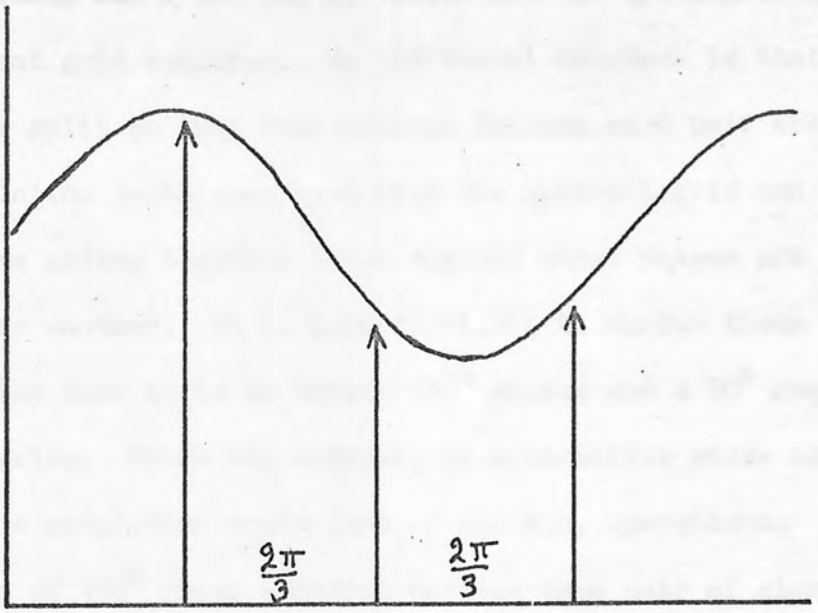

Fig. 6.20

The method of sampling a shadow is the same as that used in the four sampling systems. That is, each sample is taken by placing a sinewave grid in the plane of the shadow.and parallel with it. Square wave grids were used in practice (see note at the end of this chapter).

In principle, the same general techniques can be used in determining amplitude and phase of a periodic shadow, using a triple sampling grid, as those already discussed for the quadrant grid. One exception to this being the oscillating polarisation vector.

The total light flux transmitted by each sampling grid can be expressed mathematically in the form:-

$$P = H' + a' \sin \phi$$

$$Q = H' + a' \sin (\phi + 120^{\circ})$$

$$R = H' + a' \sin (\phi + 240^{\circ})$$

6.12 Operating Modes

The d.c. technique necessitates 3 subtractions plus one addition in determining Sin ϕ and Cos ϕ. These are two operations more than the quadrant grid requires. An additional drawback is that the signals have to be split so that subtractions between each pair are possible.

Modulation techniques used with the quadrant grid can be employed but involve adding together three signals whose phases are mutually at 120° to one another. It is more difficult to derive these phases electrically than it is to derive 180° phases and a 90° required for the quadrant grids. There is, however, an alternative phase adding sequence. This is the modulation equivalent of the d.c. operations. It involves three sets of 180° phase addition between each pair of signals and one inphase addition to derive Sin ϕ and Cos ϕ. A 90° phase shift is then required for the final 90° addition.

Using the rotating polarisation vector method, the triple grid scores in a number of ways over the quadrant grid. The concept is the same as in the quadrant grid case, where the quadrants have analysing polaroids to produce light modulation with phases corresponding to the spatial phases of the respective grids. Again, with the triple sampling grids, an analysing polaroid is placed over each grid and orientated such as to modulate the light transmitted, with phase corresponding to the spatial phase of the grid. The total light flux transmitted by all three grids is mixed optically and collected onto a single detector.

The modulation equations are:-

$$A = \lceil H' + a' \text{Sin } \phi \rfloor \quad \lceil 1 + \text{Sin } wt \rfloor$$

$$B = \lceil H' + a' \text{Sin } (\phi + 120) \rfloor \quad \lceil 1 + \text{Sin } (wt + 120) \rfloor$$

$$C = \lceil H' + a' \text{Sin } (\phi + 240) \rfloor \quad \lceil 1 + \text{Sin } (wt + 240) \rfloor$$

This produces a resultant modulation term:-

$$(A + B + C)_{mod} = \frac{3a'}{2} \text{ Cos } (wt - \emptyset)$$

which contains both phase and amplitude information, about the spatial shadow.

A rotating polarisation vector must be used to produce the modulation at the triple grid. The system is described together with other phase sensitive systems in incoherent optical processing by Rogers[86(b)].

The design of the triple grid used experimentally is shown in Fig. 6.21.

6.13 Balancing

The triple grid is topologically well suited to balance the light transmitted by the three grids before being mixed for detection by a single photo cell. This is illustrated by considering the light being collected via a circular aperture, placed over the 3 grids - shown in Fig. 6.22. As long as the aperture has 2 degrees of freedom in the plane of the grids, it is possible to collect an equal amount of light from each segment. This is not possible with a quadrant grid.

6.14 Experimental Details

The triple grid method was developed initially using a rotating polarisation vector produced by rotating a circular polaroid sheet mounted on the shaft of a small gramaphone motor.

The character was illuminated from behind using a quartz iodine lamp with a suitable condensing system and heat filters. A diffusing screen was placed behind the character. Light from the character was collimated by a 7" f/2.5 collimating lens.

The collimator is not essential but eliminates problems associated with projected magnification of the shadows and was therefore convenient to use during an experimental stage. The rotating polaroid was placed between the character and the collimator. The basic components are shown in Fig. 6.23.

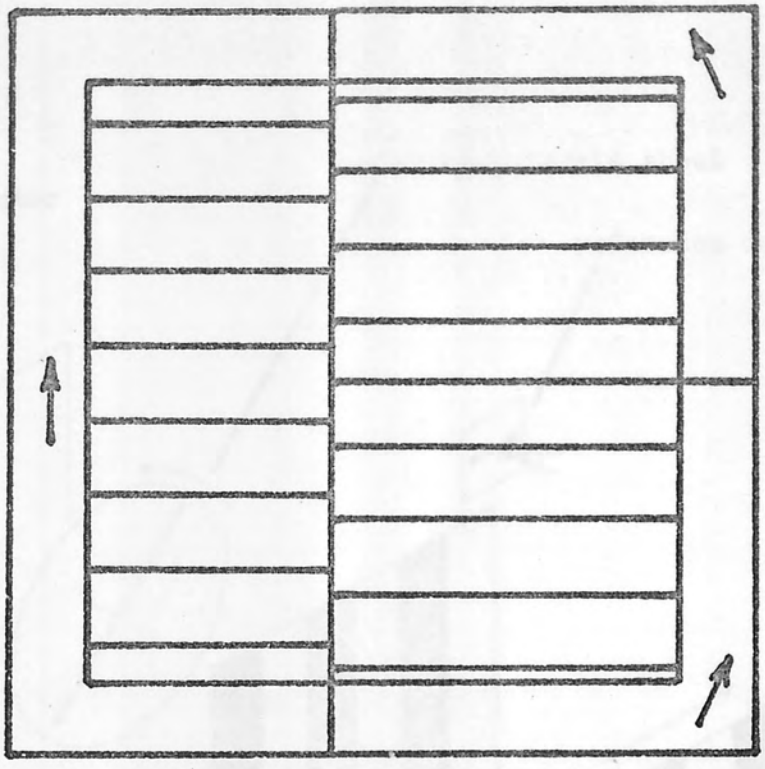

Fig. 6·21

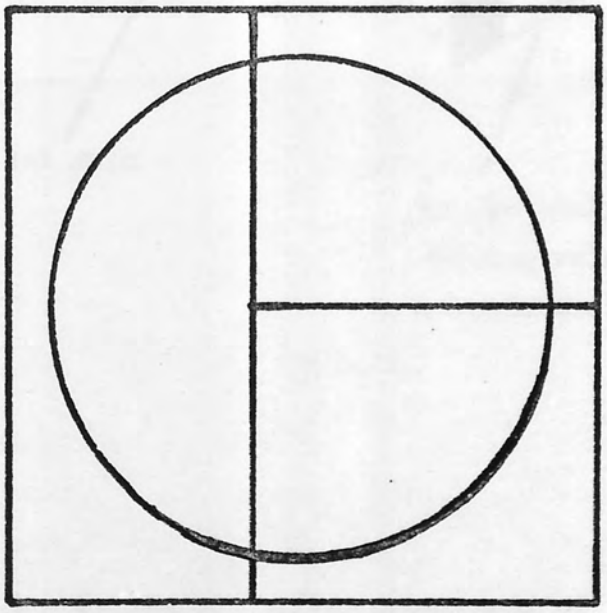

Fig. 6·22

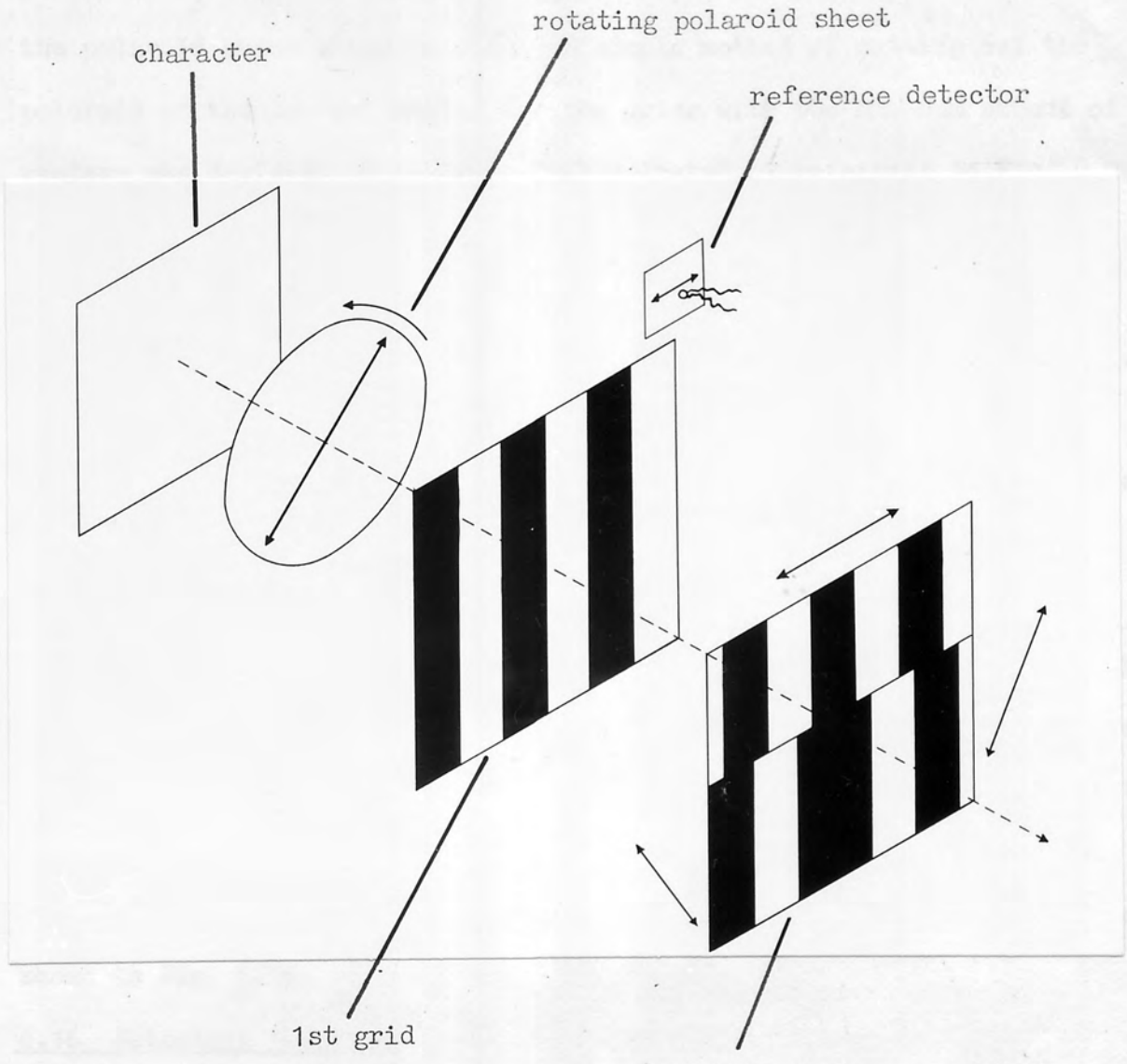

Fig. 6.23 Essential optical components of the triple grid system

6.15 Cutting Polaroid for Triple Grids

The polaroids must be cut precisely so that they modulate in 3 phases at $\frac{2\pi}{3}$ to one another. This involves 60° physical rotations of the polaroid sheet after cutting. A simple method of cutting out the polaroid at the correct angles for the grids with the minimum amount of wastage was devised. This is best illustrated by reference to Fig. 6.24 (a) and (b).

A rectangular strip of polaroid is selected which will contain the number of units required. The polaroid is then cut along the lines shown in Fig. 6.24 (a) thus forming 60° equilateral triangles. The triangles are then rotated through 60° in the directions indicated in Fig. 6.24 (a), that is, (alternate) ones in the same direction and the remainder in the opposite direction.

Each of these triangles are then cut across from base to apex as shown in Fig. 6.24 (b). Finally, the right angle triangles are moved into the positions shown, producing the unit triple polaroid cells. The cell fits over the triple grid as shown in Fig. 6.25. If only a single cell is required with minimal waste, then the polaroid is cut in the proportions shown in Fig. 6.26.

6.16 Detecting the Light

Two different light collecting systems emerged:-

(i) Using field lens;

(ii) Without field lens.

6.16.1 Field Lens

The first light collecting system devised comprised of a short focus field lens which concentrated the light onto a small photo-diode. This was mounted in a short tube and supported by a holder having vertical and horizontal traverse facilities for balancing.

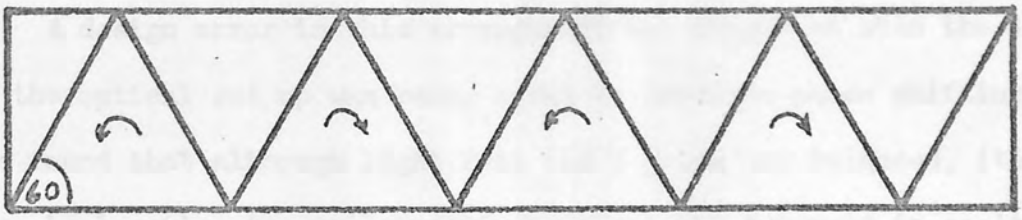

Fig. 6·24 (a)

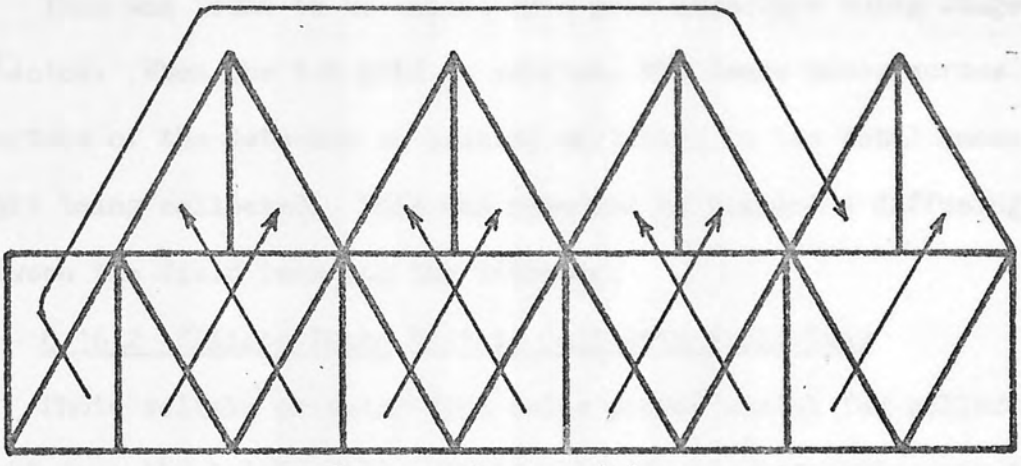

Fig. 6·24 (b)

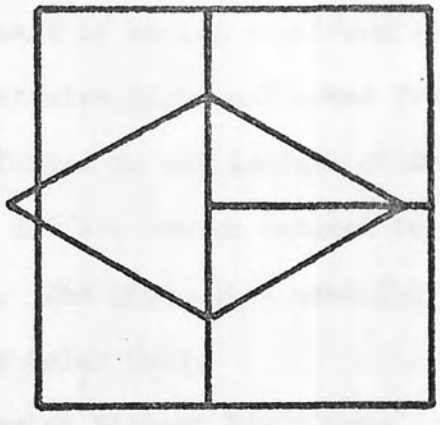

Fig. 6·25

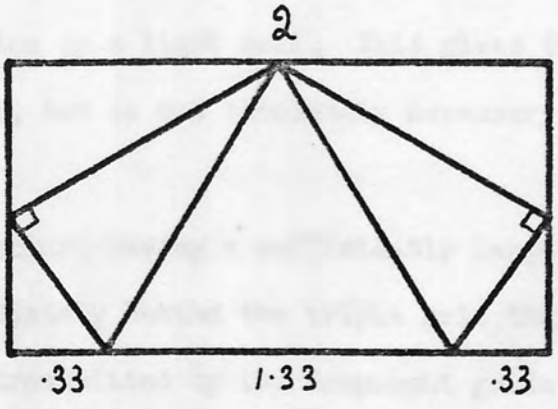

Fig. 6·26

A design error in this arrangement was diagnosed when the 1st grid in the optical set up was being moved to simulate phase shifting. It was found that although light from the 3 grids was balanced, (this is done by locating the null position without the 1st grid in position) amplitude variations occurred during shiftings of the 1st grid.

This was found to be caused by a grid structure being imaged on the detector. When the 1st grid is shifted, the image moves across the small aperture of the detector so causing variation in the total amount of light being collected. This was remedied by placing a diffusing screen between the field lens and the detector.

6.16.2 Silicon Photo Voltaic Cell with Field Lens

Photo voltaic or solar type cells proved useful for collection of light from the triple grid. Their main advantage in this work is their comparatively large uniform sensitive surface which can be chosen to be anything up to 3 cm. in diameter.

The advantage of having a uniform sensitive area is self evident. The lens concentrates light collected from the 3 grids. If the image of the character formed on the surface of the detector is within the sensitive area, then the diffuse screen between the lens and detector can be dispensed with. The photo-cell used for this was a Photain Control SPD 102 Silicon Solar Cell.

6.16.3 System Without Field Lens

The triple grid philosophy implies perfect mixing of light transmitted by each grid before detection by a light cell. This gives the condition for maximum drift stability, but is not absolutely necessary for phasal addition.

This means that a detector, having a sufficiently large sensitive area, may be situated immediately behind the triple grid thus dispensing with a field lens. Light transmitted by the component grids falls onto different regions of the sensitive surface.

A detector used for this was a Photain Control SPD111 or SPD110 Silicon Solar Cell, the former being encapsulated. The encapsulated version was found ideal, having a circular uniform sensitive area, 2 cm. in diameter. The unencapsulated version tended to pick up stray light especially from its reverse surface.

6.17 Electronics

The triple grid system converts both the spatial modulation and d.c. light terms contained in the shadow into equivalent temporal electrical signals in the detector. In essence, the only electronics required are phase and amplitude detectors described in chapter 3. At this stage, however, possible approaches to the problem of normalisation were being investigated. One such approach uses the d.c. term generated as an electrical d.c. signal in the detector as the zero order term for normalisation. The associated circuitry together with other experimental normaliser circuits are dealt with in full in the following chapter.

This system was also used in testing the rotating half-wave-plate for increasing the angular velocity of the rotating polarisation vector. A two stage half-wave-plate modulator was tested successfully. A single stage was used in the main for convenience.

6.18 The Pseudo-Rotating Polarisation Vector

This was proposed by Dr. Rogers to substitute the rotating polarisation vector particularly in high speed applications, and is filed under a provisional patent application No. 37145/70. It produces an identical effect at the triple grid but with a decreased modulation depth.

Illumination is derived from 3 lamps modulated in 3 phase with respect to one another. Light eminating from the lamps is polarised using separate polaroids so that the 3 polarisation vectors are at 120° to one another. The three beams are then combined either by directing the beams towards the object or a point on a diffusing screen placed

immediately behind the character; or using a holographic recombiner. Care must be taken not to depolarise the beams before being analysed at the triple grid.

In order to simulate the effect of a rotating polarisation vector, the three analysing polaroids at the triple grid must be orientated at the same angles as the polaroids at the light sources, though the order is not important.

6.18.1 Experimental Detail

Some experimentation was performed to verify the feasibility of the scheme, using a 3 phase 50 cycle mains supply.

Three small bayonet sockets were mounted on a dished wooden board so that they were directed towards a point approximately 12" in front of the board. The board is supported vertically so that the "average" beam is projected horizontally. This arrangement is shown in Fig. 6.27.

Two types of lamps were used: 15w Tungsten filament and Neon bulbs. The tungsten lamps ran directly off the three phase supply corrected in star. Visible and infrared polaroid was used. Infrared polaroid was marginally better but signals for both were obscured by the high d.c. component.

Bayonet neon bulbs were substituted to increase the modulation depth. These required a d.c. bias of 240 volts so as to produce sinusoidal modulation at the central electrode when the a.c. mains is applied. The circuit designed for this is shown in Fig. 6.28.

Visible polaroid was used in this case. A diffuse screen was placed in the mixing plane. No object was used. A grid that was located just in front of the triple grid simulated a shadow. So long as the detector receives light from all three grids, balancing can be done using P_1, P_2 and P_3. This eliminates the necessity for a moveable detector.

Fig. 6.27

Three lamps for generating a pseudo-rotating polarisation vector

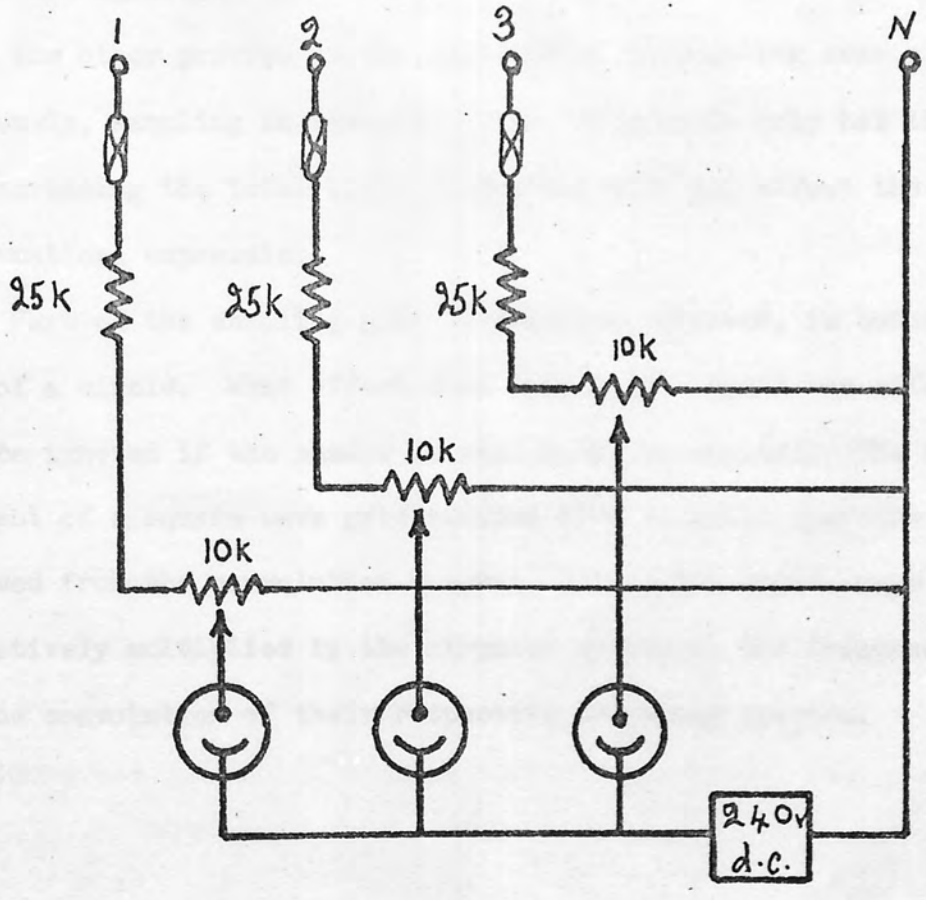

Fig. 6.28 Three phase mains circuit for driving three neon bulbs

6.19 Note on Sampling Grids

In deriving a mathematical expression for the total light flux transmitted by a sampling grid, the sampling grid is assumed to have a sinusoidal profile and the integration is performed over a period.

In practice a high contrast square-wave grating is used. This type of grid is much simpler to manufacture than a sinewave grid. It does, however, contain odd harmonics, the third being the most significant. A square-wave grid may be used legitimately to sample a shadow providing that the shadow is sinusoidal. This is a consequence of a sinewave resulting from the convolution of a square-wave with a sinewave.

The shadows sampled, however, are not strictly sinusoidal since they are produced using a square-wave primary grid. Sampling via square-wave grids constitutes a further convolution which suppresses the effect of odd harmonics. Possible error due to effects of third harmonic was therefore ignored.

The other proviso of the mathematics is sampling over a single period. Obviously, sampling an integral number of periods only has the effect of increasing the total light output and does not effect the form of the mathematical expression.

Part of the sampling grid in practice, however, is bounded by the arc of a circle. What effect does this have? Again the effects of this can be ignored if the shadow is reasonably sinusoidal. The frequency content of a square-wave grid stopped by a circular aperture is easily derived from the convolution theorem. Since the square-wave grid is effectively multiplied by the circular aperture, the frequency content is the convolution of their respective frequency spectra.

CHAPTER 7

NORMALISATION

7.1 Introduction

Normalisation was outlined in chapter 1 in relation to preprocessing video signals.

In designing a character reading machine it is standard practice to incorporate some means of normalising electrical signals derived from the character. Normalisation is an operation or series of operations performed on the electrical signals representing the character, in order to bring them into a standard form. Ideally standardisation means that the signals after normalisation are independent of factors such as: illumination level; print/paper contrast; size of characters; stroke width; broken characters and other shape deformations. Perfect standardisation is never achieved in practice, only attempts at approximations are possible.

Machines that collect primary data by some form of spot scanning often use a pre-scan for the purpose of normalisation. This is useful because all a priori knowledge necessary for normalisation may be determined on analysis of the pre-scan. The most important form of standardisation of signals is that which renders them independent of illumination level and print/paper contrast. The pre-scan can be used to assess these factors. Threshold levels of comparators or weights in decision networks are then set accordingly in preparation for the scan which collects the primary information proper in order that a more accurate final decision is made. A normalising technique aimed at improving the quality of printed characters is described in "Character Recognition" 1967[87].

7.2 Area Normalisation

This form of normalisation is flexible and most commonly used in machines which perform an inverse transform on primary data. Signals are made invarient to character area by dividing signals, detected by each photo-cell, by another signal which is proportional to the character area. The division may be performed analoguely or digitally but analogue methods are normally adopted.

Area of characters is influenced by their shape, size, stroke thickness. Area normalisation therefore implicitly compensates for variations in these factors.

7.3 Normalised Fourier Transform

Normalisation of a Fourier Transform involves operating on amplitude only leaving phase information unchanged. It is performed by dividing amplitude values of all points in the frequency spectrum by the zero order term. This is expressed mathematically:-

$$\frac{\left| F(U,V) \right|}{\int_{-\infty}^{+\infty} \int_{-\infty}^{+\infty} f(x,y)\, dx\, dy}$$

where F(U,V) is the Fourier transform of the function f(x,y).

If the frequency spectrum is sampled discretely, then normalisation is effected by dividing amplitude values obtained from each sampling point by the zero order term.

The zero order term of high contrast characters becomes a measure of the area of characters. In particular, if characters are in the form of transparencies, the zero order term is proportional to the total amount of light transmitted (or more accurately, the sum of all light intensities transmitted by each point on the character). A fraction of

this can be detected and used to normalise Fourier coefficients. In this case, values of coefficients will also be invarient to fluctuations in the intensity of illumination.

7.4 Approaches to Electronic Normalisation of Fourier Coefficients

7.4.1 Electronic Realisation of Division

Division is a non-linear process and as such, normally requires the use of non-linear elements in order that it may be performed electronically. An example is taking the logarithm of the input analogue signals using logarithmic amplifiers prior to their subtraction, (which is a linear process). Logarithmic amplifier design is treated by Gilmour[88]. Analogue antilogging can be avoided by digitising the signals after subtracting logs. Division can be performed digitally by a sequence of successive subtractions.

7.4.2 Experimental Approaches to Normalisation

Taking the logarithm of analogue voltages with a good degree of accuracy over a modest range of input voltages is fairly difficult to achieve electronically. This approach to division was not investigated experimentally. Log. circuits were used in another mode. Experimental normalisation circuits described in this chapter can be classified into two categories:-

1. Those based on generating the reciprocal value of the normalising signal which is multiplied by the amplitude voltage of a Fourier coefficient.
2. Compensating systems.

A complete d.c. analogue divider circuit has been designed by Newell[89] consisting of a reciprocal circuit and a multiplier.

7.5 The Multiplier Circuit and its Modes of Operation

The basic circuit for an analogue multiplier shown in Fig. 7.1 consists of a long tailed pair or differential pair, the emitter current of which is supplied by a simple amplifier. The linearity of the

multiplier is determined by the linearity of the individual amplifiers.

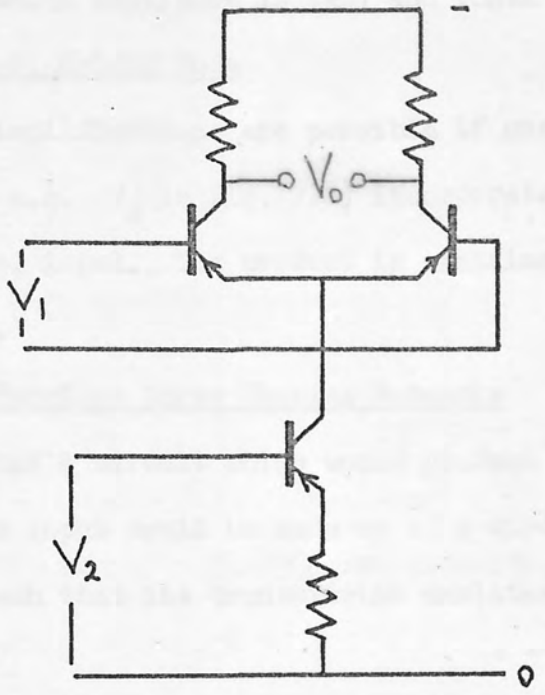

Fig. 7.1

7.5.1 A.C. Mode

Alternating voltages may be multiplied but attention must be given to the d.c. terms. Two sinusoidally varying signals at the same frequency whose amplitudes are to be multiplied may be applied to the two inputs of the multiplier. The d.c. offset at V_1 can virtually be eliminated but the input at V_2 will include a constant d.c. voltage.

The signal input V_1 will typically be in the form:-

$$a \text{ Sin } (wt + \phi)$$

while the normalising input V_2 or divisor will be b Sin wt, but accompanied by a d.c. term say, d. The product at the output is thus;

$$a \text{ Sin } (wt + \phi) \left[d + b \text{ Sin } wt \right]$$

$$ad \text{ Sin } (wt + \phi) + ab \text{ Sin } (wt + \phi) \text{ Sin } wt$$

The first term is not required and can be suppressed. The second term contains a phase and amplitude dependent d.c. term and a frequency doubled a.c. term whose amplitude is (ab) and whose phase is Ø.

7.5.2 D.C./A.C. Hybrid Mode

A number of simplifications are possible if one input is d.c. while the other is a.c. V_2 (in Fig. 7.1) incorporates the a.c. input while V_1 is the d.c. input. The product is contained in the amplitude of the a.c. output.

7.6 Transmission Function Curve Shaping Networks

It was felt that a circuit which would produce the reciprocal or log. function of its input could be made up of a diode network whose configuration is such that its transmission emulates a reciprocal or log. function.

Transmission curves may be fabricated using an assembly of Zener diodes each with a resistor whose values dictate the overall shape of the curve. There are two basic circuit configurations shown in Figs. 7.2 (a) and 7.3 (a) giving rise to the transmission functions in Figs. 7.2 (b) and 7.3 (b). These circuits are taken from the Mullard-voltage regulator diodes publication[76]. They rely on the Zener suddenly conducting at a specified reverse bias voltage. The major drawback is the high input voltages required to actuate the Zeners.

7.6.1 Curve Shaping Using the Forward Bias Characteristic of Ge and Si Diodes

The forward V/I characteristics of silicon and germanium diodes are interesting from a curve shaping view point. Their approximate shapes are illustrated in Fig. 7.4 (a) and (b). Germanium diodes exhibit a smoothly changing curve somewhat resembling a square law curve. Silicon diodes display a fairly pronounced "knee" beyond which the diode is highly conductive.

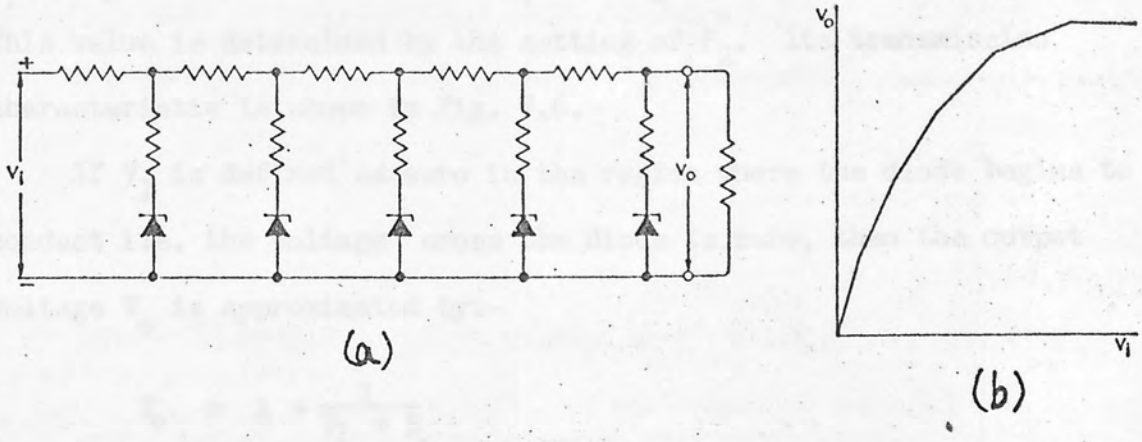

Fig. 4.2 Curve Shaping Network

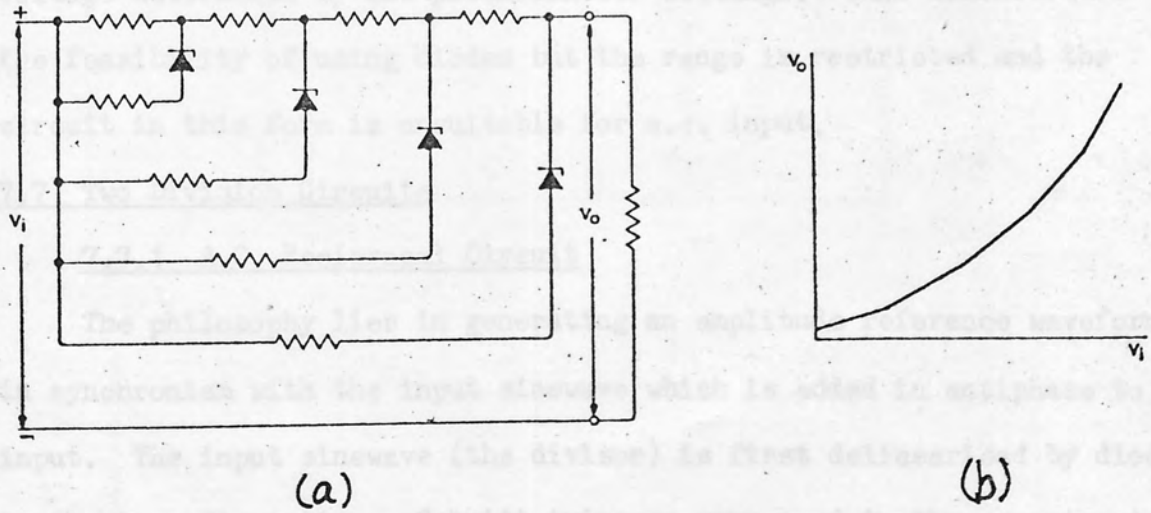

Fig. 4.3 Curve Shaping Network

(After Mullard)

A simple experimental circuit was constructed to test the possibility of using a single Ge diode for producing a reciprocal output of the input. The basic circuit diagram is shown in Fig. 7.5. The circuit effectively de-linearisers the linear inversion characteristic of a transister output. The diode will not start to conduct (and hence de-linearise) until V_I is sufficiently negative. This value is determined by the setting of P_2. Its transmission characteristic is shown in Fig. 7.6.

If V_I is defined as zero in the region where the diode begins to conduct i.e. the voltage cross the diode is zero, then the output voltage V_o is approximated by:-

$$V_o = A + \frac{1}{V_I + B}$$

'A' can effectively be zeroed over a limited range of V_I referring V_o to the appropriate voltage with P_3. Beyond this range the curve will intercept the V_I axis at some arbitrary point. 'B' is an arbitrary voltage determined by the potentiometer settings. This demonstrates the feasibility of using diodes but the range is restricted and the circuit in this form is unsuitable for a.c. input.

7.7 Two Division Circuits

7.7.1 A.C. Reciprocal Circuit

The philosophy lies in generating an amplitude reference waveform in synchronism with the input sinewave which is added in antiphase to input. The input sinewave (the divisor) is first delinearised by diodes in shunt configuration. Schmitt triggers were used in the experimental circuit for the purpose of generating a constant amplitude reference wave. Harmonics in the square wave together with those generated by delinearisation were suppressed prior to multiplication.

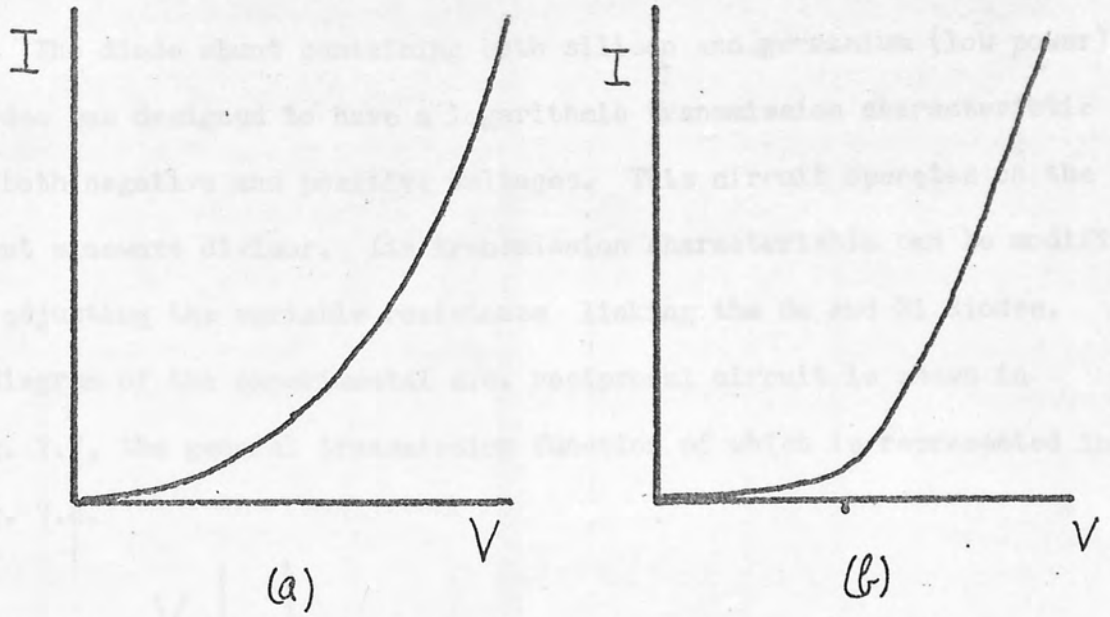

Fig. 7.4 Forward bias characteristics of (a) Germanium and (b) Silicon diodes.

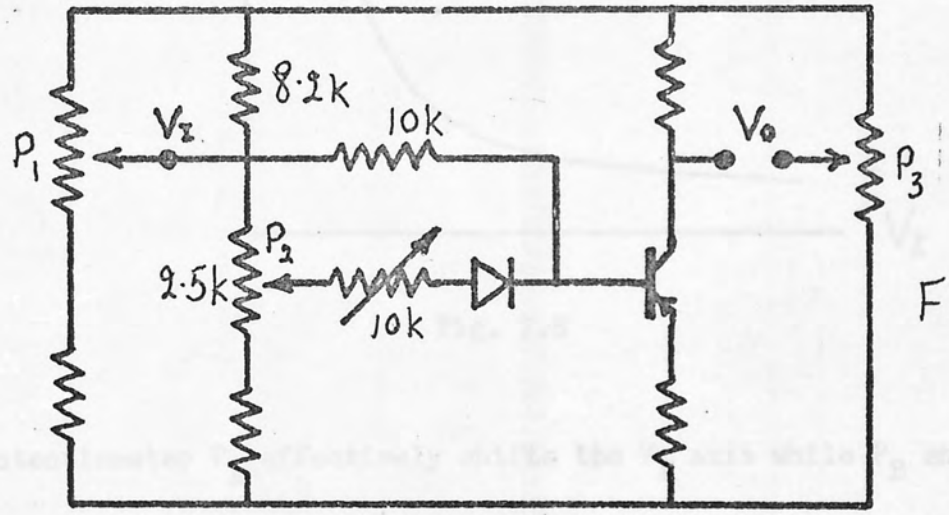

Fig. 7.5

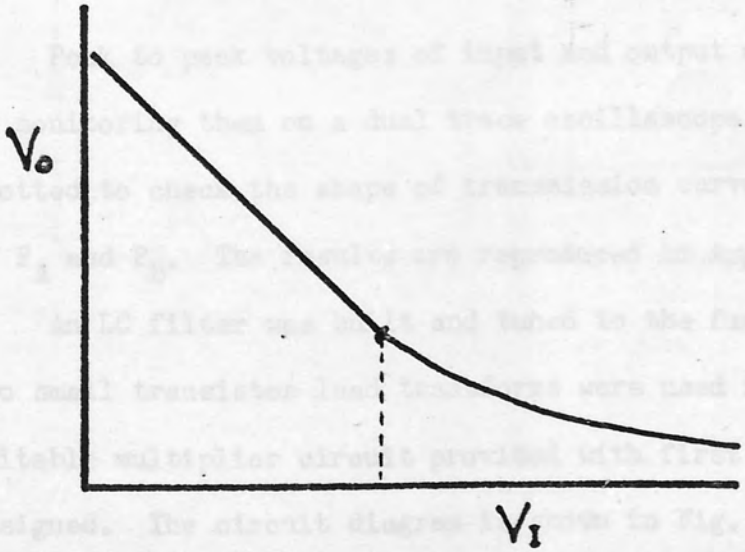

Fig. 7.6

The diode shunt containing both silicon and germanium (low power) diodes was designed to have a logarithmic transmission characteristic on both negative and positive voltages. This circuit operates on the input sinewave divisor. Its transmission characteristic can be modified by adjusting the variable resistance linking the Ge and Si diodes. A diagram of the experimental a.c. reciprocal circuit is shown in Fig. 7.7, the general transmission function of which is represented in Fig. 7.8.

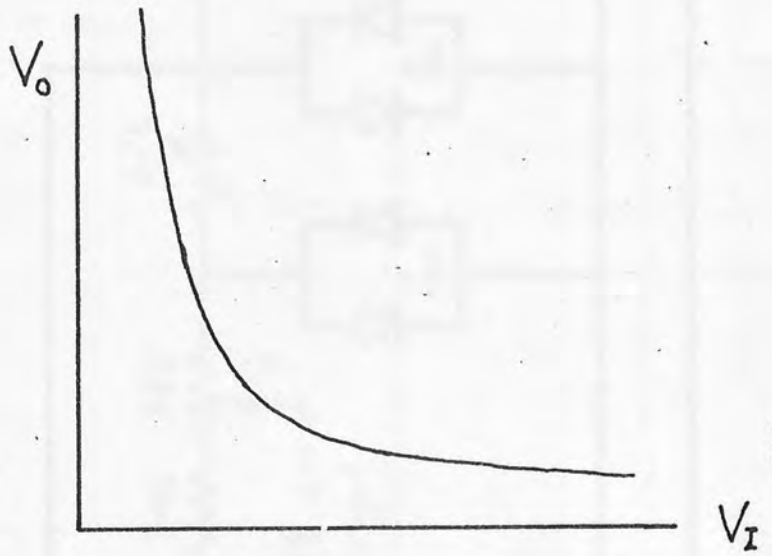

Fig. 7.8

Potentiometer P_A effectively shifts the V_I axis while P_B shifts the V_o axis. This makes for flexibility thus enabling the curve to fit $\frac{1}{V_I}$ reasonably well over a modest range of V_I.

Peak to peak voltages of input and output waveforms were measured by monitoring them on a dual trace oscillascope. V_I/V_o curves were plotted to check the shape of transmission curves for different settings of P_A and P_B. The results are reproduced in Appendix III.

An LC filter was built and tuned to the fundamental at 800 Hz. Two small transistor load transforms were used for the inductances. A suitable multiplier circuit provided with first harmonic suppression was designed. The circuit diagram is shown in Fig. 7.9.

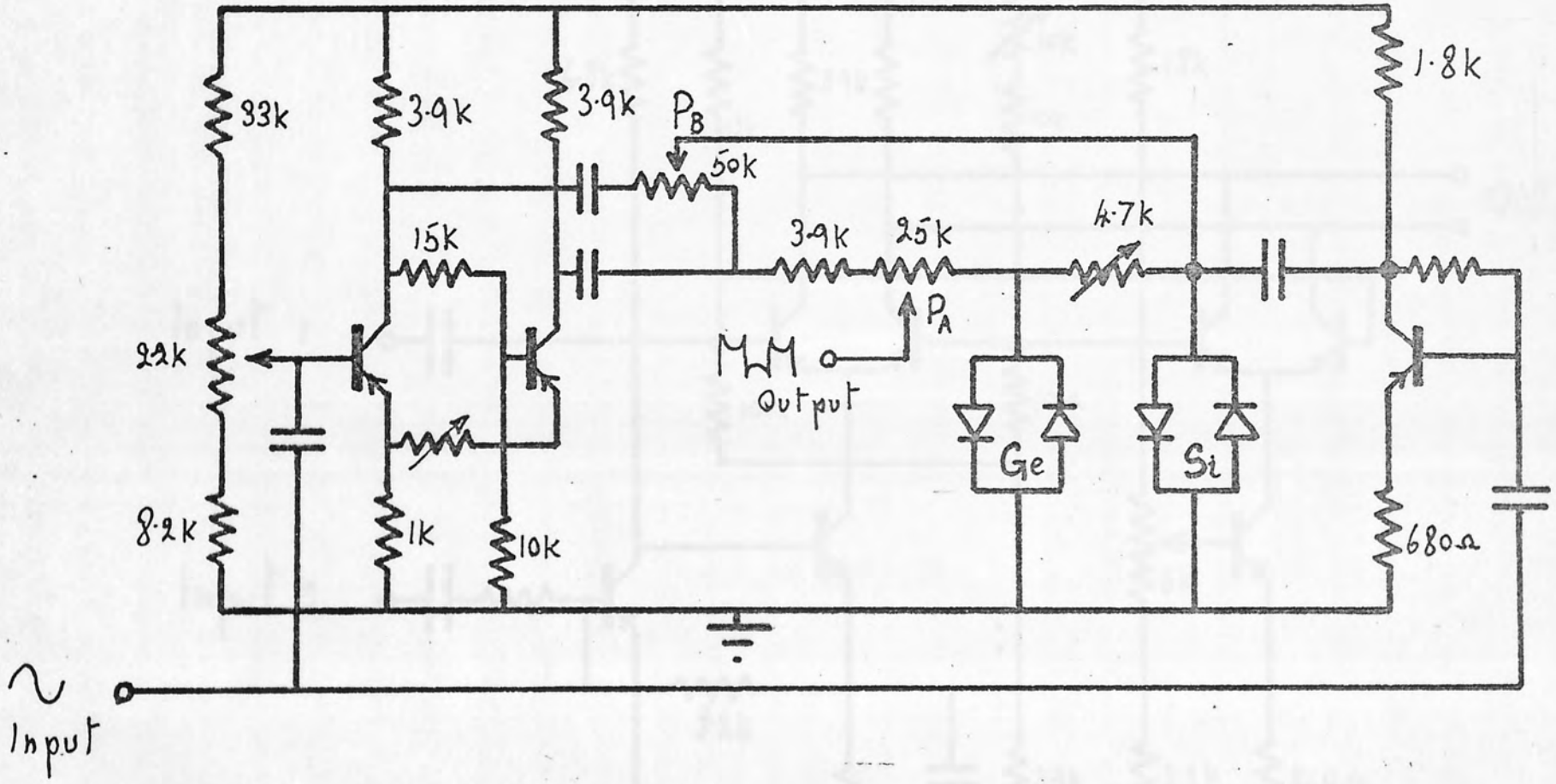

Fig. 7.7 A.C. Reciprical Circuit

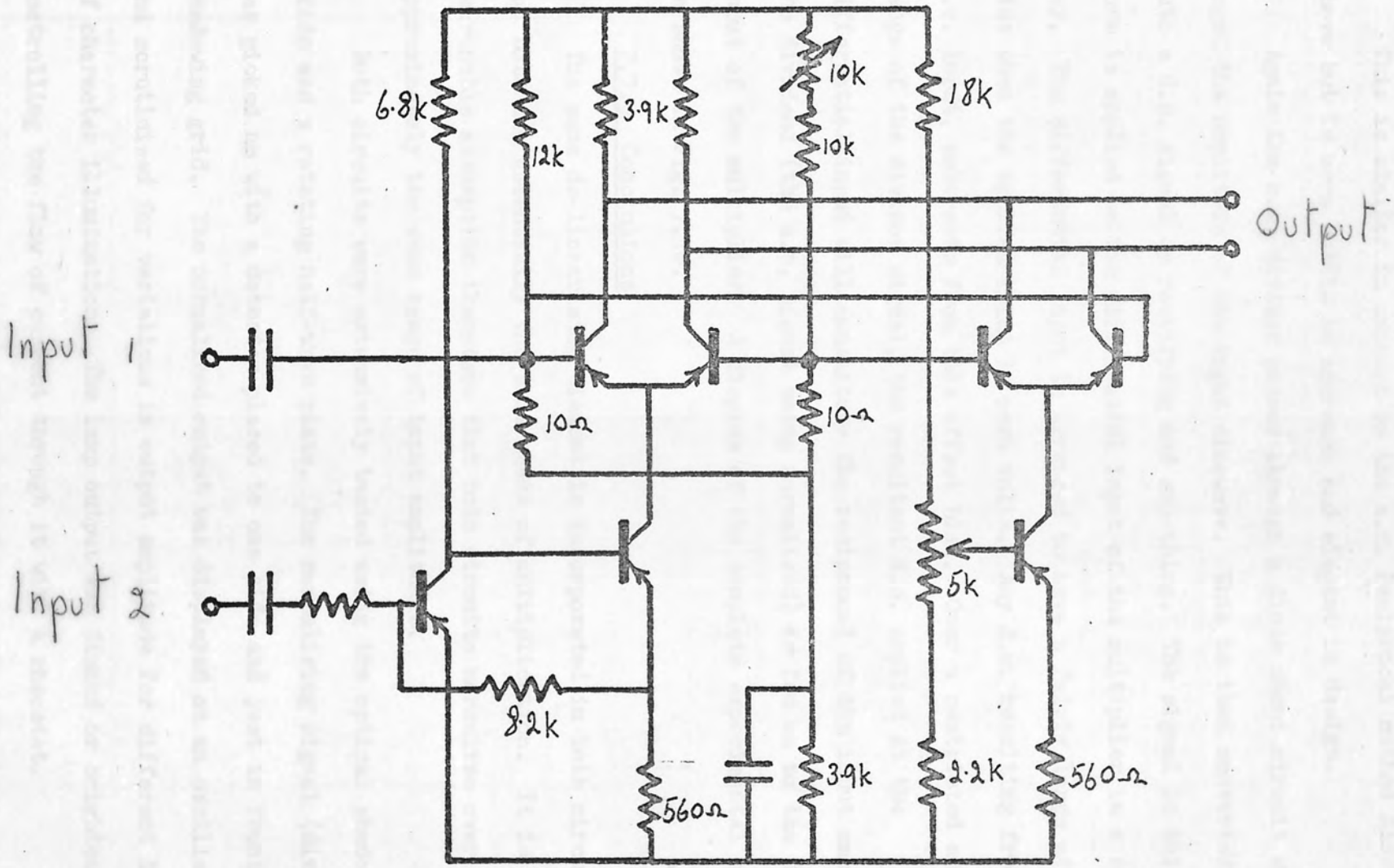

Fig. 7.9 Multiplier Circuit with First Harmonic Suppression

7.7.2 Hybrid Multiplier for Dividing A.C. Signals

This is similar in concept to the a.c. reciprocal method described above but is more subtle in approach and elegant in design.

Again the a.c. divisor passes through a diode shunt circuit which logs. the amplitude of the input sinewave. This is then converted into a d.c. signal by rectifying and smoothing. The signal in this form is applied to the differential input of the multiplier in a special way. The differential input is arranged to have a fairly large offset bias when the applied input is zero volts. Any d.c. resulting from an a.c. input, subtracts from this offset bias. Over a restricted amplitude range of the divisor signal, the resultant d.c. applied at the differential input will constitute the reciprocal of the input amplitude. The dividend (the a.c. signal being normalised) is fed on to the second input of the multiplier. A diagram of the complete experimental circuit is shown in Fig. 7.10.

7.7.3 Conclusions

The same de-linearising element is incorporated in both circuits and both use essentially the same means of multiplication. It is a reasonable assumption therefore that both circuits normalise over approximately the same range of input amplitudes.

Both circuits were extensively tested using the optical shadowing grids and a rotating half-wave plate. The normalising signal (divisor) was picked up with a detector placed to one side and just in front of the shadowing grid. The normalised output was displayed on an oscillascope and scrutinised for variations in output amplitude for different levels of character illumination. The lamp output was dimmed or brightened by controlling the flow of current through it with a rheostat.

The second circuit is superior in many respects. The first circuit has a number of inherent drawbacks, as a result of generating square waves with a Schmitt trigger. Firstly, the circuit may become unstable for

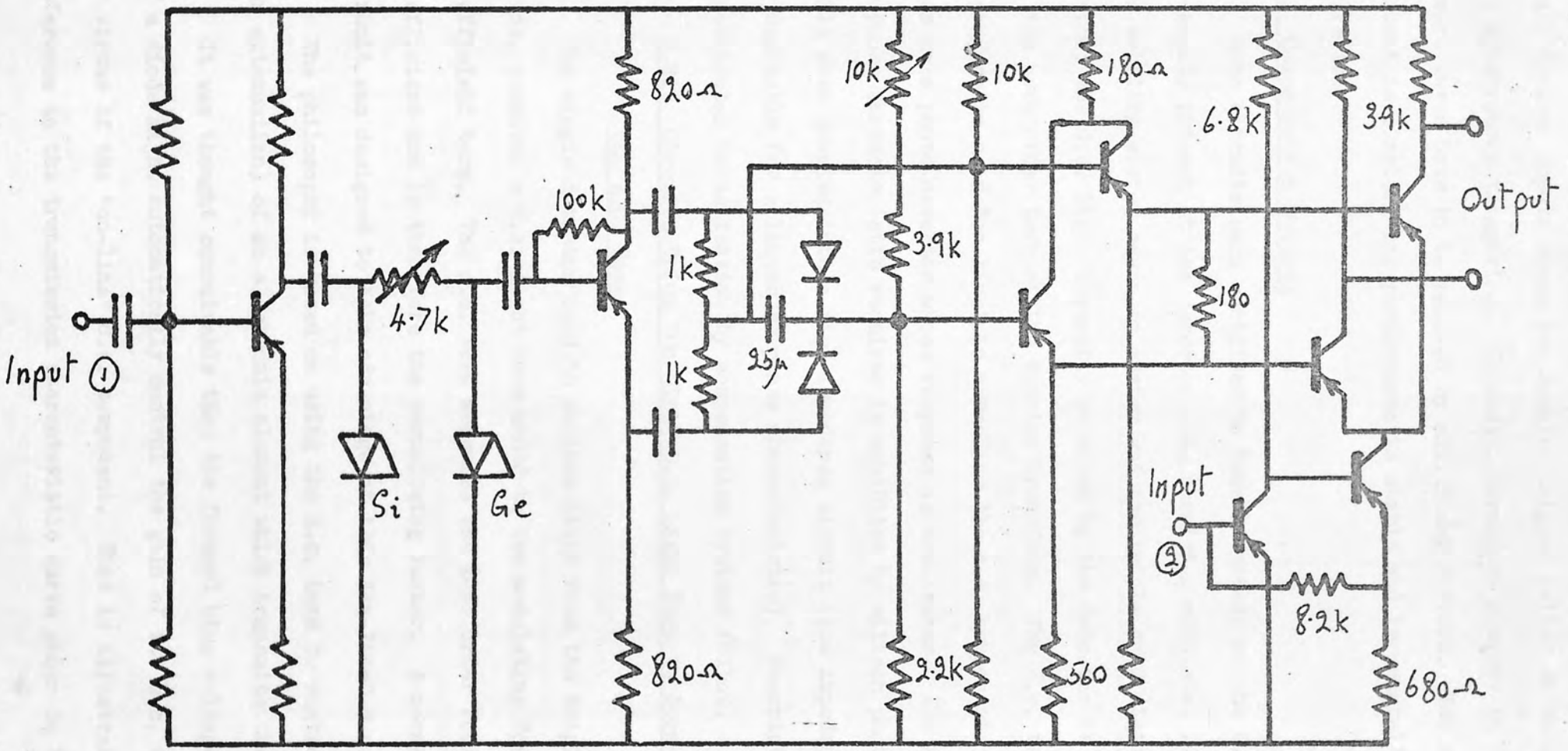

Fig. 7.10 Multiplier Circuit Modified For Division

small divisor inputs since the Schmitt trigger relies on this signal for synchronous triggering. Secondly, harmonics present in the square waves have to be removed by additional filters. The second circuit is simpler, its performance is stable and is generally more reliable.

7.8 Compensation Methods

Some circuits were contrived to take advantage of the d.c. light intensity present at the detector when receiving modulated light. In both the wobbling mirror scanning system and the triple grid static scanning system, the d.c. light intensity received by the detector is proportional to the zero order term of the Fourier transform. The d.c. term can therefore be used "on-line" to normalise the a.c. component. Its simplest form is a photo-detector whose response is non-linear. The sort of response characteristic required is exhibited by silicon photo-voltaic cells when coupled into a high impedance circuit (low impedance coupling is desirable for a linear response characteristic). Descriptions of two experimental normalisation by compensation systems follow.

7.8.1 Circuits Using "On-Line" D.C. Light Term to Normalise the A.C. Term

The single detector used to collect light from the triple analysing grids, receives a d.c. light term added to the modulating Fourier coefficient term. The d.c. term measures the zero order Fourier coefficient and is therefore the normalising factor. A normalising circuit was designed to take advantage of this "on-line" d.c. term.

The philosophy is based on using the d.c. term to control the gain (or attenuation) of an electronic element which transmits the a.c.

It was thought conceivable that the forward bias voltage characteristic of a diode might automatically control the gain of its a.c. transmission, by virtue of the "on-line" d.c. component. This is illustrated by reference to the transmission characteristic curve shown in Fig. 7.11.

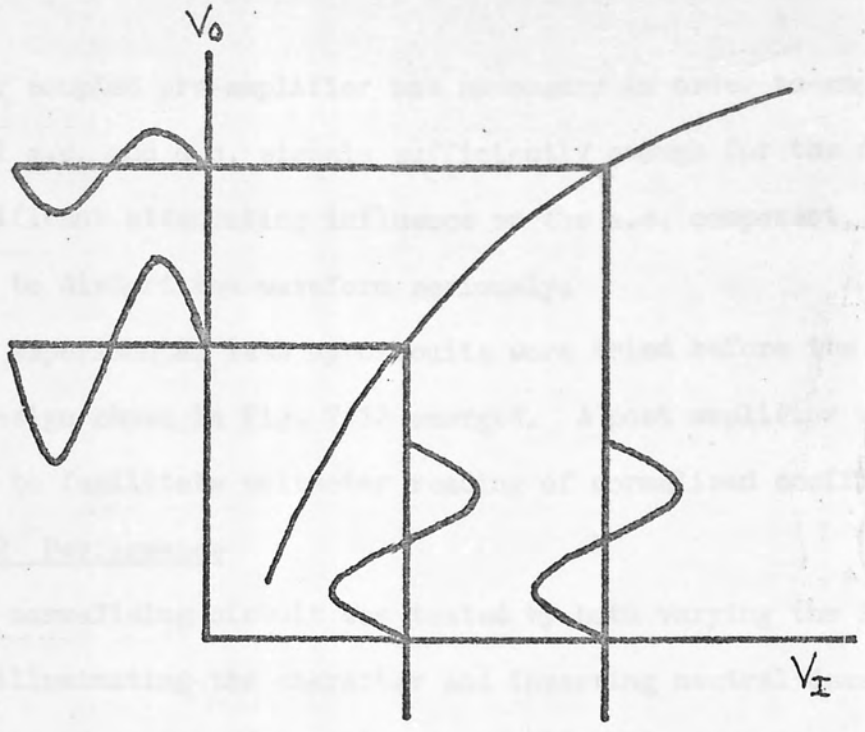

Fig 7.11

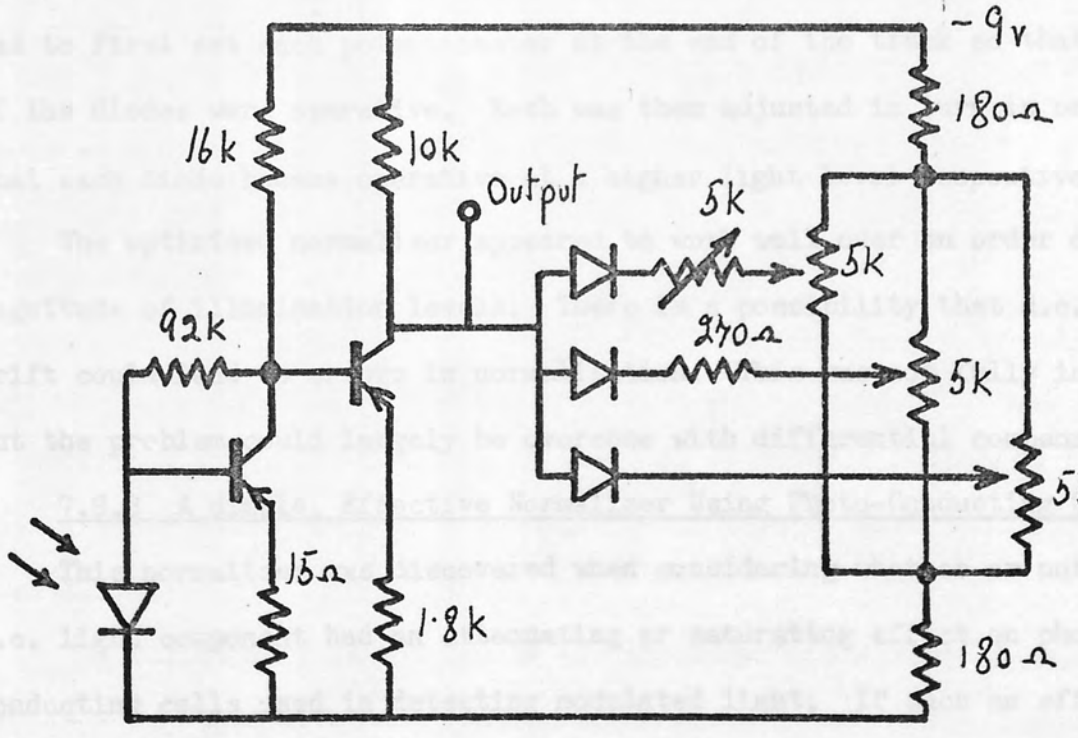

Fig. 7.12

A directly coupled pre-amplifier was necessary in order to amplify the mutual a.c. and d.c. signals sufficiently enough for the diodes to have significant attenuating influence on the a.c. component, but not too great to distort the waveform seriously.

Many experimental lash up circuits were tried before the final circuit design shown in Fig. 7.12 emerged. A post amplifier was designed and built to facilitate voltmeter reading of normalised coefficients.

7.8.2 Performance

This normalising circuit was tested by both varying the intensity of light illuminating the character and inserting neutral density filters in the beam. A number of optimisation modifications were necessary to the circuit and final optimisation was done by adjusting each of the three potentiometers and the variable resistor. Helical track potentiometers were used for stability. A certain amount of skill was required in optimising the potentiometer settings. The simplest method was to first set each potentiometer at the end of the track so that none of the diodes were operative. Each was then adjusted in turn in order that each diode became operative at a higher light level respectively.

The optimised normaliser appeared to work well over an order of magnitude of illumination levels. There is a possibility that d.c. drift could lead to errors in normalisation. This was not fully investigated but the problem could largely be overcome with differential compensation.

7.8.3 A Simple, Effective Normaliser Using Photo-Conducting Cells

This normaliser was discovered when considering whether or not the d.c. light component had an attenuating or saturating effect on photo-conducting cells used in detecting modulated light. If such an effect existed, then it might compensate for corresponding changes in amplitude of the a.c. component. This led to the idea of using two photo-conductive cells connected in parallel, one picking up the conventional a.c. and d.c. signals, while the other picked up a d.c. zero order signal only.

Experimentation was carried out on the wobbling mirror apparatus. One detector was placed towards the edge of the beam emerging from the large collimator, ensuring that light from all points on the character fell upon it. The other detector was used conventionally on the variable frequency Fourier analyser test bed. The circuit diagram including an amplifier is shown in Fig. 7.13.

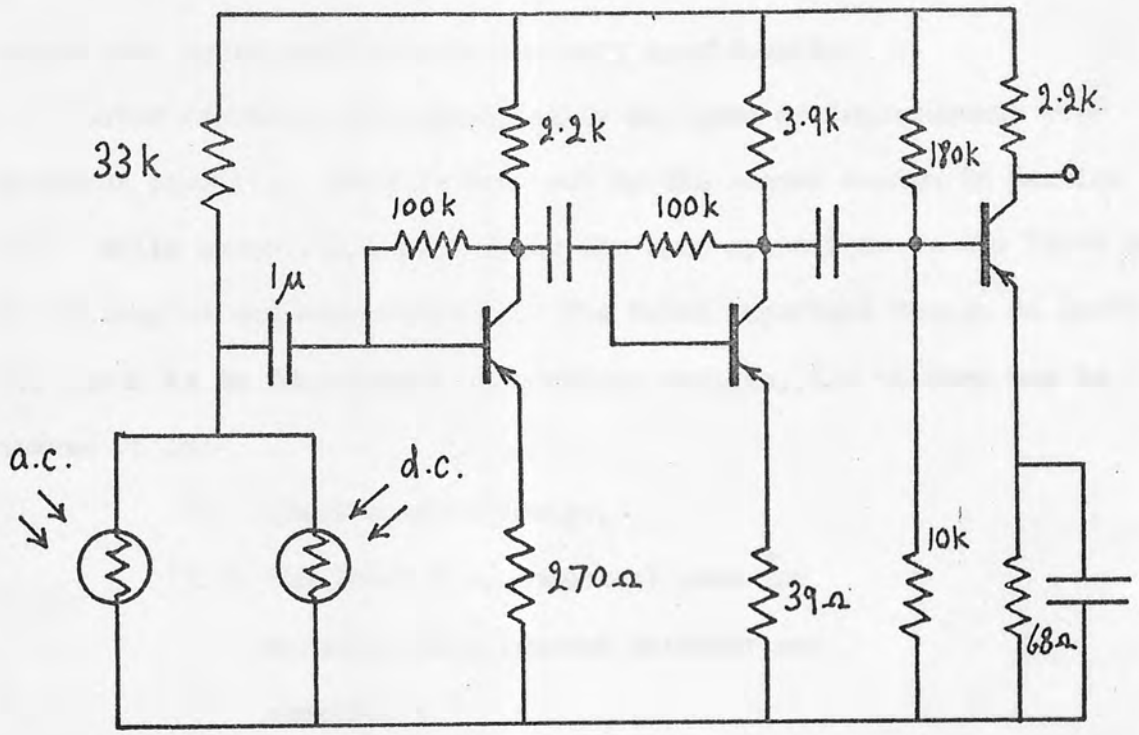

Fig. 7.13

Optimising normalising conditions was found possible by controlling the intensity of the light incident on the d.c. detector. Another way of doing this would be to insert a variable resistor in series with the d.c. detector.

The normalising action can be explained by considering the a.c. signal being shunted by the d.c. photo-conductive cell whose conductance is proportional to the light intensity incident on it.

7.9 General Conclusions on Normalisation Circuits

Three important electronic normalisation circuits have been described together with other minor experimental circuits which played a part in developing the more sophisticated circuits. They are set out in the chronological order they were developed.

The need for effective normalisation was a demanding one especially from the view of measuring Fourier coefficients of mutilated characters whose zero order coefficients can vary considerably.

Later circuits were specifically designed as improvements over previous circuits. This is born out by the second design in section 7.7. While essentially performing the same operations as the first design, it is simpler and more reliable. The third important design in section 7.8 again is an improvement in previous designs, its virtues may be summed up by:-

(i) Least complex design;

(ii) "On-line" d.c. component used for normalisation (second detector not required);

(iii) Three diodes (two Germanium and one silicon) in non-linear element, with provision for additional diodes (including Zeners), make for extended range of normalisation.

Circuits were tested largely by assessing their performance visually on an oscillascope. This was done by comparing the normalised signal with the unnormalised signal on a dual trace oscillascope while inserting neutral density filters in the beam or varying the intensity of the light illuminating the character. For this reason, formal performance results were not recorded.

Finally, a standard normalising technique used in many commercially developed machines should be mentioned. This consists of controlling the threshold level of comparators on analogue to digital conversion. The normalising voltage is applied as a bias to one of the two differential inputs of a comparator used to threshold the d.c. analogue signal. The same bias may be applied to a system containing many comparators.

CHAPTER 8

ARRAY LOGIC FOR ISOLATING CHARACTERS

8.1 Introduction

This is a theoretical study proposing a document reading head backed with array logic to isolate characters from neighbouring ones to assist in their recognition. A similar idea is proposed by the International Standard Electric Corporation, U.S.A.[90] for suppressing spurious noise present in printed characters. This study is not directly connected with the experimental work described in this thesis but speculates a possible solution to a fairly general problem encountered in document reading.

Active array logic layers are proposed for isolating characters found under real conditions in which they are often crammed together and overhanging into each other's vertical space.

Two layout configurations for implementing the logic were conceived. These are described together with circuit variations.

The preprocessing of 2-dimensional information in pattern recognition using functional parallel array logic has become popular in recent years with advances in integrated circuit technology. Their potential has been realised by: Levialdi[37]; Sheinberg[35]; the International Standard Electric Corporation, U.S.A.[90]; Chalmers[36], who have designed parallel array logic to perform a range of operations on the input image.

8.2 Large Detector Array and Parallel Logic

This concept envisages an array of photo-detectors having sufficient resolution to collect information necessary not only for effective recognition of characters but also to detect small gaps between pairs of characters.

The design of the logic relies on the detector outputs being available in parallel; this does not however discount the possible use of a scanned detector array which is commercially a more viable proposition for high resolution arrays.

A detector array should ideally consist of approximately 50 columns and 30 rows. A 30 x 20 array however may be tolerated. The detector array is used as a reading head to frame characters, and scan texts line by line.

The task is to transmit a character whose shape is retained in parallel array form, in isolation from its neighbours. This is a fundamental requirement of machines which read by recognising individual characters.

The logic layers are designed to operate in binary mode, it is therefore necessary to threshold the output of each detector so as to read ON or OFF. Comparators are the most suitable threshold devices since their threshold levels may be conveniently controlled from a common point to cope with changes in contrast and illumination level. The character isolation logic comprises of two layers. The first layer consists of propagation logic. The shape of an input character appears in binary form at the output of this layer, only after its shape has been traced out by a propagation process throughout the constituent logic elements.

Tracing can be initiated when a character, moving across the input array, strikes a preselected column. This is a triggering column. Tracing then proceeds by propagation in two dimensions throughout the logic starting from the point or points at which the character strikes the triggering column. Propagation terminates at any discontinuity, i.e. tracing only proceeds to an adjacent logic element if it is occupied by part of the character in the input matrix. This ensures that only one character at a time appears at the output.

The second layer of logic is inhibition or erase logic. It serves to remove remains of the previous character from the output array so as not to interfere with the following character. Operation of the inhibition logic is very similar to that of the propagation logic. The character is erased by the same tracing mechanism.

8.3 Broken Characters

The resolution of the propagation logic or its ability to detect small gaps between characters is dependent on:-

(i) Spatial resolution of the detector array;

(ii) Threshold level setting.

The logic, of course, will not be able to discriminate between broken characters and small gaps between adjacent characters in certain instances. The above factors, however, may be optimised for best performance. Many characters consist of closed loops, so that provided there are not two breaks in a loop, propagation of such characters will be completed.

8.4 Propagation Logic Elements

Three basic propagation logic elements are illustrated in Fig. 8.1 shown linked with feedback in one dimension for clarity.

Using the convention ON to mean the presence of part of a character, then any particular output is ON subject to the conditions that:-

1. Its corresponding input is on;
2. Any one or more of its neighbouring outputs are on.

The Boolean expression for output f_2 is:

$$f_2 = (f_1 + f_2) \cdot B$$

8.5 Inhibition Logic Elements

Again, three logic elements connected in one dimension are shown in Fig. 8.2. It incorporates propagation logic but includes an additional layer to perform erasure. Before propagation of the inhibition logic is initiated, the outputs match the inputs. When triggered at an appropriate column, namely when the character touches the left hand edge of the array, the character shape is traced out by propagation through the logic elements and erased from the outputs.

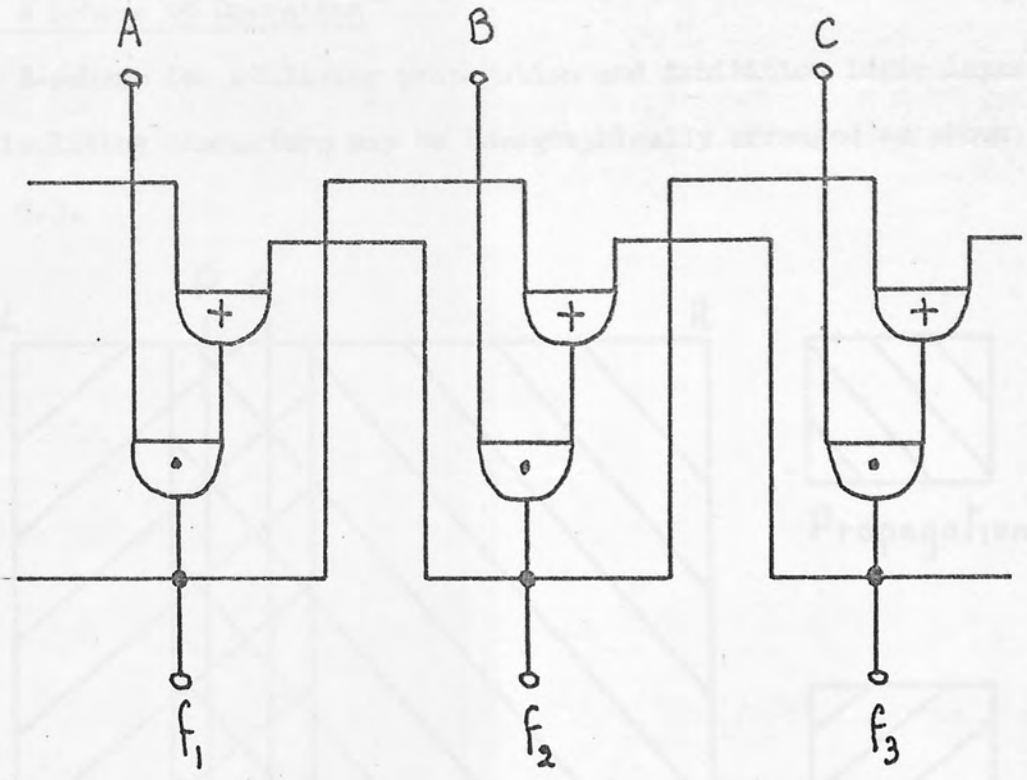

Fig. 8·1 Propagation logic elements

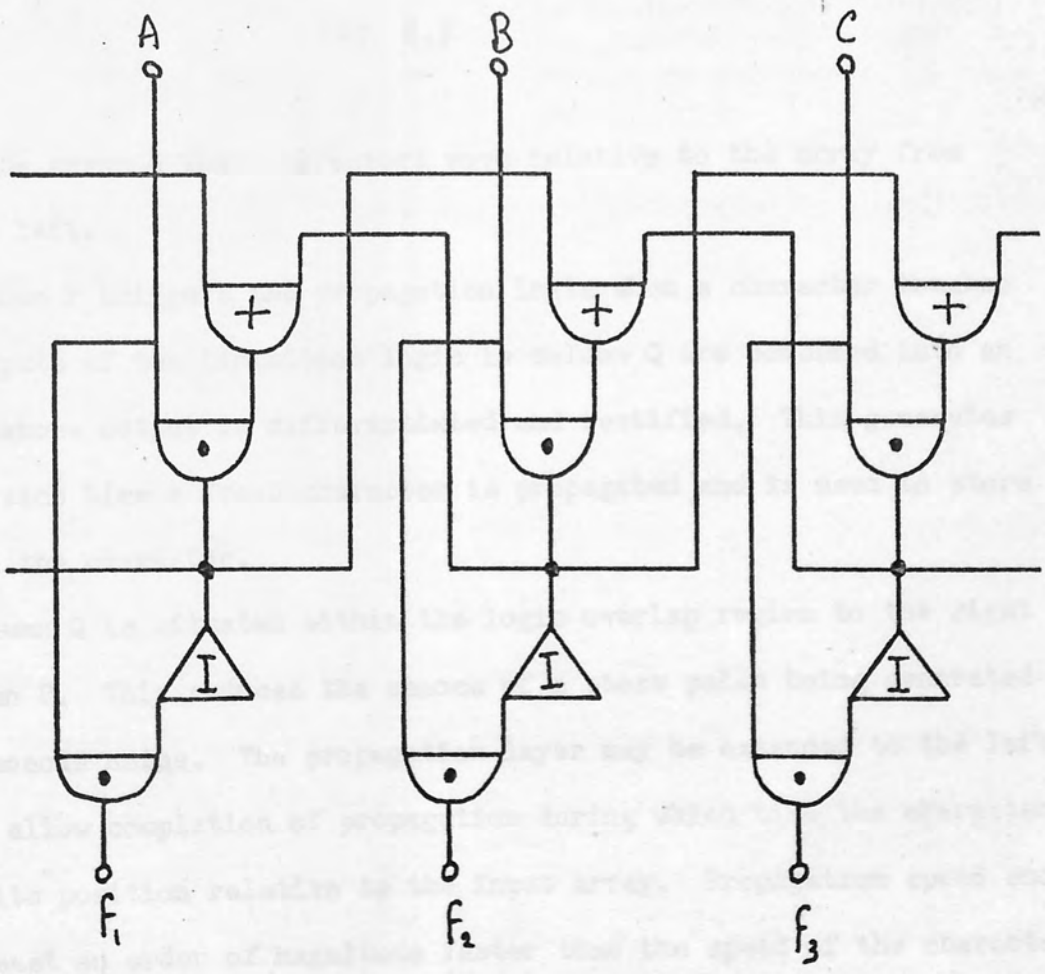

Fig. 8·2 Inhibition logic elements

8.6 A Scheme of Operation

A scheme for utilising propagation and inhibition logic layers for isolating characters may be topographically arranged as shown in Fig. 8.3.

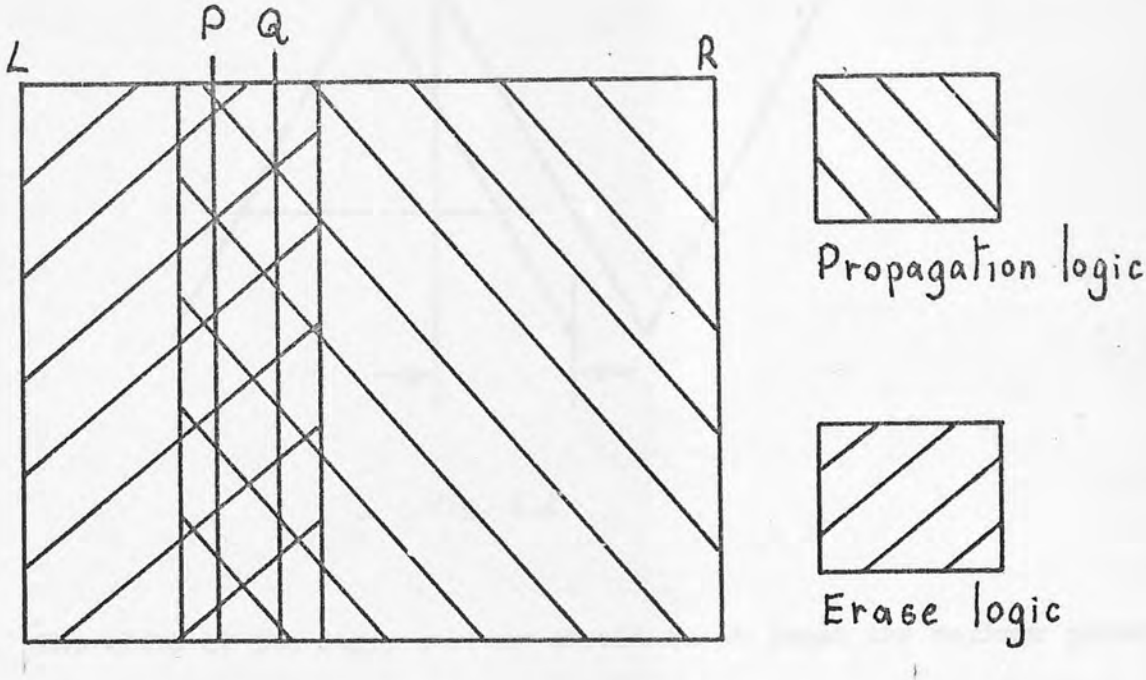

Fig. 8.3

It will be assumed that characters move relative to the array from right to left.

Column P triggers the propagation logic when a character touches it. Outputs of the inhibition logic in column Q are combined into an OR gate whose output is differentiated and rectified. This generates a pulse each time a fresh character is propagated and is used to store and hold the character.

Column Q is situated within the logic overlap region to the right of column P. This reduces the chance of a store pulse being generated by extraneous noise. The propagation layer may be extended to the left of P to allow completion of propagation during which time the character shifts its position relative to the input array. Propagation speed should be at least an order of magnitude faster than the speed of the character relative to the input array.

The ingibition logic layer is situated below and overlaps the propagation logic layer to cope with characters that overhang into its neighbour's vertical space. This effect is illustrated in Fig. 8.4.

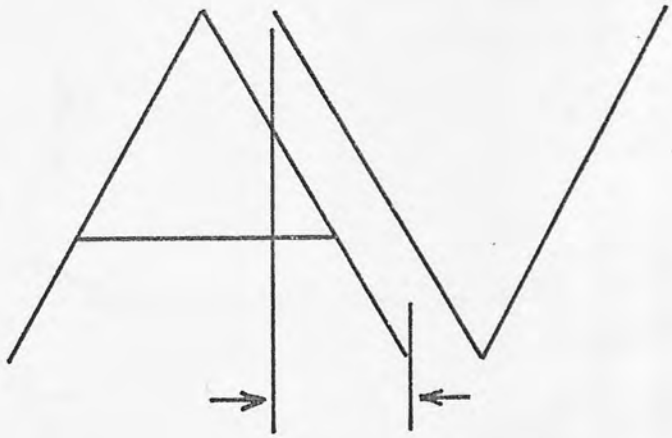

Fig. 8.4

The width of the logic overlap should be at least the maximum probable overhang between character pairs. A cross section through the logic layers made parallel to the direction of motion of characters is shown in Fig. 8.5. Feedback connections are shown in one dimension only for clarity. The circuit also includes a store, controlled by pulses derived from column Q.

8.7 System Using Narrow Detector Array with Corresponding Narrow Logic Layers

In this system, a minimal extent of propagation and inhibition logic is used to isolate characters.

Most of a character's form is built up in rows of parallel access shift registers fed from outputs of one end of the inhibition layer. A section through the logic layers of such a scheme is shown diagrammatically in Fig. 8.6. The detector array, propagation array and inhibition array are the same in extent typically 5 x 20 and situated one under the other. Their columns may be "narrower" (having higher resolution) than the shift register columns if required for detecting small gaps. This means that

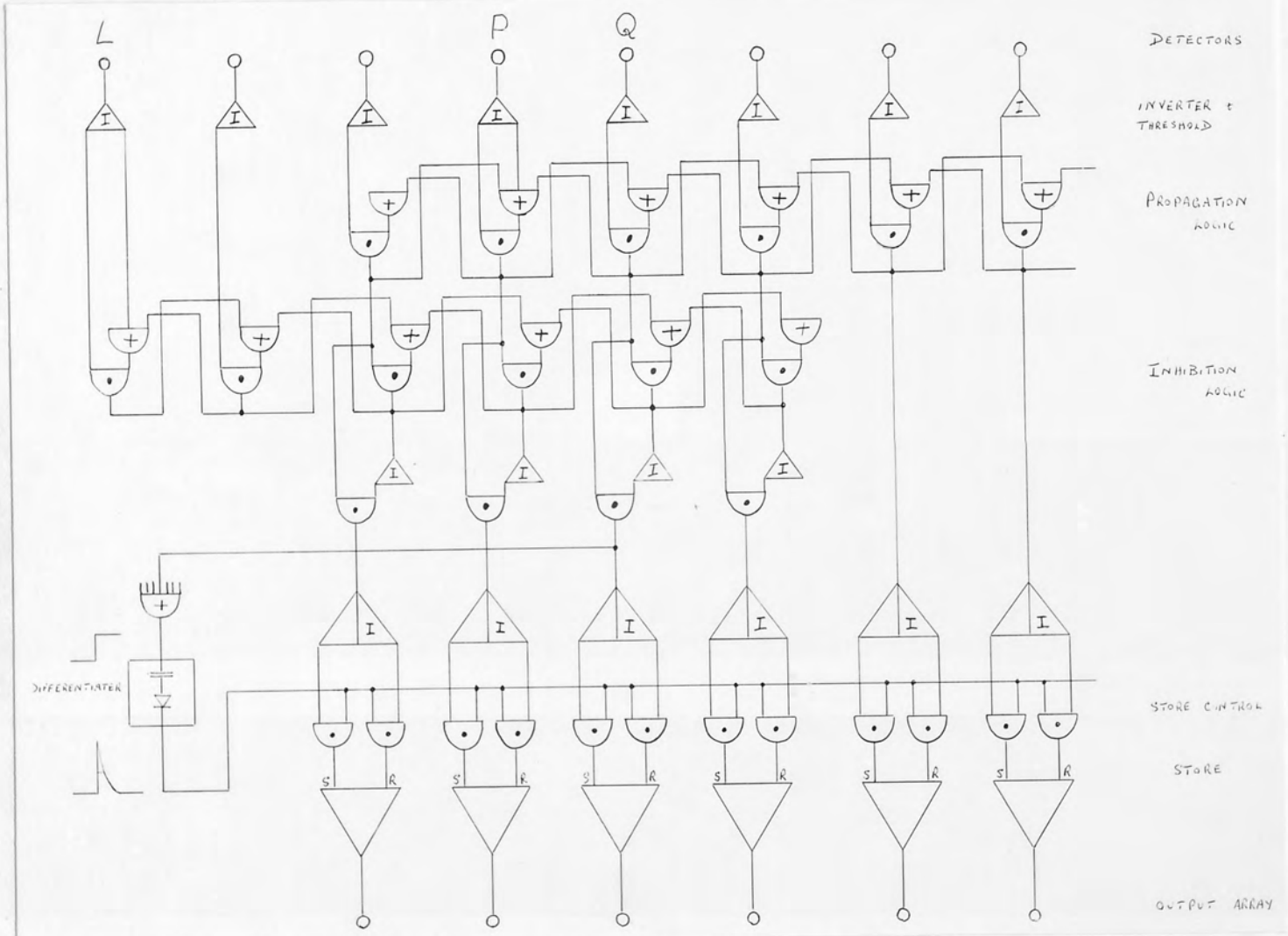

Fig. 8.5 A scheme using propogation logic to isolate characters

not all the information collected passes into the shift register. The inhibition logic outputs of adjacent columns can then be tied together to match the shift register outputs as indicated in Fig. 8.6.

The number of columns in the logic layers is dictated by the maximum probable overhang between any character pair. The width of the logic is at least the width of this overhang.

8.7.1 Mode of Operation

Characters move from right to left across the detector array. It is assumed that the detector outputs are suitably thresholded, thus providing binary inputs for the logic layers.

The propagation layer is activated when a character touches the extreme left column in the propagation logic, column A. The rate of propagation is fast compared with the progress the character makes across the array. The shape of the character thus immediately appears at the outputs of the inhibition logic since this logic is not activated at this stage.

The information is shifted column by column into rows of parallel access shift registers by clock pulses synchronised such that progress through the register matches the progress of the character across the input detector array. A read or store signal is given only when the outputs from column B are all in the OFF state simultaneously, that is, an entire character appears at the output array to the left of column B. This can be done by feeding all outputs from B into an AND gate followed by an inverter. Of course, any overhanging characters that follow cannot appear at the output until it touches column A.

The shift registers must all be reset and the inhibition logic triggered from column A before the following character touches A, which is propagated in the propagation layer. The character may be held in a store until the next character is available for reading. Advantage may be taken of the spatial redundancy provided by more than one column of detectors by overlapping the shift register with the logic layers.

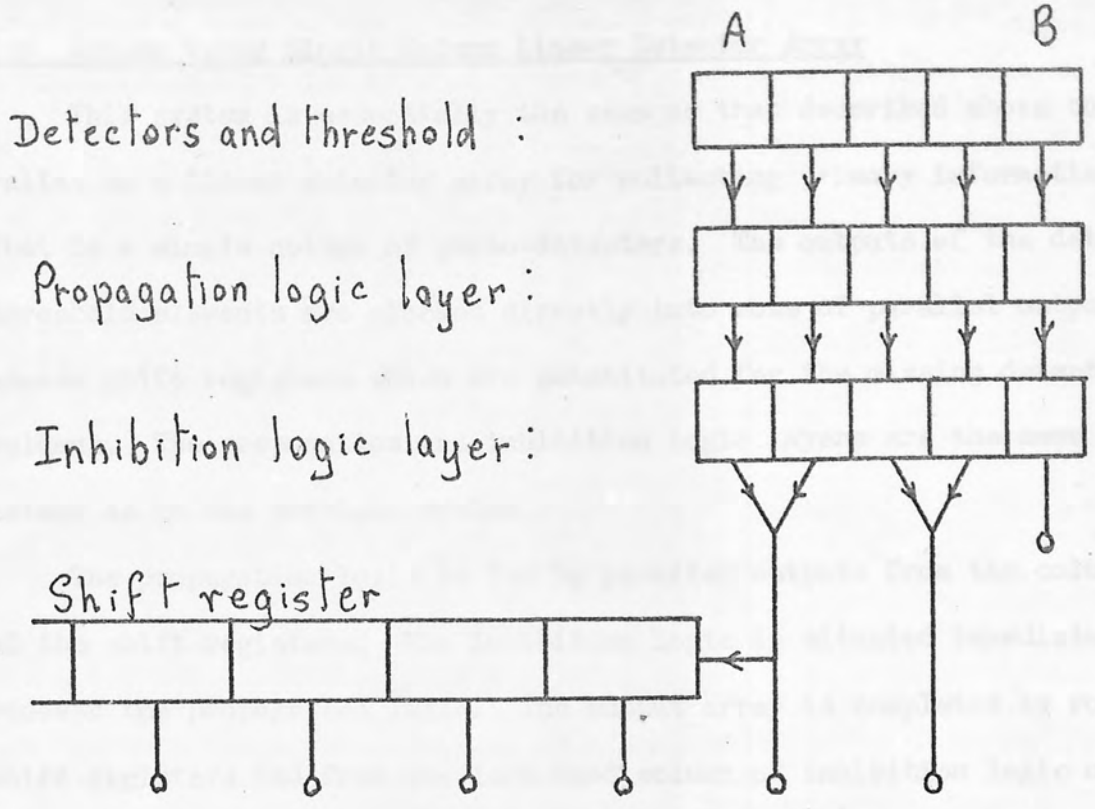
A
B
Detectors and threshold :
Propagation logic layer :
Inhibition logic layer :
Shift register

Fig. 8.6

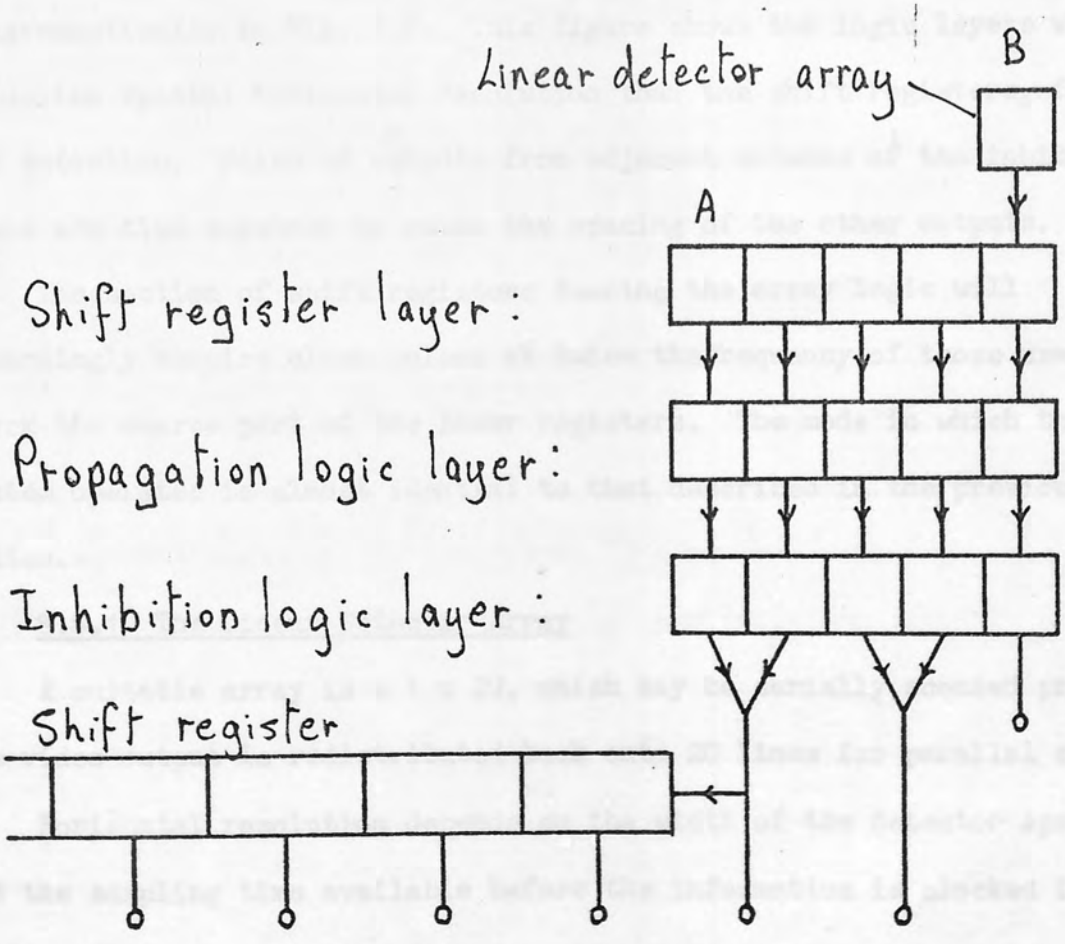
Linear detector array
B
A
Shift register layer :
Propagation logic layer :
Inhibition logic layer :
Shift register

Fig. 8.7

8.8 Scheme Using Single Column Linear Detector Array

This system is essentially the same as that described above but relies on a linear detector array for collecting primary information. That is a single column of photo-detectors. The outputs of the detector threshold elements are clocked directly into rows of parallel output access shift registers which are substituted for the missing detector columns. The propagation and inhibition logic layers are the same in extent as in the previous system.

The propagation logic is fed by parallel outputs from the columns of the shift registers. The inhibition logic is situated immediately beneath the propagation logic. The output array is completed by rows of shift registers fed from the left hand column of inhibition logic outputs as before.

A section through the various layers along a row is shown diagrammatically in Fig. 8.7. This figure shows the logic layers with twice the spatial horizontal resolution than the shift registers, for gap detection. Pairs of outputs from adjacent columns of the inhibition logic are tied together to match the spacing of the other outputs.

The section of shift registers feeding the array logic will accordingly require clock pulses at twice the frequency of those used to clock the coarse part of the lower registers. The mode in which this system operates is almost idential to that described in the previous system.

8.8.1 The Linear Detector Array

A suitable array is a 1 x 20, which may be serially scanned provided the video output is redistributed back onto 20 lines for parallel access.

Horizontal resolution depends on the width of the detector aperture and the sampling time available before the information is clocked into a shift register.

8.9 Design for a Parallel Access Shift Register

Fig. 8.8 shows a diagrammatical circuit design plan for a shift register. This form of register is now available in integrated form at economic prices.

8.10 Other Active Operational Logic Arrays

Edge Detection

Edge detection is often a desirable means of rejecting redundant information in pattern recognition machines. A simple analogue form of edge detection is achieved by feeding pairs of output from adjacent detector array elements onto the differential inputs of integrated differential amplifiers.

An amplifier will register an output voltage only if a differential in light intensity exists between the two detector elements feeding the amplifier. More sophisticated forms of edge detection have been proposed using lateral inhibition circuits[91].

Edge detection may be performed digitally by means of a simple form of lateral inhibition logic in the form of an array. The logic array receives information in parallel channels, each conveying a "bit" of information. Fig. 8.9 illustrates the basic connections between 3 logic elements. This logic may be modified to perform edge following or edge tracing by incorporating propagation logic as shown in Fig. 8.10. Tracing is initiated from any preselected point or column in the array, either automatically by the pattern or by a control pulse.

8.11 Summing Up of Array Logic for Character Isolation

The logic was originally propounded to operate in the mode described under section 1 of this chapter with a full photo-detector array.

Manufacturing costs of such a device would be high. Two major cost factors are:-

1. The parallel detector array backed by comparators for thresholding;
2. Extensive special purpose array logic.

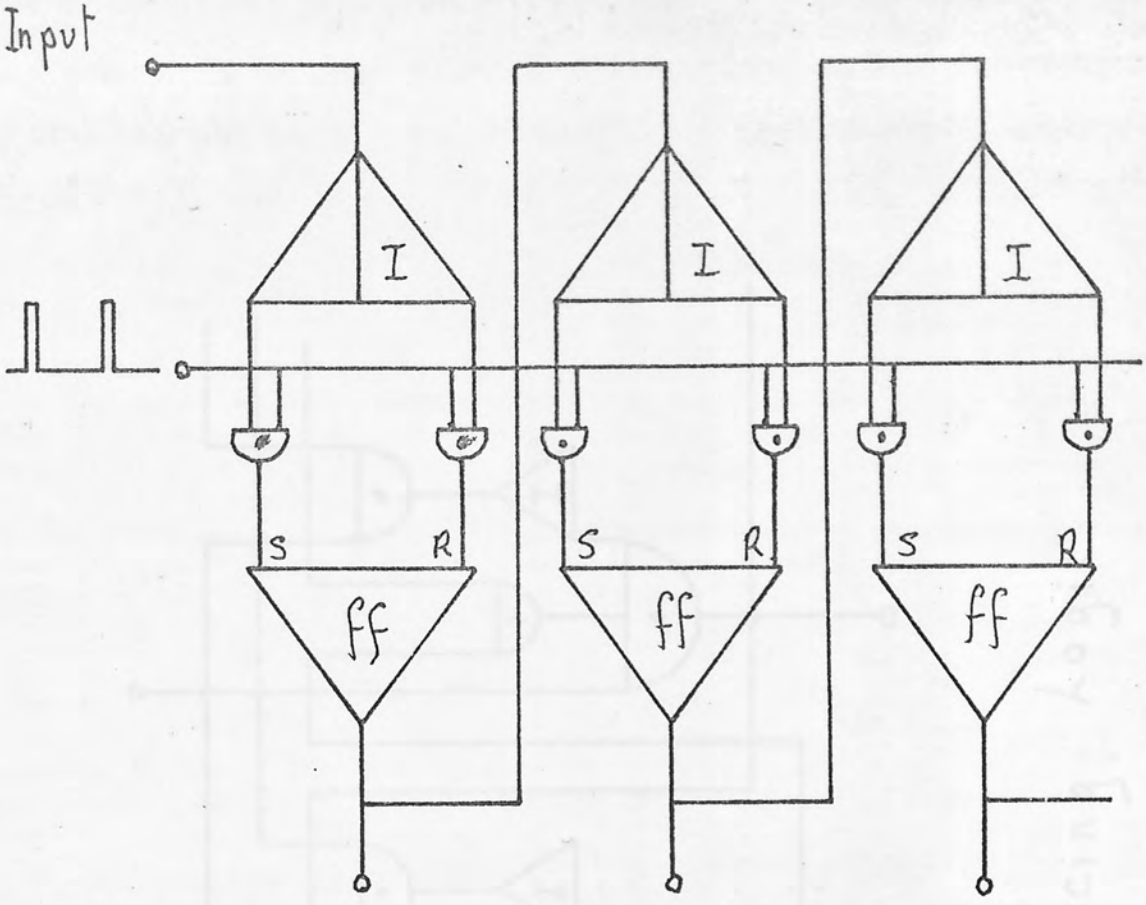

Fig. 8·8 Parallel Access Shift Register

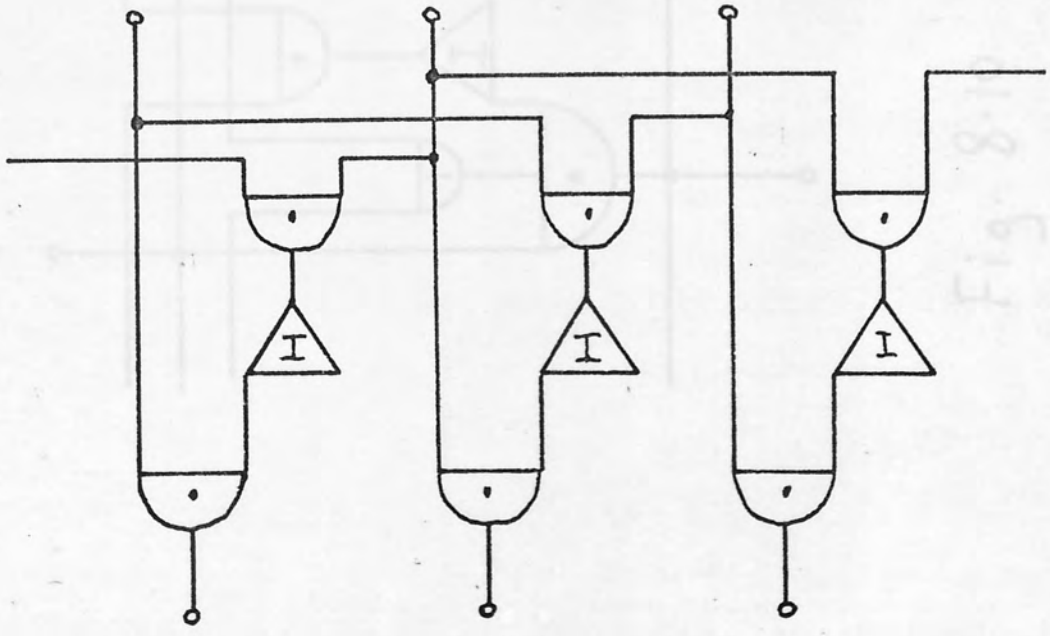

Fig. 8·9 Edge Detection Logic

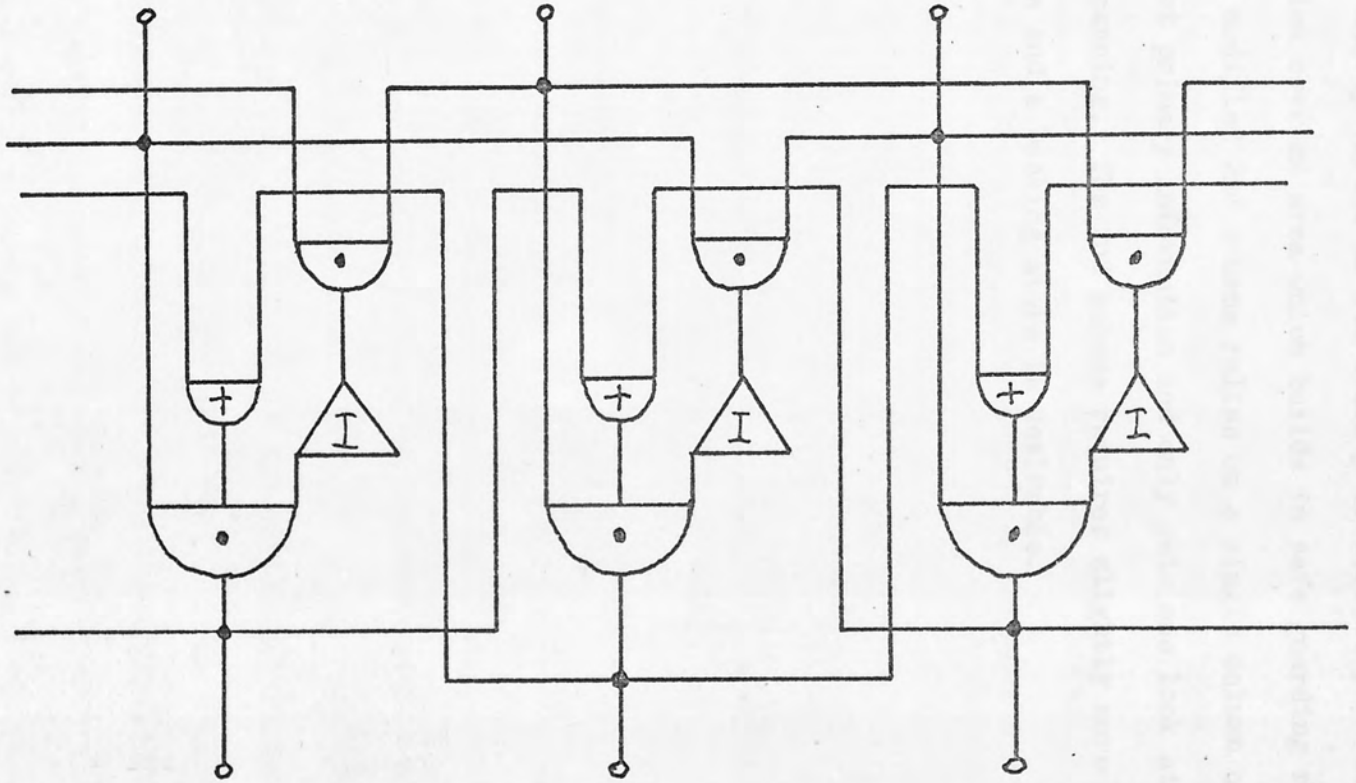

Fig. 8.10 Edge Tracing Logic

The 2nd design is an alternative scheme minimising the requirements of these factors and using production line components where possible, for example, shift registers. The 1st scheme is inherently more reliable than the 2nd by virtue of its ability to collect parallel primary information over an area which builds in safe guarding redundancy.

The modified 2nd scheme relies on a single column of photo-detectors to collect primary information and only gets one look at a character during scanning. The 2nd scheme requires slightly more complex control procedure and a backing store is desirable.

CHAPTER 9

MARK I AND MARK II CHARACTER RECOGNITION MACHINES

SUMMING UP AND CONCLUSIONS

9.1 Introduction

During the course of research on character recognition by incoherent Fourier transformation, two experimental character recognition machines were built. These were the Mark I and Mark II machines. A third high speed film machine is now in the course of construction based on the Mark II design.

The Mark I machine was built up from the hardware described in chapter 3 to collect Fourier transform data of characters which in turn was computed in order to locate high efficiency Fourier coefficients for character recognition.

This machine is really a pilot plant built to demonstrate the existence of a machine which recognises characters by measuring their discrete low spatial frequency content, using incoherent optical means.

The Mark II machine is based on the same optical principle, but incorporates features desirable for high speed operation. The optics are generally more streamlined and the electronic processing simplified by virtue of one bit encoding. Both machines are important stepping stones in development of character recognition by frequency analysis.

The salient features of the Mark I machine are: the wobbling mirror mechanical scanner; use of collimator; 3 bit encoding logic. Mark II was designed primarily for potential high speed operation. Its salient features are: static scanning; shadowing without a collimator; one bit encoding logic. Both machines are broadly described below under optical hardware and electronic hardware.

9.2 Mark I Machine

This machine consists of hardware developed in association with the wobbling mirror scanner. The optics are essentially the same as the continuous spectrum Fourier analyser described in the latter part of chapter 3. The single "variable" grid is replaced by a set of grids whose frequencies and orientations are pre-determined so as to generate given Fourier frequencies in the detector plane.

The spatial frequencies of the grids in this composite grid are the ones associated with the Fourier coefficients used as features for recognising Gill Sans numerals with 3 bit encoding. The 3 Fourier frequencies are the ones selected using computer and optical test bed procedures described in chapter 5. Fig. 9.1 shows the composite grid containing these frequencies.

The oblique grid is extended to accommodate a reference detector for phase measurement. The phases of coefficients generated by this frequency are needed to distinguish between 6 and 9, not otherwise possible by amplitude. The characters are displayed in the back focal plane of the collimator together with a reference spot situated to one side of the character. Light from the character is cross polarised with respect to light from the reference spot, so that they can be separated at the detectors. A reference slit may be used, situated parallel to the stripes of the phase grid.

9.2.1 Detector Plane

A composite detector mask is identical in every respect to the frequency shadowing grids, and orientated so that the shadows produced by the first grids match up with the corresponding frequencies in the detector mask. This ensures that the shadow profiles are sampled efficiently by the detectors. The detector mask is equipped with polarisers to separate the signal and reference beams. OAP12 Germanium photo-diodes were the detectors used.

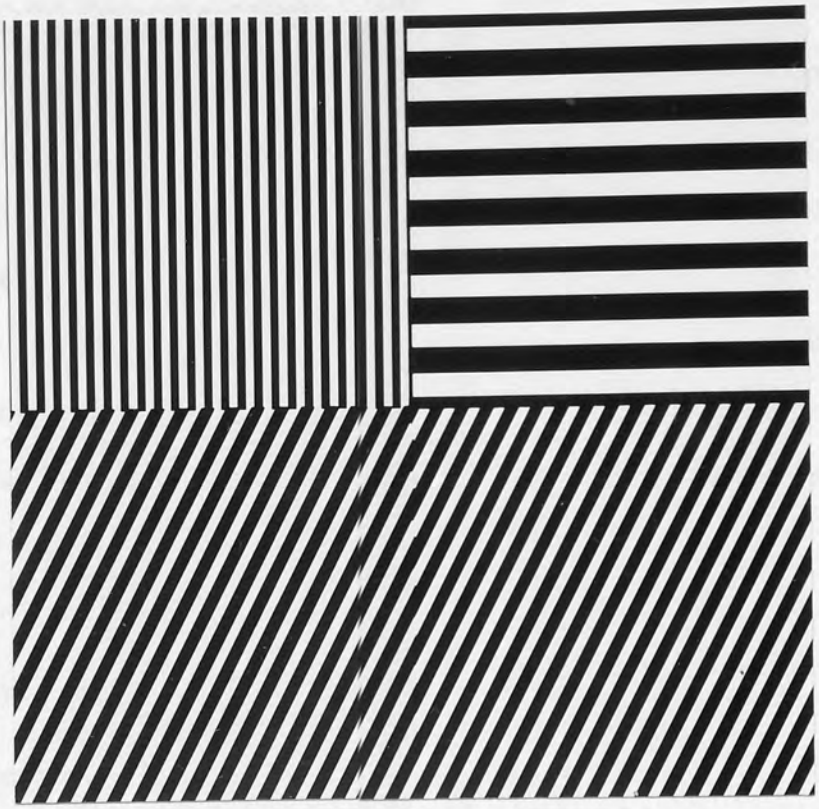

Fig. 9.1 Composite three grids for Mark I machine

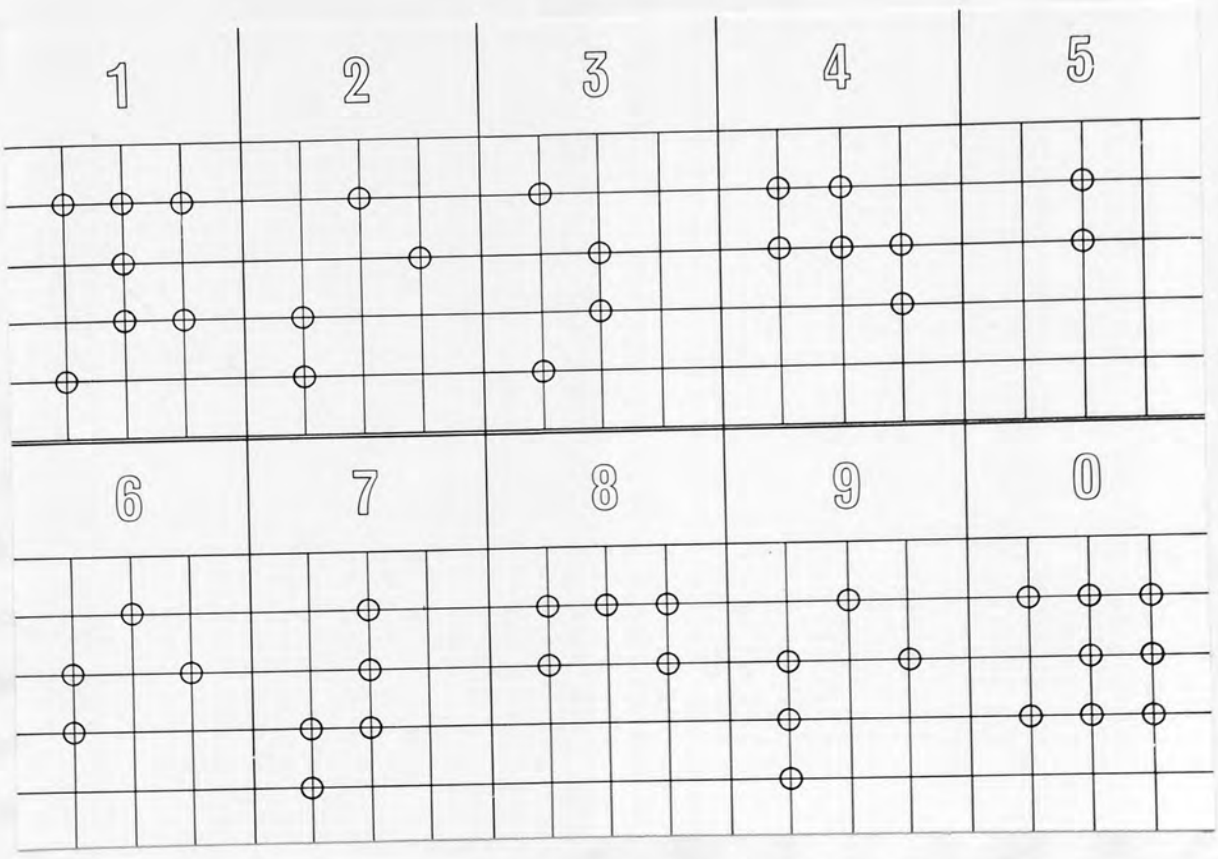

Fig. 9.2 Binary lamp codes produced by Gill Sans numerals

9.2.2 Grid Specifications

The grid frequencies are based on a square frame round the characters (in this case a one inch square) which defines the unit frequency. The height of the characters themselves are approximately 0.7 of an inch.

Factors determining the sampling period, T, are the focal length, f, of the lens, the grid spacing, d, and the separation distance between the grids and the shadows, r. These are linked by the equation derived in chapter 3 for frequency calibration of the optical bench:-

$$T = \frac{df}{r}$$

The frequency sampled by the grid is: $\frac{r}{df}$

Thus the spacing of a grid required to sample the unit frame frequency is:-

$$d = \frac{1 \times r}{36"}$$

If $r = 3"$ $\quad d = \frac{1}{12}$ inch or 12 lines per inch.

The spatial frequencies of grids actually used are:-

1. $(1, 90^{\circ})$: 8 lines/inch
2. $(3, 0^{\circ})$: 24 lines/inch
3. $(\sqrt{5}, -27^{\circ})$: 18 lines/inch

9.2.3 Electronic Hardware

Analogue: Electronic circuitry, handling modulated analogue signals for their phase and amplitude measurement, is described in chapter 3 for a single variable frequency channel. Each of the three fixed frequency grids is provided with a similar electronic channel. Only the channel associated with the oblique grating requires a phase detector. The signals in the other two channels are merely amplified and rectified for amplitude detection.

Digital: Amplitude and phase information is converted into d.c. voltages prior to digitisation. Each analogue amplitude voltage is encoded in 3 bit binary. 7 Schmitt triggers, with their threshold voltages set in ladder configuration, are followed by a 3 bit encoding logic described in chapter 4. Phase voltage is encoded into 1 bit binary for IN or OUT of phase discrimination only. The Mark I machine was not provided with a decoding logic. Instead, the binary coding is displayed visually on 3 rows of 3 lamps representing binary digits, plus a single lamp for phase. The coded signals produced by Gill Sans numerals are shown in Fig. 9.2. Ordinary low voltage filament bulbs are used, driven by Schmitt triggers for good ON/OFF discrimination.

General layout of the Mark I machine is shown in Figs. 9.3 (a) and (b) viewed from two different angles. Electronic circuitry and bulb display panel is in the foreground of Fig. 9.3(b).

9.3 Mark II Machine

The development of the hardware for this machine is treated largely in part II of chapter 6 which describes the triple grid static scanner.

The Mark II machine is designed to recognise OCRB type using 1 bit encoding. A composite grid consisting of four frequency grids corresponding to the 4 Fourier sampling frequencies selected by procedures described in chapter 5 is used for shadowing. This grid is shown in Fig. 9.4.

Diffusely illuminated characters are shadowed directly through the grids without using a collimator, this produces projected magnification of the shadows in the detector plane. 4 detectors, one for each frequency, are each equipped with a triple analysing grid, magnified by an appropriate amount so that they precisely match the spatial frequency of the shadows falling upon them. (Fig. 9.5).

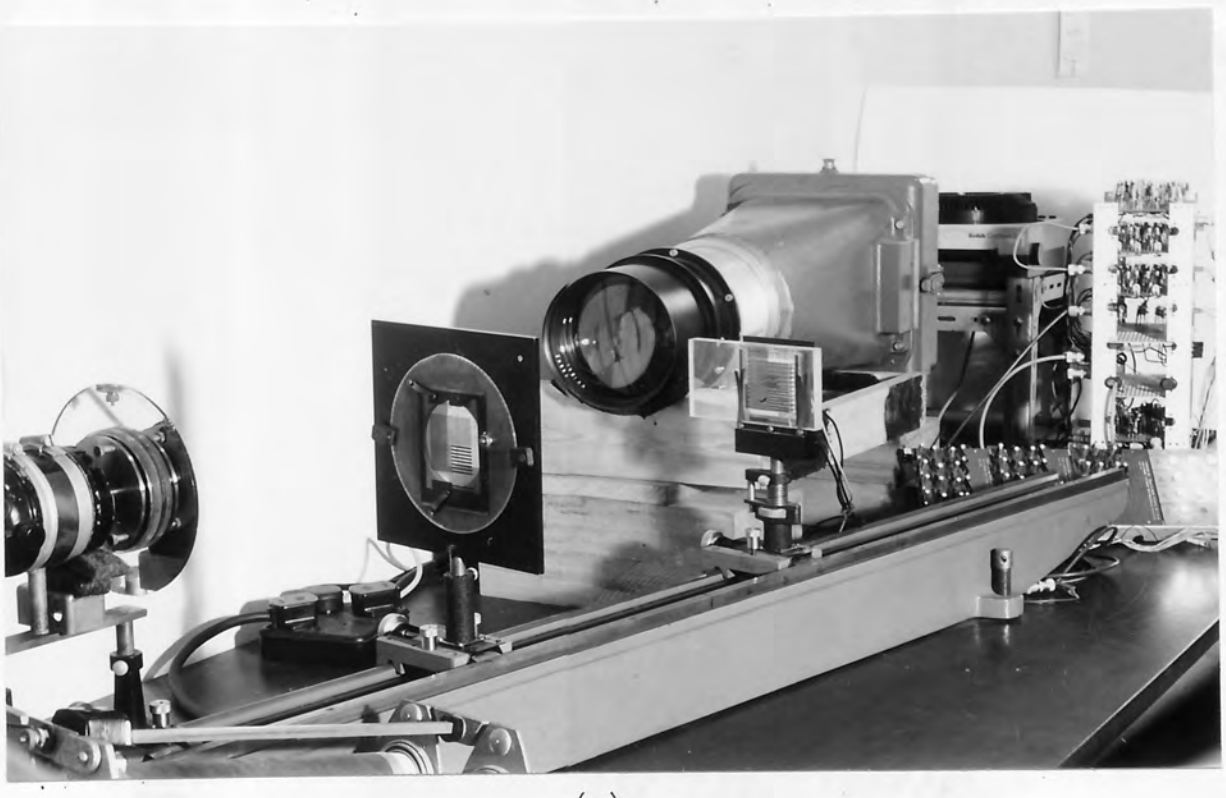

(a)

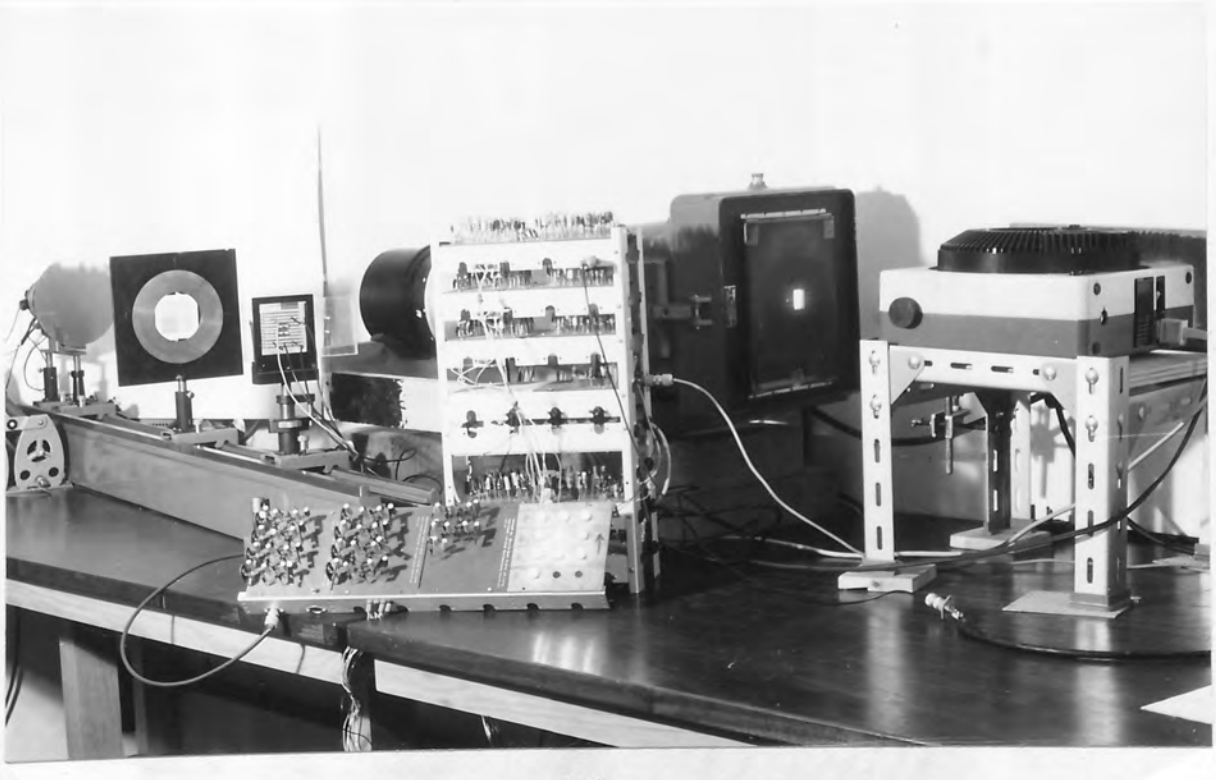

(b)

Fig. 9.3 Two views of the general layout of the Mark I machine

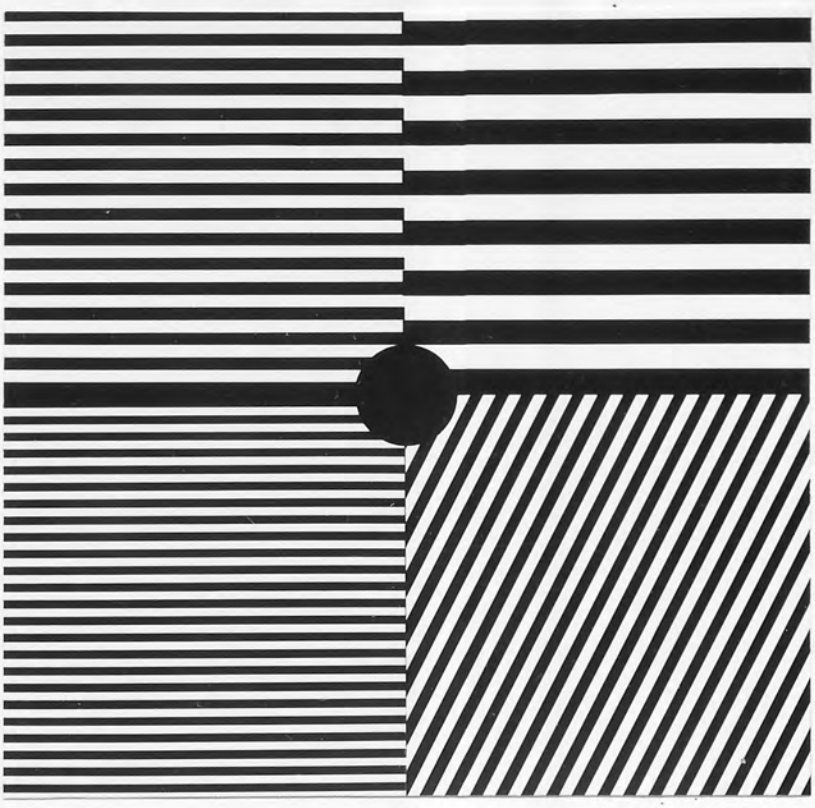

Fig. 9.4 Composite grid containing four frequencies used in the Mark II machine

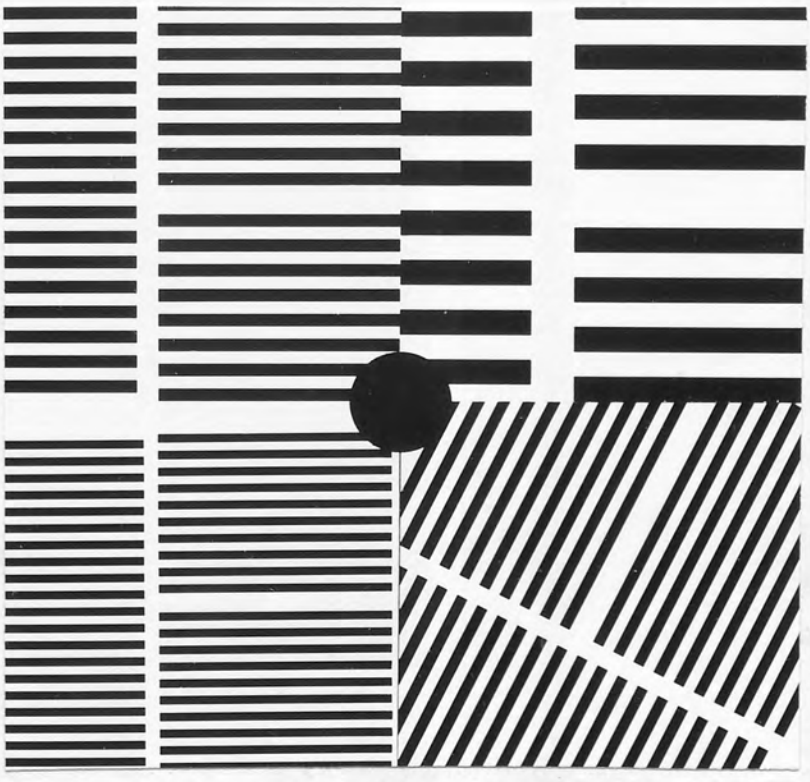

Fig. 9.5 Composite triple grids for analysing shadows produced by grid shown in Fig. 9.4

The detectors (SPL111) are silicon solar cells chosen for their large uniform sensitive areas and relatively fast response. Each one is placed immediately behind a triple grid so as to collect light from each segment. Balancing is achieved by adjusting its position in a plane parallel to the grids. A composite detector jig for independently adjusting the position of 4 detectors situated behind the 4 triple grids was designed and built by Mr. McKenzie.

A polariser is placed immediately in front of the character and the plane of polarisation rotated, by spinning a half-wave plate, mounted on the shaft of a small electric motor, in the beam between the polariser and the first grid. This produced modulation at about 180 Hz.

9.3.1 Phase

Phase measurement at only one Fourier frequency is required to distinguish between 6 and 9. These coefficients are generated by the oblique grid. A reference signal is obtained by placing a small detector, equipped with a polarising filter, anywhere in the beam after the rotating half-wave plate, as long as it does not obstruct light forming the shadows. A convenient place is a small aperture between the 4 triple grids in the centre of the detector plane. The phase of this signal may be set at any value by rotating the polaroid filter on the detector.

9.3.2 Grid Specification

Characters are shadowed directly through the grids without a collimator. This is illustrated in Fig. 9.6.

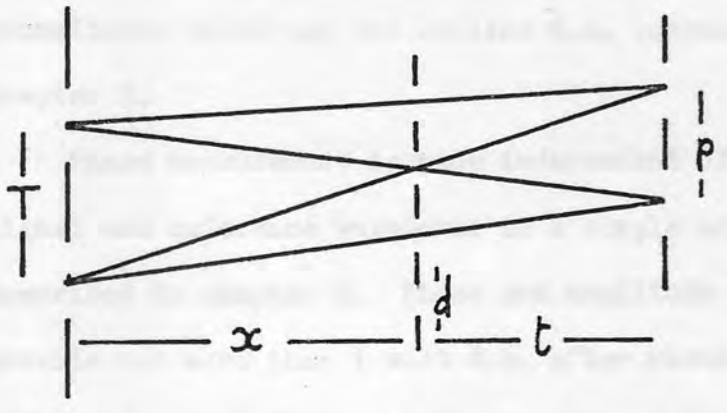

Unit frame period, in the Mark II machine, is 1 cm.

Fig. 9.6

The grid interacts with a periodicity T in the object producing a strong shadow when:-

$$\frac{T}{d} = \frac{(x + t)}{t}$$

or $$T = (\frac{x}{t} + 1)d$$

subject to $d < T$

Projected magnification of the shadow is given by:-

$$\frac{p}{d} = \frac{(x + t)}{x}$$

The important thing to notice is that the frequency picked out in the object is determined by the ratio: $(\frac{x}{t})$ and not by specific values of x and t using a particular grid. This is also true of the projected magnification.

The ratio $\frac{x}{t} = \frac{3}{1}$ was used.

Three vertical sampling frequencies were 1, 2 and 3 times the unit frequency of 4 lines/cm. The oblique frequency is $\sqrt{5}$ the unit frequency. The 4 triple analysing grids are photographically enlarged and arranged on a single $\frac{1}{4}$ plate as shown in Fig. 9.5.

9.3.3 Electronic Hardware

The detectors convert optically modulated signals into electrically modulated signals whose amplitude and phase are detected using similar techniques to those of the Mark I machine. The amplifiers incorporate normalisers which use the on-line d.c. component technique described in chapter 7.

Phase measurement is made independent of amplitude by clipping both signal and reference waveforms in a simple silicon diode clipper circuit described in chapter 3. Phase and amplitude signals are amplified to provide not more than 1 volt d.c. after rectification. Transister instead of transformer driven rectifiers are used for high speed operation.

Each phase and amplitude voltage is encoded into 1 bit binary using Schmitt triggers. The precise threshold voltage of each Schmitt is optimised for maximum character pair discrimination. In a production model, integrated circuit comparators would be used for thresholding, an applied bias determines their switching level. This has the advantage that the bias may be controlled automatically according to the previous experience of the machine.

The binary outputs are decoded or re-encoded via a simple decoding logic so as to be compatible with the logic configuration of a paper tape readout punch.

9.4 Performance Evaluation

9.4.1 Mark I Machine

Performance evaluation involves the factors:-

(i) Stability: estimation of fraction of not-read and erroneous signals;

(ii) Typeface handling capabilities;

(iii) Identification of weaknesses in the system.

The first can only be studied within limits as the system is a slow reading one, typically one character per second. Owing to the need to develop a.c. signals, typically 30 - 300 Hz, depending on the grid frequency, it is necessary to drive the projector lamps from d.c. This involves the use of accumulators and there is a steady downward drift in output intensity. The use of floating batteries improves stability. This machine was built without normalisation facility and therefore does not compensate for fluctuations in illumination level. Variations in motor speed also produced instability. The behaviour of the transistor circuits was found to be temperature dependent.

Most critical are the Schmitt trigger circuits. Instability in this area was largely overcome using silicon transistors, and ensuring that the values of the d.c. voltages, before thresholding, are an order

of magnitude higher than the drift limits in the threshold voltage of the trigger. Specially designed temperature stable, integrated circuits are superior in this respect.

Variations in the tarnish on the mirror surface produces signals even when the field is open (i.e. has no grid in it). Regular resurfacing is therefore required. There is also an inevitable amount of electronic noise and interference. External a.c. pick up from fan motors etc. can only be cured by good screening. The intrinsic detector noise is noticeable but is not found troublesome. This could be reduced further by using larger detectors with larger areas behind the second grids. The wobbling mirror scanner generates a waveform whose frequency is modulated by twice the mirror rotation frequency, and can lead to bandwidth restrictions.

Removing this frequency using a parallel T rejection filter as a coupling between stages of amplification, cleans up the waveform considerably without serious bandwidth loss.

Testing Internal Consistency

This has been restricted to 100 runs of the character sequence 0, 1, 2, 3 ..... 9, with the result that no erroneous signals were obtained. Redundancy built into the 3 level discrimination criterion described in chapter 4 was such that occasional variations of one bit did not cause any confusion. On this limited scale the system is reliable.

Type Face Invariance

Some type face work was done on the variable frequency bed described in chapter 5. Type face handling capabilities of the machine could therefore be predicted with some conviction. Only Gill Sans numerals are completely recognised while OCRB numerals are partially recognised. It proved difficult to find a set of low frequency coefficients to distinguish between all pairs of Rockwell numerals. Only a few Rockwell 371 characters produced the same signals as corresponding Gill Sans characters.

9.4.2 Mark II Machine

This is a later machine and opportunity was taken to obviate and rectify many faults found in the Mark I machine.

The system of scanning used in the Mark II machine for high speed operation introduces new possible sources of error. The positioning of each detector behind its triple grid is fairly critical when maintaining proper balance. Any accidental shift in the position of a detector immediately introduces gross error. This is overcome using rigid mountings. The optics of the Mark II machine are shown in Fig. 9.7.

One virtue of the triple grid static scanner is that it produces a clean continuous temporal sinusoidal output wave for as long as the shadow it represents, remains in position. This waveform is more convenient to handle electronically. A tuner may be incorporated to improve signal to noise ratio at the expense of bandwidth.

Coefficients are normalised by the on-line d.c. zero order coefficient which also automatically compensates for fluctuations in illumination level. This dispenses with a stabilised light source.

Proper performance evaluation of the Mark II machine was not carried out for two reasons. Firstly, only one channel of the electronics was completed and secondly a high speed character input display is not available. Work is proceeding along these lines so as to make a full evaluation possible.

Each frequency was, however, tested by balancing the detector behind each of the four triple grids in turn. The detector was mounted on an optical bench holder having vertical and horizontal traverse facilities for balancing. The detector was established behind the oblique striped frequency grid for further tests. Balancing was easily achieved by removing the shadowing grids for a uniform field before manipulating the horizontal and vertical traverses whilst observing the signal trace on an oscillascope. Scratch noise from the rotating half wave plate was

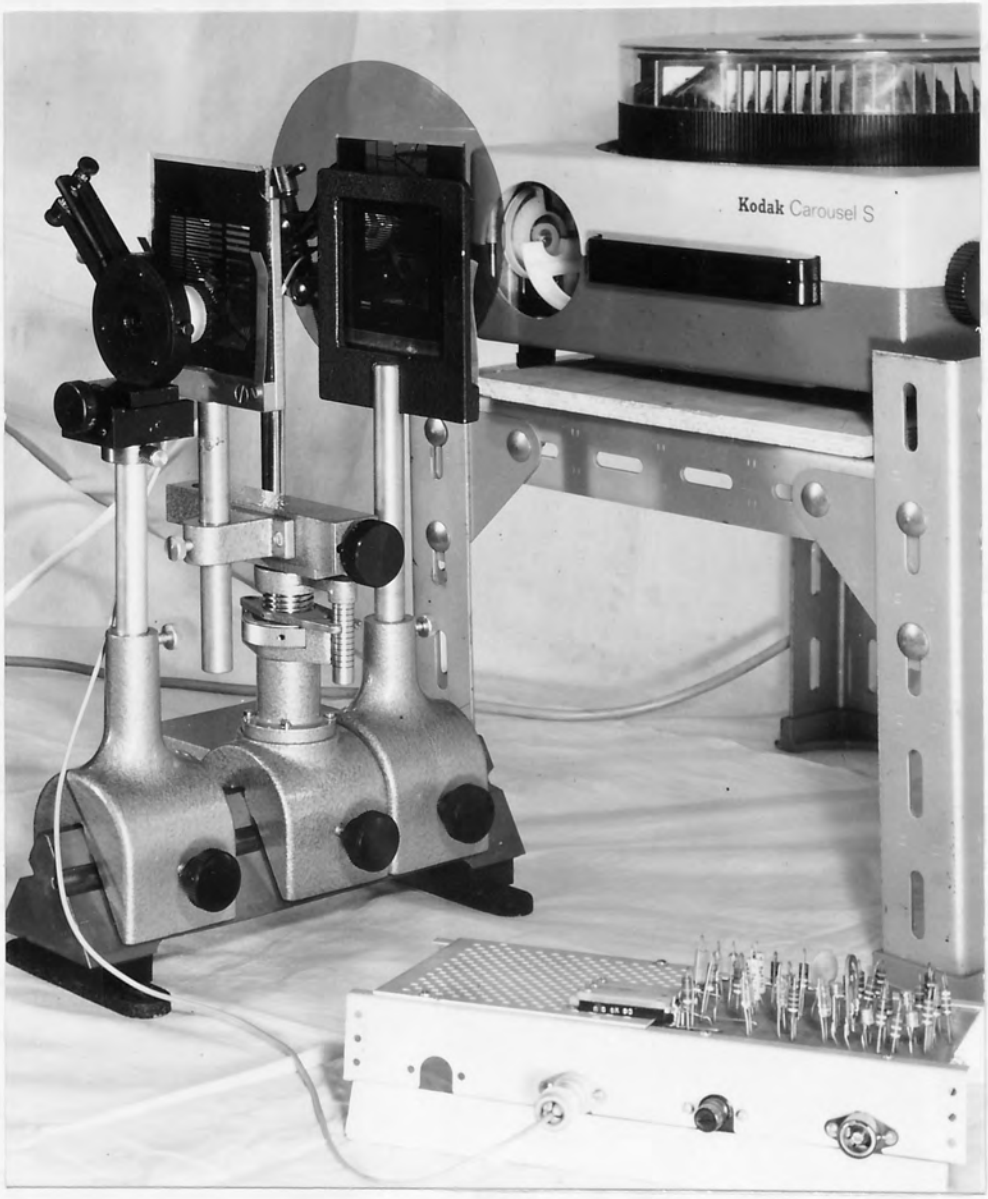

Fig. 9.7 The optics of the Mark II machine

observed on the trace when the detectors were balanced. Balance could easily be disturbed by knocking the detector.

Phase discrimination of 6 and 9 was checked on an oscillascope. A reference detector provided external synchronising of the time base. Signal to noise ratio was noticeably better than for the Mark I machine, despite the characters being much smaller and despite the absence of collimation.

A point about the Mark II machine is that the same temporal modulation frequency is generated in every detector. Identical amplifiers (including tuned filters) may be used in each channel, but precaution should be taken to ensure against cross channel interference. Each channel is consistent in the rate at which it is capable of transmitting information. This is not so in the Mark I machine where the temporal frequency is proportional to the spatial frequency of the shadowing grids.

9.5 Summing Up

Both machines read high contrast white characters on a black background. The sort of printed characters one meets in real life situations are usually black on a white paper background and the contrast can often be poor, depending on ink and paper quality[92].

It is unlikely that a Mark II style machine could cope with these characters without additional hardware such as a television link for converting characters into white on black and enhancing their contrast. The video signal for such a television link may be derived using a vidicon tube, a flying-spot scanner, or even a photo-diode array. These are described in the literature survey of chapter 1. Characters may be displayed on a television screen or on a galium phosphide photo-emitting diode array, the latter generally being of much lower resolution. The latter has the advantage that if used in parallel mode it would provide an ideal output display for the array logic character reader proposed in chapter 8.

9.5.1 Directly Reading Black Characters on a White Background without Electronic Imaging Systems

Babinet's principle[93] for Fraunhoffer diffraction states that the sum of energies of the light diffracted in a given direction by complementary screens equals the energy of the light diffracted in that direction when both screens are removed. Under certain conditions this may be interpreted to mean the diffraction patterns produced by complementary screens are approximately the same at all points except very near to the centre of the diffraction pattern. In consequence, the frequency content of white characters on a black background may be regarded as being sensibly the same as black characters on a white background (neglecting phase reversal). This, however, requires the white background to be bound by large aperture or frame.

If the black character is bound by a rectangular frame then its frequency content is derived by convolving the spectral function of the character (by applying the convolution theorem). Consequently the frequency spectrum of the character becomes confused with the spectrum of the aperture and is rendered useless for recognition by incoherent Fourier transformation.

If, however, the frequency content of the aperture can be confined within a narrow spectral band, then the frequency content of characters will not be seriously disturbed by the aperture. The practical realisation of this type of aperture is an aperdizing mask whose transmission profile function is Gaussian. This has a Gaussian frequency distribution whose width is inversely proportional to the width of the mask function.

A two dimensional Gaussian transmission function can be approximated by recording the convolution of two circular apertures on photographic emulsion. The negative of this is the required mask.

The Mark I and Mark II machines are both suitable for testing the efficiency of such a mask. The system of normalisation in the Mark II machine would need revising.

9.5.2 Mutilation Mask Experiments

A mutilation mask, shown in Fig. 9.8 (a), was devised by Dr. Leifer to simulate distorted characters. Its effect when placed in contact with Rockwell numbers 5 and 6 is demonstrated in Fig. 9.8(b) and (c).

It consists of a fairly random distribution of transparent dots on an opaque background. The mask cuts down the total light intensity, transmitted by characters, to around a third. The Mark II machine, with its built-in normaliser circuits, compensates for this reduction in light level and is therefore suitable for use in conducting experiments to investigate the effects of mutilation on the frequency content of characters.

The Mark I machine was used to perform some crude experiments into the effect the mutilation mask has on the value of Fourier coefficients. The main problem was found to be adjusting the gain of the amplifiers accurately enough to properly compensate for the reduced light level on introducing the mask. A set of results were taken with and without the mask at 6 frequency sampling points for both OCRB and Gill Sans numerals. These are reproduced in Table 9.1.

9.5.3 Direct Applications of a Mark II Machine without Additional Hardware

Two direct fast reading applications of the Mark II machine are: film reading, that is reading information stored on film in the form of transparent characters suitable for presentation to the machine; reading data presented in the form of characters on a cathode ray output display screen of computers.

The Mark II machine is now being adapted as a high speed film reader capable of reading characters at a rate of a 100 per second. A rotating polarisation vector is generated by rotating a half-wave-plate at 1000 revolutions per second mounted inside the hollow spindle of the air turbine shown in Fig. 9.9.

(a)

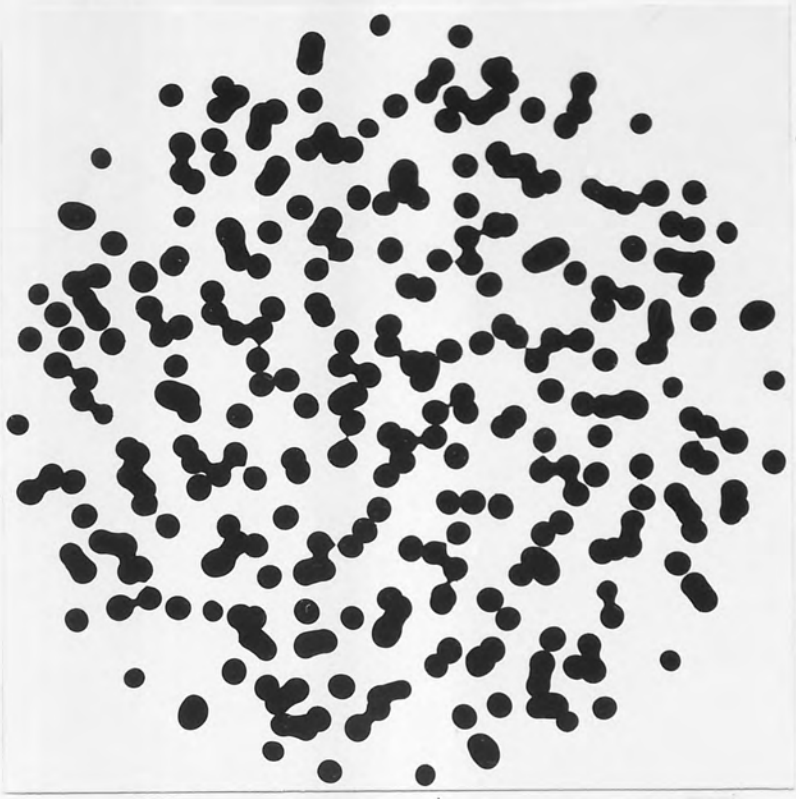

(b)

(c)

Figs. 9.8 (a) Mutilation mask
(b) Mutilated Rockwell 5
(c) Mutilated Rockwell 6

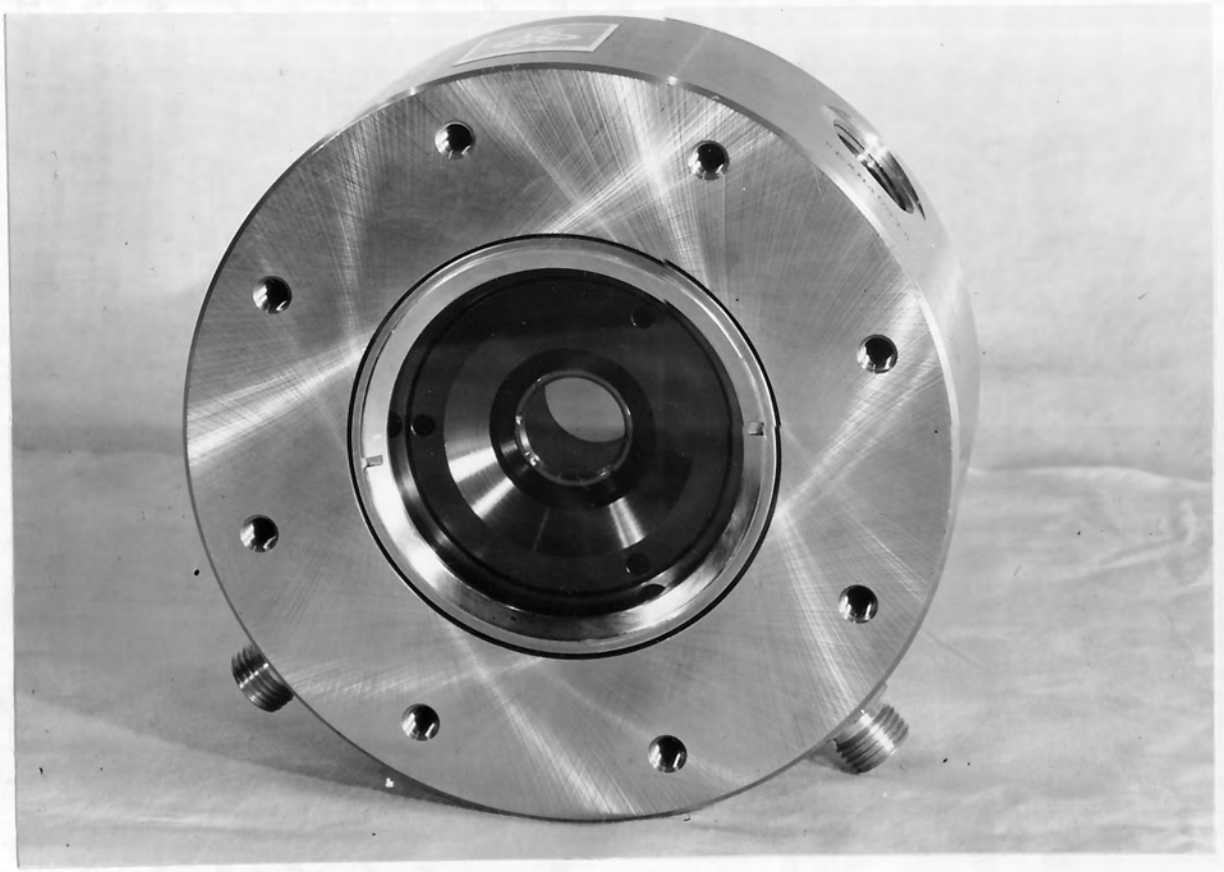

Fig. 9.9 Air turbine for spinning half-wave plate at 1000 revolutions per second

9.6 Character Recognition by Incoherent Fourier Transformation: Conclusions and Closing Remarks

Disadvantages

The optical system of deriving Fourier coefficients is not directly compatible with recognition of black characters on a white background, which is how they nearly always appear on printed documents. Possible solutions of this problem have been discussed already.

The frequency content of characters can change completely if variations in their size occur. Character recognition by incoherent Fourier transformation is thus not invariant to changes in character size unless some form of size compensation or normalisation is incorporated.

One of the few machines that can recognise characters occurring in different sizes was developed by Hawker Siddley Dynamics[46].

Advantages

Fourier coefficients provide two distinct bits of information: amplitude and phase. Amplitude is invariant to shift of the input data but phase is not in general shift invariant. Most of the recognition of characters is performed by features derived from amplitude of Fourier coefficients. A few character pairs are distinguishable only on including phase information of particular shadow frequencies. Character recognition by incoherent Fourier transformation is therefore not, in general, invariant to shift of characters in their input plane, although it will be invariant for most characters. If phase information, derived from a single Fourier frequency, is sufficient to complete the recognition of an alphabet, then recognition will be invariant to shift of characters along one particular direction in the data input plane. This direction is the one which does not disturb phase values of coefficients generated at the phase point or any other Fourier frequencies having that orientation.

One distinct advantage of character recognition by incoherent Fourier transformation lies in the illumination of characters. There are no special constraints or conditions as there are when generating a coherent Fourier transform. Diffuse and completely incoherent illumination is ideal (temporally coherent illumination might produce spurious diffraction effects at the grids). This offers a real possibility of reading characters directly from pages or any form of character display such as: cathode ray or television screens; lamp displays.

A number of advantages are embodiments of the system of optically preprocessing information. The optical preprocessing can be tailored to meet the requirements of the machine. The grids are selected to generate optimum Fourier frequencies used in recognising an alphabet (c.f. chapter 5). Consequently, the absolute minimum amount of information is collected by detectors for electronic processing and classification. The spatial bandpass restrictions, imposed by using discrete Fourier frequencies as features, automatically reject spatial noise existing outside these frequencies. Moreover, because relatively low Fourier frequencies are successful as features, coefficients generated by them can tolerate, to some degree, distortion of characters before their values become seriously disrupted. This is demonstrated in Table 9.1.

Finally, an incoherent Fourier transform can provide information or features in parallel. This means that it is potentially possible to read characters at very fast rates, limited only by the response time of the detecting system.

	Sampling Frequencies											
	(1,90°)		(1.55,80°)		(1.85,63°)		(2.5,0°)		(2.5,-27°)		(3.2,0°)	
Character	OCRB											
	*	**	*	**	*	**	*	**	*	**	*	**
1	3.6	3.2	5.1	5.2	4.2	4.7	7.6	7.1	1.8	1.8	6.5	5.8
2	1.0	1.3	9.8	7.3	9.8	7.7	3.5	2.9	5.3	5.9	4.9	4.7
3	1.9	2.1	7.2	5.7	4.8	3.1	3.5	3.5	2.7	3.7	3.4	3.8
4	6.2	4.8	6.0	5.9	5.6	5.2	1.0	1.6	8.0	7.9	2.8	1.9
5	3.2	3.4	4.2	4.1	3.7	2.9	3.2	2.7	5.8	4.2	5.4	4.6
6	6.6	5.9	1.6	1.2	2.2	1.8	4.9	4.4	9.8	9.3	4.8	3.9
7	3.3	2.6	7.6	6.3	7.0	5.0	2.1	1.7	8.7	8.3	2.7	1.9
8	5.8	5.4	6.1	4.4	5.0	3.7	8.1	6.8	4.0	4.3	8.5	7.8
9	6.8	6.3	2.1	1.3	2.1	1.7	5.3	4.4	9.9	7.6	5.1	4.9
0	4.9	3.5	6.2	6.8	6.8	6.6	9.8	9.4	8.1	6.8	9.8	9.5
	GILL SANS											
	*	**	*	**	*	**	*	**	*	**	*	**
1	2.7	3.1	1.7	0.9	1.7	0.9	8.1	8.0	2.2	3.2	7.0	7.0
2	1.1	1.1	9.5	8.8	9.0	8.0	2.8	2.2	6.1	5.2	2.4	2.4
3	2.1	2.1	6.8	6.0	4.7	4.0	4.2	4.0	1.9	3.1	3.3	2.9
4	9.8	8.4	6.0	5.8	3.8	4.2	4.6	3.6	3.6	4.0	5.0	3.4
5	2.5	2.6	4.4	3.9	1.6	1.7	3.4	3.7	2.2	1.8	1.2	1.3
6	6.7	5.7	2.2	2.5	1.8	1.7	1.8	1.8	7.0	6.5	4.0	3.6
7	3.0	2.3	8.1	8.0	7.1	6.3	1.6	2.1	8.2	7.4	2.6	2.6
8	6.6	5.9	3.9	3.7	3.6	3.4	4.5	4.1	2.8	2.5	7.8	7.4
9	7.2	6.8	3.2	2.7	2.5	1.8	1.6	1.2	6.6	4.7	4.2	3.6
0	4.6	4.2	7.5	7.0	8.1	7.4	9.8	8.7	7.9	7.5	5.3	5.3
Switching Levels:	4.7		5.2		5.9		6.45		7.0		6.2	
Calibration Character:	G-4		0-2		0-2		G-0		0-6 or 9		0-0	

TABLE 9.1 Voltages representing Fourier Coefficients of Mutilated** and Unmutilated* OCRB and Gill Sans numerals taken at the Six Best Frequencies selected to recognise both sets of numerals without necessitating the use of extra decoding logic.

APPENDIX I - The OCRB Repertoire of Characters

Sampling Frequencies

Character	(1,90°)	(1.55,80°)	(1.85,63°)	(2.5,0°)	(2.5,-27°)	(3.2,0°)
A	2	0	0	0	2	1
B	2	1	0	2	0	2
C	0	2	2	1	1	2
D	2	2	2	2	2	2
E	1	2	1	2	0	2
F	2	0	0	2	0	2
G	2	2	1	2	1	2
H	2	0	0	2	0	2
I	0	2	2	2	0	2
J	2	2	2	2	0	2
K	2	0	0	2	0	2
L	1	2	1	2	0	2
M	2	1	0	2	0	2
N	2	0	0	2	0	2
O	2	2	2	2	2	2
P	2	0	0	2	0	2
Q	2	2	2	2	2	2
R	2	1	0	2	0	2
S	1	2	0	0	0	2
T	1	2	1	2	0	2
U	2	2	1	2	1	2
V	2	0	0	0	2	0
W	2	2	1	2	0	2
X	2	1	0	0	1	0
Y	2	1	0	0	1	0
Z	0	2	2	0	2	0
Calibration Character:	M or W	Z	Z	U	0	H

2 ≡ ON 0 ≡ OFF 1 ≡ voltage within the error margin

APPENDIX II (a) One bit binary coded Fourier Coefficients of OCRB capital letters taken at the six best frequencies selected for numerals in two fonts.

	Sampling Frequencies								
	1	2	3	4	5	6	7	8	9
	$(\sqrt{10},-18^\circ)$	$(\sqrt{5},63^\circ)$	$(1,90^\circ)$	$(2,0^\circ)$	$(\sqrt{2},-45^\circ)$	$(\sqrt{5},-27^\circ)$	$(2\sqrt{2},-45^\circ)$	$(3,0^\circ)$	$(\sqrt{10},55^\circ)$
Character									
A	7	2	6	2	7	7	0	2	3
B	5	2	5	1	4	2	1	7	3
C	5	6	1	3	4	5	3	5	1
D	7	6	4	2	2	5	4	7	1
E	3	2	2	4	4	3	0	5	3
F	2	0	3	6	6	4	3	4	2
G	6	2	3	1	1	6	4	6	4
H	5	0	6	4	6	1	4	7	1
I	4	4	0	7	2	2	3	5	0
J	2	4	3	4	7	5	1	5	2
K	0	3	5	3	7	5	4	5	1
L	3	5	2	6	0	3	0	6	1
M	3	1	7	7	7	1	7	7	1
N	7	0	7	3	4	4	1	7	0
O	7	6	4	6	0	7	3	7	2
P	5	3	5	4	7	0	7	6	3
Q	7	7	5	3	1	7	6	7	1
R	6	4	6	1	6	0	6	7	4
S	3	0	2	1	0	2	2	4	7
T	4	4	2	7	3	3	1	5	0
U	7	4	4	7	2	7	2	7	2
V	7	1	5	1	6	7	2	3	0
W	4	3	7	5	7	5	5	7	0
X	2	2	4	2	6	5	6	2	0
Y	7	2	4	5	5	5	2	0	2
Z	4	7	0	3	6	7	7	0	0
Calibration Character:	V	Q	M	I	W	O	2	H	S

APPENDIX II (b) 3-bit binary coded Fourier Coefficients of OCRB capital letters taken at 9 Frequencies.

V_I	V_o
3 mm	30 mm
6	19
9	14
12	10
15	8
18	6
21	5

(a)

V_I	V_o
1 mm	23 mm
2	19
3	16
4	13.5
5	11.5
6	10
7	9
8	8
10	6
12	5
14	4

(b)

V_I	V_o
1 mm	22 mm
2	17
3	14
4	11.5
5	10
6	8.5
8	6
10	5
12	4
14	3
16	2.5
20	2.0

(c)

V_I	V_o
2 mm	32 mm
4	25
6	18
8	14
10	10
12	8
14	6
16	5
18	4
20	$3\frac{1}{2}$
22	3

(d)

APPENDIX III Results of tests on A.C. Reciprocal Circuit (7.7.1). Measurements were made using an oscillascope.

REFERENCES

1(a) Corcoran D.W.J., 1971, "Pattern Recognition", Penguin sci. of behaviour.

1(b) Casey R.G. and Nagy G., 1971, Scientific American, 224, 4, 56 - 71.

2. Fournier d'Albe, E.E., 1914, Proc. Roy. Soc., A. Vol. XC, p. 373.

3. Shannon E.E. and Weaver W., 1949, "The Mathematical Theory of Communication", Illinois press.

4. Parkes J.R. and Bell D.A., 1968, New Scientist, 38, 602, 624 - 626.

5. Ullmann J.R., 1968, I.E.E.-N.P.L. Conference on Pattern Recognition, conf. pubn. 42, p. 197 - 206.

6. Bledsoe W.W. and Browning I, 1959, Proc. Eastern Joint Computer Conference. p.225.

7. Nilsson N.J., 1965, "Learning Machines". McGraw Hill.

8. Arkadev A.G. and Braverman E.M., 1967, "Teaching Computers to Recognise Patterns". Academic Press, London and New York.

9. Kovalevsky V.A., 1968, "Character Readers and Pattern Recognition". Spartan/McMillan and Co. Ltd.

10. Mason C.J.W. and McFall C.H., 1968, I.E.E.-N.P.L. Conference on Pattern Recognition, conf. pubn. 42. p. 69 - 76.

11. Holt A.W., 1968, Computer Group News, 2, 6, 3 - 11.

12. Wilson R.A., 1966, "Optical Page Reading Devices", Reinhold Publishing Corporation.

13. The British Computer Society, 1967, "Character Recognition 1967". The Gresham Press, Unwin Bros. Ltd.

14. Nadler M., 1969, Computer Group News, 2.

15. Hammans B., 1969, The Marconi Review, Vol. XXXII, No. 172, p. 31 - 48.

16. Davis J.H., 1961, Bulletin of the Institute of Physics, 12, 12, 333 - 338.

17. Greanias E.C., 1962, "Optical Character Recognition", p. 129 - 145. McGregor and Werner Inc.

18. Griffin E., 1962, "Optical Character Recognition", p. 73 - 83. McGregor and Werner Inc.

19. Bell H.A., 1967, Systems Technology, p. 32 - 37.

20. Noble P.J.W., 1967, Components Technology, 2, 8, 23 - 28.

21. Sarage P., Weaver J.A., and Woollons D.J., 1967, Philips Technical Review, 28, 5/6/7, 197 - 203.

22. Aleksander I. and Albrow R.C., 1968, I.E.E.-N.P.L. Conference on Pattern Recognition, conf. pubn. 42. p. 1 - 10.

23. Weaver J.A., 1968, Sci. J., 4, 10, 66 - 71.

24. Britt R.H., 1968, I.E.E.-N.P.L. Conference on Pattern Recognition, conf. pubn. 42. p. 347 - 354.

25. Hosking K.H. and Thompson J., 1968, I.E.E.-N.P.L. Conference on Pattern Recognition, conf. pubn. 42. p. 271 - 281.

26. Hosking K.H., 1969, The Marconi Rev., Vol. XXXII, No. 172. p. 3 - 20.

27. The Marconi Review, 1969, (First Quarter) Vol. XXXII No. 172.

28. Hall P.M., 1968, Electronics and Power, April, p. 149 - 153.

29. Saraga P. and Woollons D.J., 1968, I.E.E.-N.P.L. Conference on Pattern Recognition, conf. pubn. 42. p. 106 - 116.

30. Deutch E.S., 1968, I.E.E.-N.P.L. Conference on Pattern Recognition. p. 179 - 190.

31. Bomba J.S., 1959, Proc. Eastern Joint Computer Conference, p. 218 - 224.

32. Block H.D., 1962, Rev. Mod. Phys. 34, 1, 123 - 135.

33. Holmes W.S., Leland H.R., and Muerle J.L., 1962, "Optical Character Recognition". (Edited by Hannan W.J.) p. 213 - 225. McGregor and Werner Inc.

34. Bell D.A., 1964, Patent No. 972,054.

35. Sheinberg I., 1970, Pattern Recognition (J. of the P.R. Soc. of America.) Pergamon Press. Vol. 2. p. 167 - 173.

36. Chalmers J. and Stein A., 1969, Electronics Letters, 5, 18. p. 431 - 433.

37. Levialdi S., 1971, Inst. P. Phys. Exhibition, Italian Exhibit.

38(a) Vander Lugt A., 1968, Optica Acta, 15, 1, 1 - 33.

38(b) Yeliseyev V.K., 1968, "Character Readers and Pattern Recognition (Edited by Kovalevsky V.A.) p. 195.

39. Babcock R.C. et. al., 1963, "Optical Processing of Information" (Edited by Pollack D.K. et. al). Chapt. 12, p. 145 - 167.

40. Lee Y.W., 1964, "Statistical Theory of Communication". John Wiley and Sons Inc.

41. Panter P.F., 1965, "Modulation, Noise and Spectral Analysis". McGraw Hill.

42. McLachlan D., 1962, J. Opt. Soc. Am. 52, 4, 454 - 459.

43. Mazurowski J.J., 1969, New Sci., 44, p. 636 - 639.

44. Goodman J.W., 1968, "Introduction to Fourier Optics". McGraw Hill.

45. Horwitz L.P. and Shelton G.L., 1961, Proc. I.R.E., 49, 1, 175 - 185.

46. Holden S., 1968, J. of Sci. Instruments (J. of Phy. E.) Series 2, 1, p. 827 - 828.

47. Clowes M.B., 1962, "Optical Character Recognition" (Edited by Hannan W.J.) p. 305 - 318. McGregor and Werner Inc.

48. Kovasznay L.S.G. and Arman A., 1957, Rev. Sci. Instruments. 28, 10, 793 - 797.

49. Edgar R.F., 1969, Optics Technology, Aug. p. 183 - 189.

50. Mertz L., 1965, "Transformations in Optics", John Wiley and Sons Inc.

51. Mertz L. and Young N.O., 1961 Proc. I.C.O. Conf. Opt. Instruments, London, p. 305.

52. Goodman J.W., 1968, "Introduction to Fourier Optics". p. 177. McGraw Hill.

53(a) Smith H.M., 1969, "Principles of Holography", John Wiley and Sons Inc.

53(b) Lendaris G.G., and Stanley G.L., 1965, Optical and Electro-optical Processing of Information, edited by J.T. Tippett et. al. (M.I.T. Press), p. 535 - 550.

53(c) Lendaris G.G. and Stanley G.L., 1970, Proc. I.E.E.E., 58, 2, 198 - 216.

54. Keyte G.E., 1970, "The Use of Complex Spatial Frequency Filters in Correlation Processes". Ph.D. Thesis, University of Aston.

55(a) Gabor D., 1969, Optica Acta, 16, p. 519 - 533.

55(b) Rogers G.L., 1970, The Proceedings of the Technical Programme Electro-optical Systems Design Conference, New York.

56. Douglass A.E., 1915, The Astrophysical Journal, XLI, 3, 173 - 186.

57. Douglass A.E., 1914, The Astrophysical Journal, XL, 3, 326 - 331.

58. Foster G.A.R., 1930, J. Text. Inst. 21, T18.

59. Baker L.R., 1968, Symposium on the Engineering Uses of Holography. University of Strathclyde.

60. Born M., Furth R. and Pringle R.W., 1945, Nature, Lond., 156, p. 756.

61. Edgar R.F. and Clarke D., 1967, Infrared Astronomical Instrumentation: Polarimeters and Multiplex Radiometers. Report Contract AF61(052) - 968. University of Hull, Edgar R.F., Lawrenson B. and Ring J., 1967, J. de Phys. Radium, Paris, Suppl. 3 - 4, 28, C2 - 73/78.

62. Barber N.F., 1961, "Experimental Correlograms and Fourier Transforms". Pergamon Press.

63. Leifer I., Rogers G.L. and Stephens N.W.F., 1969, Optica Acta, 16, 5, 535 - 553.

64. Hannan W.J., 1962, "Optical Character Recognition". McGregor and Werner Inc.

65. International Business Forms Industries, 1969, "Optical Character Recognition and the Years Ahead". The Business Press, Elmhurst, Illinois.

66. Balm G.J., 1970, J. of the Pattern Recognition Soc. Am. 2, p. 151 - 166. Pergamon Press.

67. Nagy G., 1968, Proc. of the I.E.E.E., 56, 5, 836 - 862.

68. Carslaw H.S., 1921, "Introduction to the Theory of Fourier's Series and Integrals". McMillan and Co. Ltd.

69. Shulman A.R., 1970, "Optical Data Processing", John Wiley and Sons Inc.

70. Cooley J.W. and Tukey J.W., 1965, "Mathematics of Computation", 19, 297 - 301.

71. Cochran W.T. et. al., 1967, Proc. I.E.E.E., 55, 10, 1664 - 1674.

72. Goodman J.W., 1968, "Introduction to Fourier Optics", p. 21, McGraw Hill.

73. Radoy C.M., 1967, "Pattern Recognition by Fourier Series". Transformations, MSEE Thesis, GE/EE/67A-11, U.S.A. F. Inst. Tech. (Washington, D.C.)

74. Jennison R.C., 1961, "Fourier Transforms and Convolutions", Pergamon Press.

75. Tucker D.G., 1958, J. Brit. Inst. Radio Engineers, 18, 233 - 235.

75(a) Mertz P. and Gray F., 1934, Bell Systems Tech. J., 13, p. 472.

76. Mullard, 1966, "Voltage Regulator (Zener) Diodes", Wightman and Co. Ltd.

77. Crump A.E., 1967, Wireless World, 73, 3, 122 - 127.

78. Crump A.E., 1967, Wireless World, 73, 4, 175 - 177.

79. Crump A.E., 1969, Wireless World, 75, 1404, 269.

80. Batchelor B.G. and Wilkins B.R., 1968, I.E.E.-N.P.L. Conference on Pattern Recognition, conf. pubn. 42, p. 168 - 178.

81. Uttley A.M., 1968, I.E.E.-N.P.L. Conference on Pattern Recognition conf. pubn. 42, p. 338 - 346.

82. Lendaris G.G. and Stanley G.L., 1963, On the Structure-Dependent Properties of Adaptive Logic Networks, General Motors Corporation, GM Defense Research Labs., Santa Barbara. TR63 - 219.

83. Weaver W., 1949, "Recent Contributions to the Mathematical Theory of Communication". Illinois Press, p. 23.

84. Peek, Th., de Lang H. and Bouwhins G., 1969, Lasers and Opto-Electronics conference, Southampton, Paper S177.

85. Rogers G.L., 1970, Applied Optics, 9, 10, 2396 - 2397.

86(a) Jaumann G., 1891, Sitzungsberichte der Wiener Akad. Math. Nat. K.L. 1239.

86(b) Rogers G.L., 1971, Proc. Electro-Optics. '71 International Conf., Southampton, p. 365 - 368.

87. The British Computer Society, 1967, "Character Recognition 1967", p. 64. The Gresham Press.

88. Gilmour G.A., 1967, I.E.E.E. Trans. on Nuclear Science, Feb. p. 321 - 324.

89. Newell A.F., 1969, Wireless World, 75, 1404, 285 - 289.

90. International Standard Electric Corporation, 1965, Patent Spec. 1,110,923.

91. Ratliff F., 1961, Sensory Communication, edited by W.A. Rosenblith (M.I.T. Press).

92. Arps R.B. et. al., 1969, I.E.E.E. Trans. on Man-Machine Systems, Vol. MMS - 10, 3, 66 - 71.

93. Ditchburn R.W., 1963, "Light", p. 204, Blackie and Sons Ltd.

94. European Computer Manufacturers' Association, 1965, "ECMA Standard for the Alpha-Numeric Character Set OCR-B for Optical Recognition", Geneva.

ACKNOWLEDGEMENTS

I am extremely indebted to my supervisor, Dr. G. L. Rogers, for proposing the original theme for this thesis and for his advice, assistance and encouragement throughout each stage of the research.

I would also like to express my gratitude to Dr. I. Leifer for much stimulating and useful discussion. My thanks are also due to Professor S. E. Hunt for the use of laboratory facilities within the department.

Acknowledgements should be made to the S.R.C. for initially sponsoring the research and to the U.G.C. for their follow-up grant.

Grateful thanks are given to B. Brookes for his photographic skill in assisting in the manufacture of grids, also to A. G. McKenzie for building a composite detector holder and to J. Sidwell for his advice during the early stages of developing the electronics.

Finally, I would like to record my thanks to Wendy Farrington for the invaluable work done when typing the manuscript.